Possible Roles for Tropomyosin During Anaphase Chromosome Movement

Jessica Di Salvo

A thesis submitted to the Faculty of Graduate Studies in partial fulfillment of the requirements for the degree of Master of Science

Graduate Program in Biology

York University

Toronto, Ontario

August 2017

Abstract

During anaphase, chromosomes move toward the spindle poles by forces transmitted through their kinetochore fibres. The fibres contain microtubules, as well as actin and myosin, which work together to produce the force that moves chromosomes. If tropomyosin functions in the spindle, as it does in other actin microfilament systems, then it may regulate actin filaments along kinetochore fibres. The purpose of my thesis was to investigate whether tropomyosin has possible roles during anaphase chromosome movement.

Anaphase cells were treated with different inhibitory drugs against tropomyosin. Chromosome movement was altered by an upstream kinase inhibitor and was sometimes altered by a direct binding inhibitor. This may be due to possible time constraints. Furthermore, tropomyosin localized to the spindle poles and kinetochore fibres of the meiotic spindle of crane-fly primary spermatocytes. Overall, the data support the idea that tropomyosin is present in the spindle, where it may function during anaphase chromosome movement.

Acknowledgments

First and foremost, I would like to thank my supervising professor, Dr. Arthur Forer. Throughout my graduate degree, Art provided me with continual support and advice and I could not have done this without him. I feel very lucky to have had the chance to work with Art and learn from him. He is kind, caring, patient and inspiring and I am thankful for everything that he taught me. Even in the most challenging situations throughout my research, Art was there to guide and motivate me. I always looked forward to coming in to the lab, to hear one of Art's funny jokes, talk about our days and, of course, check in on the crane-flies. Art has also helped me in pursuing the next phase of my academic life and I cannot be more grateful. Thank you so much Art for all of your time and effort, you made my graduate degree enjoyable, educational and unforgettable.

I would also like to thank my advisor, Dr. Jean-Paul Paluzzi. Dr. Paluzzi was encouraging and supportive throughout my graduate degree and I am very thankful for all of his time and effort in helping me improve my work.

Thank you as well to Dr. Logan Donaldson and Dr. Michael Connor for reading and attending my thesis defense. I am very appreciative of all of your time and effort in helping me.

I would also like to thank my fellow lab members, Eleni Fegaras and Amanda Silverio. Eleni was very helpful in getting me started in the laboratory and showed me many of the experimental procedures. I am very thankful for all the time that she spent helping and listening to me. I will miss her support and her friendship and I will also miss the delicious home-grown vegetables that she would share with us. I wish Eleni the best of luck in her PhD degree, I am confident that she will do great work. I would also like to thank Amanda, who was a great friend to me. Amanda and I learned a lot about the lab together and I am thankful for her support. Eleni and Amanda both helped to make my graduate degree a great experience.

Lastly, I am endlessly thankfully to my family and friends who believed in me and supported me over the last two years. They were a large source of my motivation and their support helped in keeping me focused and dedicated.

Table of Contents

Abstract ii

Acknowledgments iii

Table of Contents v

List of Tables viii

List of Figures ix

General Introduction 1

A. The Spindle 1

B. The Mitosis Spindle 3

B.1 Prophase 3

B.2 Prometaphase 3

B.3 Metaphase 4

B.4 Anaphase 4

B.5 Telophase 4

B.6 Cytokinesis 5

C. The Meiotic Spindle 5

D. The Spindle: Microtubules as force producers 6

D.1 The Flux model 8

D.2 The Pac-Man model 10

D.3 Confounding evidence regarding microtubules as force producers 12

E. The spindle: Actin and Myosin as force producers 14

F. Complementary systems 16

F.1 Complementary systems: Actin and myosin in muscle cells 17

F.2 Complementary systems: Tropomyosin in non-muscle cells 25

G. Tropomyosin inhibition 30

G.1 Upstream kinase inhibition of tropomyosin 31
G.2 Direct binding inhibition of tropomyosin 33
H. Tropomyosin in the spindle 36
I. Crane-fly spermatocytes provide an excellent model for studying meiotic processes and cytoskeletal components 38
Title page 41
Introduction 42
Materials and Methods 48
Crane fly stock 48
Larval selection 48
Solutions 49
Live cell preparations 50
Phase-contrast light microscopy and data analysis 51
Lysing and fixation 52
Antibody staining 53
Confocal microscopy and image processing 55
Results 57
Control divisions 57
Anaphase chromosome movement following treatment 61
DMSO treatment 65
PD treatment 67
TR100 treatment 75
Cytoskeletal effects following treatment 85
Membrane blebbing 85
Cleavage furrows 87
Actin fingers 91
Tropomyosin localization in the spindle 93

Non-constant poleward velocity during anaphase 100

Discussion 108

Anaphase chromosome movement following drug treatments 108

PD treatment 109

TR100 treatment 112

Tropomyosin localization in the spindle 117

Chromosome movement and tropomyosin function 118

Chromosome arms and non-constant poleward velocity 120

References 122

Appendix 134

List of Tables

Table 1: Average relative anaphase speeds following DMSO, PD and TR100 treatments 63

Table 2: Summary of chromosome movements after control (DMSO) and drug treatments (PD and TR100) added during anaphase 64

Table 3: Average speeds during anaphase in Insect Ringer's for kinetochores with constant and non-constant poleward velocity 103

Table 4: Summary of chromosome are extensions and retractions for autosomal half-bivalents during anaphase in Insect Ringer's 106

Table 5: Absolute difference in time between chromosome arm retraction and resumed poleward movement during anaphase in Insect Ringer's 107

List of Figures

Figure 1: Different types of kinetochore fibre attachment observed in the spindle 1

Figure 2: Microtubule dynamics showing dynamic instability and treadmilling 7

Figure 3: Proteins involved in the Flux model for chromosome movement 10

Figure 4: Schematic of the sarcomere repeat in striated muscle 18

Figure 5: "Decorated" actin filaments treated with HMM showing arrowhead complexes oriented with definite structural polarity 20

Figure 6: Schematic representation of the protein arrangement in the thin filaments of striated muscle 22

Figure 7: Intron-exon organization of the mammalian tropomyosin genes 26

Figure 8: Structure of PD 098059 (PD) (2'-amino-3'-methoxyflavone) 31

Figure 9: Sequence of events leading to tropomyosin phosphorylation by DAP kinase-I in the MAPKK pathway 33

Figure 10: Structure of TR100 and predicted modelling for interaction with 9d exon sequence of tropomyosin 35

Figure 11: Tropomyosin localization to the spindle in *Drosophila* S2 cells during mitosis 37

Figure 12: Illustrating constant poleward velocity during anaphase in Insect Ringer's 58

Figure 13: Illustrating constant poleward velocity during anaphase in Insect Ringer's 59

Figure 14: Average control speeds during anaphase in Insect Ringer's 60

Figure 15: Illustrating chromosome movement following DMSO treatment 66

Figure 16: Average speeds following PD treatment that slowed anaphase movement 69

Figure 17: Illustrating slowed chromosome movement following PD treatment 70

Figure 18: Average speeds following PD treatment that slowed and then stopped anaphase movement 71

Figure 19: Illustrating slowed and then stopped chromosome movement following PD treatment 72

Figure 20: Average speeds following PD treatment that stopped anaphase movement 73

Figure 21: Illustrating stopped chromosome movement following PD treatment 74

Figure 22: Average speed following TR100 treatment in which chromosome movement was unaffected 77

Figure 23: Illustrating chromosome movement that was unaffected following TR100 treatment 78

Figure 24: Average speeds following TR100 treatment that slowed anaphase movement 79

Figure 25: Illustrating slowed chromosome movement following TR100 treatment 80

Figure 26: Average speeds following TR100 treatment that stopped anaphase movement 81

Figure 27: Illustrating stopped chromosome movement following TR100 treatment 82

Figure 28: Average speeds following TR100 treatment that had a delayed effect 83

Figure 29: Illustrating chromosome movement that showed a delayed effect following TR100 treatment 84

Figure 30: Membrane blebbing following TR100 treatment 86

Figure 31: Relative percent of cells with cleavage furrow ingression in different treatments 88

Figure 32: Average time after anaphase onset that cleavage furrows begin to ingress (minutes) 89

Figure 33: Cleavage furrow attempt in TR100 90

Figure 34: Loss of actin fingers following TR100 treatment 92

Figure 35: Three different cells stained for tropomyosin in prometaphase-I to metaphase-I stages of cell division 94

Figure 36: Three different cells stained for tropomyosin in anaphase-I, as autosomal half-bivalents move toward spindle poles 96

Figure 37: Three different cells stained for tropomyosin in prometaphase-I to anaphase-I stages of cell division 98

Figure 38: Average speeds for kinetochores with non-constant poleward velocity in Insect Ringer's 101

Figure 39: Illustrating non-constant poleward velocity during anaphase in Insect Ringer's 102

Figure 40: Chromosome arm extension and retraction during non-constant anpahase movement in Insect Ringer's 105

General Introduction

A. The Spindle

The spindle apparatus assembles during cell division and is responsible for separating chromosomes into two daughter nuclei (Schrader 1953). In animal cells, it is fusiform in shape, with spindle poles on opposite ends, and composed of birefringent material (Inoue 1953, Forer and Zimmerman 1976, Inoue 1988). Three types of birefringent fibres can be observed in the spindle including continuous fibres, that extend between spindle poles, interzonal fibres, that extend between separating chromosomes during anaphase or telophase, and chromosomal fibres, that extend between the kinetochores of the chromosomes and the spindle poles (Inoue 1953). The kinetochore is the site on the chromosome to which the chromosomal or kinetochore fibre attaches. The fibres can attach to kinetochores in one of several ways (Compton *et al.* 2007) although, for the purposes of my thesis, I will on focus amphitelic or bioriented attachment (Figure 1). The kinetochore fibres are responsible for transmitting force to the chromosomes which causes them to move (Forer 1980).

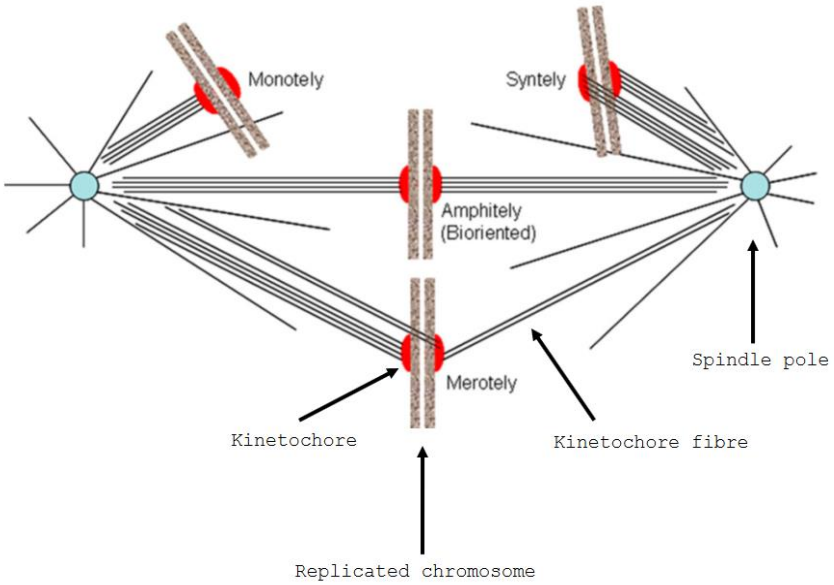

Figure 1 – Different types of kinetochore fibre attachment observed in the spindle. Kinetochore fibres from one spindle pole can attach to one (monotely) or both (syntely) of the sister kinetochores. Kinetochore fibres from opposite spindle poles can attach to sister kinetochores equally (amphitely) or unequally (merotely). Image modified from Compton *et al.* (2007). Originally published in *Journal of Cell Biology*. DOI: 10.1083/jcb.200709152.

Cell division can occur through mitosis or meiosis. Mitosis occurs in somatic tissue while meiosis occurs exclusively in germ line cells. In mitosis, replicated chromosomes are separated through an equational division producing two identical diploid daughter cells. Meiosis, on the other hand, generally occurs through two rounds of division, meiosis-I and meiosis-II, and produces four unique daughter cells with haploid numbers of chromosomes. The meiotic divisions include one reductional and

one equational division (Ris 1949). The reductional division, generally first, divides the number of chromosomes in half, producing haploid daughter cells. Mitosis and meiosis progress through similar stages, with some critical exceptions. The stages of mitosis generally include prophase, prometaphase, metaphase, anaphase, telophase and cytokinesis. The stages of meiosis-I and -II include prophases-I and -II through telophases-I and -II, respectively. The stages of mitosis as well as the unique events of meiosis will be discussed in the following sections.

B. The Mitosis Spindle:

B.1 Prophase

During prophase, chromosomes condense and duplicated centrosomes, which are the microtubule organizing centers (MTOC), move apart. Replicated chromosomes are composed of sister chromatids that are attached at the centromere and appear as paired chromatids by late prophase (Sumner 1991).

B.2 Prometaphase

Prometaphase begins with nuclear membrane breakdown which allows kinetochore fibres to capture chromosomes at their kinetochores and move them toward the equator. Chromosomes congress toward

the equator and, moving past and back, either prior to or after becoming bioriented (Kapoor *et al.* 2006).

B.3 Metaphase

Chromosomes become aligned at the equator at metaphase and bioriented sister kinetochores attach to opposite spindle poles through their kinetochore fibres (reviewed in Scholey *et al.* 2003).

B.4 Anaphase

During anaphase, the cohesin complex which holds paired sister chromatids together disassembles (Nasymth 2002) and the chromatids move toward opposite spindle poles. Anaphase includes two distinct phases; during the first phase, kinetochore fibres shorten as kinetochores move toward spindle poles and, during the second phase, the spindle elongates as the spindle poles move apart (Hughes and Swann 1948, Ris 1943, Ris 1949, Taylor 1965). These phases, referred to as anaphases A and B, can occur simultaneously, concurrently in either order or exclusively.

B.5 Telophase

By telophase, the two sets of daughter chromosomes arrive at opposite spindle poles and decondense. New nuclear membranes assemble around each set of chromosomes creating two daughter

nuclei and marking the end of mitosis (reviewed in Scholey *et al.* 2003). The division of cytoplasm begins after the contractile ring forms and constricts.

B.6 Cytokinesis

During cytokinesis, the contractile ring forms a cleavage furrow which ingresses, creating two daughter cells. The contractile ring is composed primarily of actin and myosin (Schroeder 1973, Fujiwara and Pollard 1976, Fujiwara *et al.* 1978, Vavylonis *et al.* 2008).

C. The Meiotic Spindle

Meiosis is responsible for producing genetically unique haploid sex cells through a process called gametogenesis. Briefly, primary gametocytes undergo meiosis-I division and produce secondary gametocytes, which in turn undergo meiosis-II division and produce gametids. These later develop into haploid gametes. The stages of meiosis resemble mitosis with some critical exceptions, which will be discussed here.

Meiosis-I is typically a reductional division that results in haploid daughter cells (Ris 1949). During prophase-I, non-sister chromatids from pairs of replicated homologous chromosomes undergo crossing over at regions called chiasmata

(Henderson 1970). This crossing over allows genetic recombination to occur and the exchange of genetic material. The terms bivalent or tetrad refer to the pairs of homologous chromosomes at this stage. During the metaphase-I to anaphase-I transition, and throughout anaphase, the cohesin complex holding sister chromatids together does not disassemble and sister kinetochores are pulled toward the same spindle pole (Watanabe 2004). Unlike mitosis, replicated chromosomes therefore remain together, while homologous pairs separate. As a result, the daughter nuclei contain half of the chromosome complement of the parent cell. Meiosis-II follows meiosis-I and is an equational division, similar to mitosis. In some females, such as mammals and birds, meiosis arrests at different divisional stages such as prophase-I and, as a result, meiotic events do not occur sequentially (Mira 1998). In addition, in some organisms such as the coccids, meiosis-I is equational while meiosis-II is reductional (Brown and Nelson-Rees 1961).

D. The Spindle: Microtubules as force producers

Microtubules are ubiquitous cytoskeletal filaments involved in various types of cellular movement. They are composed of αβ-tubulin heterodimers and form hollow tubes (Downing and Nogales 1998). When microtubules assemble, the plus end typically incorporates subunits faster than the minus end and assembly is

accompanied by GTP hydrolysis by β-tubulin. In the cell, microtubules preferentially nucleate in a region called the microtubule organizing center or centrosome (Wade 2009). During cell division in animal cells, the centrosome duplicates and one centrosome locates to each spindle pole. An important feature of microtubules is that they display dynamic instability and fluctuate between growth and shrinkage (Wade and Hyman 1997). They are also capable of treadmilling, as tubulin subunits can be incorporated and lost on opposite ends of the microtubule filament without length change (Grego *et al.* 2001, Figure 2).

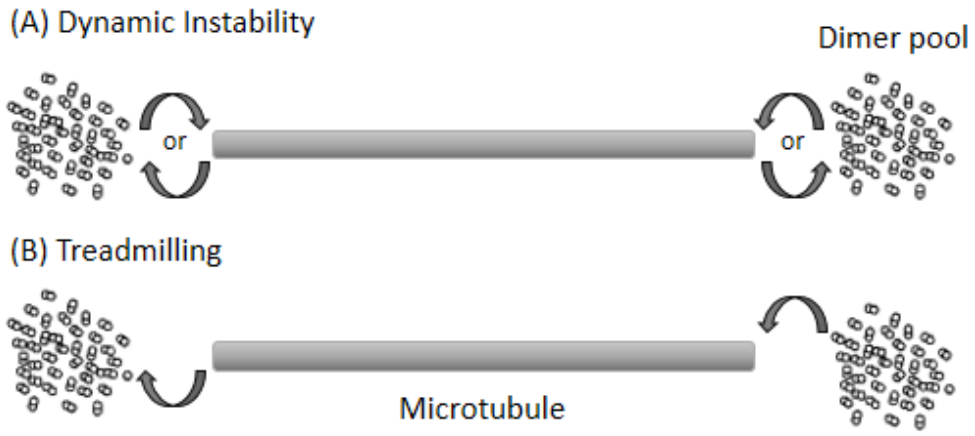

Figure 2 – Microtubule dynamics showing dynamic instability and treadmilling. A) tubulin subunits can be incorporated or lost from either end of the microtubule filament. B) tubulin subunits are added and lost on opposite ends of the microtubule filament.

Microtubules compose the majority of the spindle structure and evidence suggesting they are involved in spindle function comes from studies demonstrating the dynamic behaviour of kinetochore fibre microtubules (Mitchison 1988). These microtubules are part of the kinetochore fibres extending between the spindle pole and the kinetochores of the chromosomes. The plus ends of the microtubules are located at the kinetochores while the minus ends are located at the spindle poles. Unlike non-kinetochore microtubules, these display unique stability against agents such as cooling, hydrostatic pressure and colchicine (Cassimeris *et al.* 1988). Two models describing microtubules as the force producers for chromosome movement include the Flux and Pac-Man models which will be discussed in the following section.

D.1 The Flux model

The Flux model is based on poleward movement of microtubules because of minus end disassembly at the spindle pole (Maddox *et al.* 2003). In this model, microtubule polymerization takes place at the kinetochore and depolymerization takes place at the spindle pole (MTOC). Briefly, tubulin is incorporated at the kinetochore and moves along the kinetochore fibre toward the spindle pole where it is lost. During metaphase, equal rates of polymerization and depolymerization maintain the length of the

kinetochore fibre (Mitchison 1989). However, during anaphase A, depolymerization occurs at a faster rate than polymerization, which results in kinetochore fibre shortening as chromosomes move poleward. Tubulin flux continues throughout anaphase A while kinetochore fibres shorten (Wadsworth *et al.* 1989, LaFountain *et al.* 2004). In crane-fly primary spermatocytes (LaFountain *et al.* 2004), tubulin subunits continue to incorporate at the kinetochore showing that depolymerization occurs primarily, if not exclusively, at the pole.

Different proteins have been implicated in the Flux model (reviewed in Rogers *et al.* 2005, Figure 3). A series of experiments conducted in *Drosophila* showed that a Kin-1 kinesin, KLP10A, functioned by depolymerizing microtubules at the mitotic spindle pole as well as facilitating poleward flux during anaphase (Rogers *et al.* 2004). In another set of experiments conducted in *Drosophila*, it was shown that the CLASP orthologue, MAST/Orbit, localizes to kinetochores where it is essential for incorporating tubulin during flux (Maiato *et al.* 2005). Lastly, it has been suggested that a kinesin-5 protein, Eg5, drives flux by promoting microtubule sliding (Miyamoto *et al.* 2004). The Flux model proposes that kinesin-driven depolymerization at the spindle pole generates the force required for microtubule flux

and, furthermore, that flux exerts a pulling force moving chromosomes toward spindle poles (Rogers *et al*. 2005).

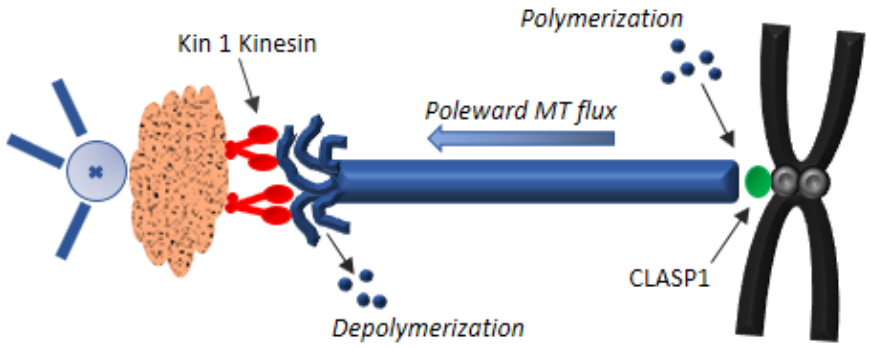

Figure 3 – Proteins involved in the Flux model for chromosome movement. Kin-1 kinesin localizes to the spindle pole where it acts to depolymerize kinetochore fibre microtubules. CLASP1 localizes to the kinetochore where it promotes mictrotubule polymerization. Mictrotubules flux toward the spindle pole during metaphase, as kinetochore fibres maintain their length, and anaphase, as kinetochore fibres shorten and chromosomes move poleward.

D. 2 The Pac-Man model

The Pac-Man model is based on evidence suggesting that poleward force is generated at the kinetochore, as opposed to being along the kinetochore fibre or at the spindle pole (Cassimeris *et al.* 1987). Contrary to the Flux model, the Pac-Man model proposes that microtubules depolymerize at the kinetochore as chromosomes chew their way poleward along kinetochore fibres. For example, chromosomes have been shown to move poleward during anaphase

while photobleached regions along the kinetochore fibres remain stationary with respect to the spindle pole to which they are attached (Gorbsky *et al.* 1987). These results suggest that kinetochore fibre shortening is due to depolymerization at the kinetochore, as opposed to the spindle pole. In addition, photobleached regions along kinetochore fibres do not move poleward during metaphase and tubulin flux does not account for fluorescence recovery (Wadsworth and Salmon 1986). Together, these data suggest that kinetochore fibre microtubules are stationary and that kinetochore fibre shortening is due to depolymerization at the kinetochore. It has also been suggested that the motor driving poleward chromosome movement is at or near the kinetochore (Nicklas 1989). Briefly, chromosomes continued moving poleward after their kinetochore fibres were cut in a region lying between the chromosome and the spindle pole. This suggests that poleward chromosome movement is driven by a force generated at or near the kinetochore, as opposed to being generated at the spindle pole.

Recent data suggests that the Pac-Man and Flux models may work concurrently to produce poleward chromosome movement during anaphase A and that microtubule severing proteins are involved (Zhang *et al.* 2007). In a series of experiments conducted in *Drosophila*, three microtubule severing proteins, including

Katanin, Spastin and Fidgetin, were shown to affect both microtubule flux and microtubule depolymerization at the kinetochore. Briefly, Katanin was proposed to sever microtubules at the kinetochore allowing them to be depolymerized in accordance with the Pac-Man model. Spastin and Fidgetin, on the other hand, were proposed to sever microtubules at the centrosomes allowing the microtubules to be depolymerized in accordance with the Flux model. These data demonstrate how the Flux and Pac-Man models can work together to produce a viable mechanism for chromosome movement during anaphase. Whether they occur independently or together, both the Flux and Pac-Man models propose that microtubules and their associated motor proteins are the force producers for chromosome movement during anaphase.

D.3 Confounding evidence regarding microtubules as force producers

Kinetochore microtubules may not be solely responsible for producing the force that moves chromosomes during anaphase. Pickett-Heaps and Forer (2001) discuss several potential issues with the Pac-Man model which will be discussed here briefly. Firstly, in diatoms, kinetochore microtubules end at an "amorphous 'collar'", as opposed to inserting at the kinetochore, which would be required for the Pac-Man model to

work. Secondly, when whole chromosomes were removed from cells using micromanipulation, the spindles remained and kinetochore fibres still shortened. This suggests that fibre shortening occurs through forces other than those at the kinetochore (Zhang and Nicklas 1996). Thirdly, when single kinetochore fibres were cut with UV microbeam, chromosomes and their associated kinetochore stubs continued moving poleward and sometimes accelerated. This suggests that suggests that microtubules may actually limit the rate at which chromosomes move toward their respective spindle poles. In sum, these data demonstrate that the Pac-Man model, which identifies kinetochore microtubules as the producers of force (Cassimeris *et al.* 1987), does not account for all chromosome movement during anaphase A. In the flux model, kinetochore microtubules exhibit polymerization and depolymerization at the kinetochore and pole, respectively, fluxing tubulin poleward (Wilson *et al.* 1994, LaFountain *et al.* 2004). The model proposes that tubulin flux is responsible for producing the force that moves chromosomes poleward (Rogers *et al.* 2005). However, although microtubule flux occurs along kinetochore fibres during anaphase A, this does not implicate microtubules as the producers of force *per se.* For example, tubulin flux may be driven by an actomyosin mechanism acting on kinetochore fibre microtubules as opposed to being intrinsically

driven or driven by microtubule motor proteins (Silverman-Gavrila and Forer 2000, Forer et al. 2007).

In consideration of the potential problems with the Flux and Pac-Man models, which focus on microtubule-based mechanisms for force production, it is important to consider other likely force producers for chromosome movement. Specifically, actin microfilaments and associated myosin motor proteins.

E. The spindle: Actin and Myosin as force producers

Actin and myosin are parts of the spindle and have been implicated as force producers for chromosome movement. Forer *et al.* (2003) provide a comprehensive review of the reports of actin and myosin in various mitotic and meiotic spindles as well as the effects of anti-actin and anti-myosin drugs on spindle function. Briefly, by 2003, actin had been localized in spindles of twenty-three different organisms through various techniques including fluorescence microscopy of fixed cells, electron microscopy and labelling with heavy meromyosin and fluorescence microscopy of living cells with fluorescently labelled actin or phalloidin. In particular, actin was shown to associate with kinetochore fibres. Myosin had been localized in the spindles of seven different organisms via fluorescence microscopy of fixed cells and fluorescently labelled myosin in living cells. Together, these data indicate that actin and myosin are parts of

the spindle apparatus and that they localize to kinetochore fibres along with microtubules. With respect to actin and myosin function in the spindle, different anti-actin and anti-myosin drugs were shown to perturb several spindle functions. Of particular interest, inhibitory drugs against either actin or myosin altered anaphase chromosome movement as well they blocked tubulin flux along kinetochore fibre microtubules. These results are important because they implicate actin and myosin as force producers for chromosome movement.

In crane-fly primary spermatocytes, actin and myosin contribute to producing the force that moves chromosomes during anaphase. The anti-actin drugs cytochalasin D (CD) and latrunculin (LAT) slow or stop chromosome movement when applied during anaphase (Forer and Pickett-Heaps 1998). These results suggest that actin is involved in poleward chromosome movement. Similar results were observed with the anti-myosin drug 2,3-butanedione 2-monoxime (BDM) (Silverman-Gavrila and Forer 2001). When applied during anaphase, chromosomes slowed, stopped or moved backward and generally resumed movement when BDM was washed out. Additionally, when the myosin inhibitory drugs ML-7 and Y27632 were applied during anaphase, chromosome movement slowed or stopped (Sheykhani *et al.* 2013). Sheykhani et al. (2013) also showed that the kinetochore fibres corresponding to

chromosomes that displayed altered movement showed reduced levels of myosin phosphorylation. This suggests that myosin is involved in anaphase chromosome movement and, in particular, myosin phosphorylation is involved in force production. Conversely, when the myosin enhancer calyculin A (CalA) was added during anaphase, poleward movement accelerated for all bivalent pairs within the same cell (Fabian *et al.* 2007). Lastly, when the actin stabilizing drug jasplakinlide was added during anaphase, chromosome movement was also altered (Xie and Forer 2008). Autosomal bivalents stopped, slowed, had no effect, or very rarely accelerated. Occasionally, movement recovered after stopping while still in jasplakinolide. In general, the autosomal bivalent pairs between cells and within a single cell did not react the same to any of these drugs, with the exception of CalA. This suggests that several force systems are operating in the spindle and that different combinations of these force generators can be used within the same cell. In order to better elucidate the mechanism of force production in the spindle, it is worthwhile investigating whether other proteins that are known to function with actin and myosin are involved.

F. Complementary systems

Actin and myosin are ubiquitous proteins present in several other cytoskeletal systems. Understanding how these proteins are

structured and function in other systems, referred to here as complementary systems, may help to understand how they may be structured and function in the spindle.

F.1 Complementary systems: Actin and myosin in muscle cells

Muscles are force generating tissues that display unique structural and functional properties. Each type of muscle including cardiac, smooth and skeletal or striated muscle, all function using actin and myosin but through somewhat different mechanisms. For the purposes of my thesis, I describe the actomyosin mechanism of force production in striated muscle. The following section will describe the composition, organization and contractile mechanism of striated muscle. Later, I expound upon how tropomyosin, a regulatory muscle protein, may function in other motile systems involving actomyosin based force production.

Striated muscle shows a characteristic banding pattern observed under phase contrast light microscopy and/or electron microscopy. This banding pattern is also observed in cardiac muscle (Moore and Ruska 1957) although it has slight structural and compositional differences. The banding pattern results from alternating bands of birefringence and non-birefringence, known as the A (anisotropic) and I (isotropic) bands respectively

(Huxley and Hanson 1957). Electron microscopy analysis reveals that the I bands contain only thin filaments while the A bands contain a compound array of both thin and thick filaments (Huxley 1953). An H zone is embedded in the center of every A band which contains a simple array of only thick filaments. It is bisected by an M line or midline which represents the center of the repeating unit of the banding pattern. The repeating units, flanked by Z lines, are referred to as sarcomeres and are the functional units of striated muscle (Figure 4).

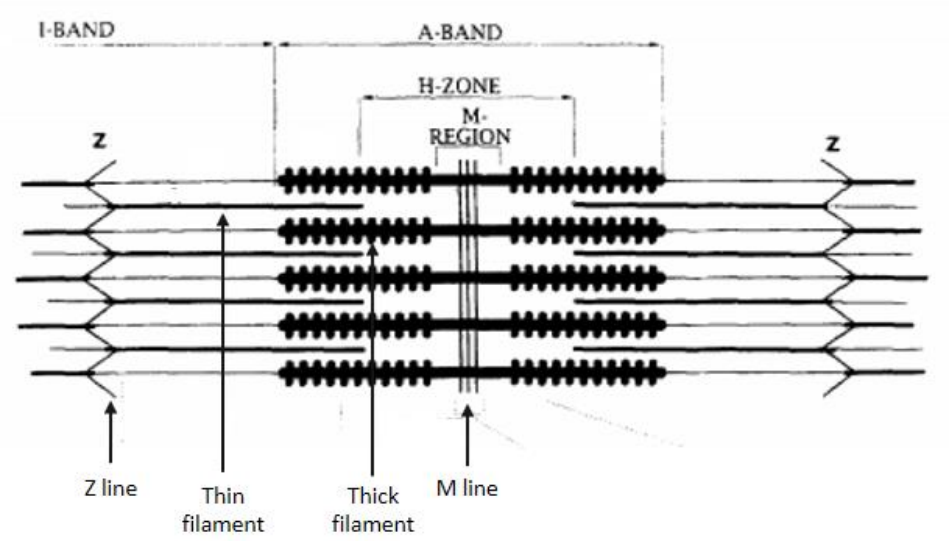

Figure 4 – Schematic of the sarcomere repeat in striated muscle. The I band contains thin filaments, the A band contains thin and thick filaments and the H zone contains only thick filaments. Thin and thick filaments overlap in the A band. The M line (midline) bissects the thick filaments in the center of the H zone. Image modified from Squire (1997). Originally published in *Current Opinion in Structural Biology*. DOI: 10.1016/S0959-440X(97)80033-4.

Muscle cells are able to convert stored chemical energy into useful mechanical work which causes muscular contractions. The sliding filament model is based on the structural arrangement of the sarcomere and describes how the thin and thick filaments work together to produce contractile force (reviewed in Huxley 1969). Briefly, actin-containing thin filaments interact with thick filaments, that are composed of myosin molecules, within the A band where they overlap. This interaction is facilitated by cross-bridges that extend between the filaments and represent the S-1 globular regions of the heavy meromyosin (HMM) heads of myosin molecules. They contain an actin binding site as well as ATPase and ATP receptor sites. The cross-bridges display opposite orientations in either half-sarcomere because they reverse orientation along the thick filaments at the M line (Huxley 1963). The cross-bridge orientation directs force production toward the center of the sarcomere, causing the sarcomere to shorten during contraction.

A common method for determining the structural polarity of actin-containing filaments is to "decorate" the filaments with HMM or the S-1 fragments of HMM (Moore *et al.* 1970, Forer 1974, Forer 1982a). Briefly, HMM or HMM-S-1 will bind to polar actin filaments and form uniformly oriented arrowhead complexes along the lengths of the filaments (Figure 5).

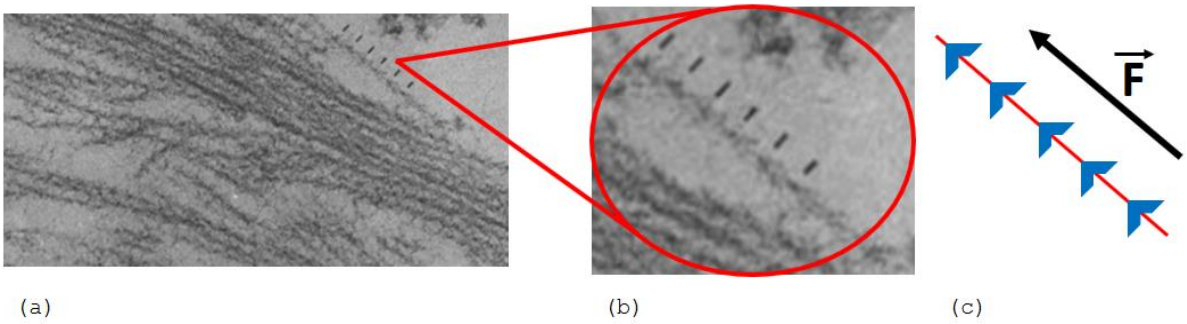

Figure 5 – "Decorated" actin filaments treated with HMM showing arrowhead complexes oriented with definite structural polarity. (a) sectioned myotube treated with HMM. (b) enlarged image of a polar actin filament showing HMM arrowhead complexes. (c) schematic of a polar actin filament with arrowheads all pointed in the direction of force production. Images (a) and (b) modified from Ishikawa *et al.* (1969). Originally published in *The Journal of Cell Biology.*

The arrowheads point in the direction in which the filaments generate force by interacting with myosin (Begg *et al.* 1978). Therefore, arrowheads can give clues to help understand the functional mechanism through which actomyosin interactions generate force. In striated muscle, the arrowhead complexes point toward the M line (Woodrum *et al.* 1975). Determining the polarity of actin-containing filaments can be useful when trying to understand their functional mechanism. Furthermore, actomyosin based motile systems that display similar filament polarity to striated muscle may also share similar functional mechanisms.

Actomyosin based force production in striated muscle is generated by cross-bridge cycling (reviewed in Fitts 2008). Briefly, the cycle begins when myosin ATPase hydrolyses ATP and the HMM heads bind to the actin filaments with weak affinity. The HMM heads then become strongly bound, causing the actomyosin complex to enter a "high force" state. In this state, the HMM heads release inorganic phosphate, which is associated with the power stroke (Kraft *et al.* 2005). During the power stroke, the myosin molecules pivot at the junction between the HMM and LMM chains (Tyska and Warshaw 2002) causing the thin filaments to slide past the thick filaments toward the center of the sarcomere. The HMM heads then release ADP, bind to a new molecule of ATP and dissociate from the actin filaments, allowing the cycle to repeat.

The force generating actomyosin interactions are governed by cofactors and other regulatory proteins. In the absence of calcium ions (Ca^{2+}) actomyosin interactions are inhibited by troponin and tropomyosin which are part of the thin filaments (reviewed in Wakabayashi *et al.* 1975, Figure 6). During a contraction, electrical impulses trigger Ca^{2+} to be released from the sarcoplasmic reticulum into the cytoplasm. The Ca^{2+} binds to troponin C which induces a conformational change and shift in tropomyosin.

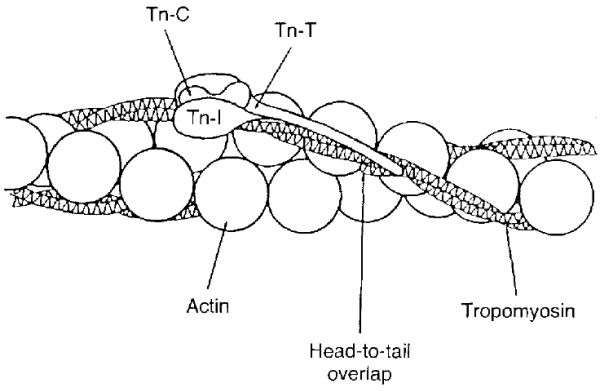

Figure 6 – Schematic representation of the protein arrangement in the thin filaments of striated muscle. The troponin molecule is composed of troponin-C, which binds Ca^{2+}, troponin-T, which binds tropomyosin, and troponin-I, which the inhibitory component of troponin (Hitchcock 1975). Tropomyosin lies in the major groove of the actin filament. Image from Lees-Miller and Helfman (1991). Originally published in *Bioessays*. DOI: 10.1002/bies.950130902.

This shift is exposes the myosin binding sites on actin, allowing myosin to bind actin with strong affinity. The actomyosin complex now enters the "high force" state, myosin releases P_i and the power stroke occurs. Troponin and tropomyosin therefore act as regulators of actomyosin interactions in striated muscle. Troponin is necessary to induce a conformational change in tropomyosin (Wakabayashi *et al.* 1975) and tropomyosin mediates actin-myosin binding affinity. By controlling actomyosin interactions, troponin and tropomyosin regulate force production and are necessary to produce purposeful contractile force. For example, purified actomyosin

is insensitive to Ca^{2+}, remaining in the active state whether Ca^{2+} is present or absent (reviewed in Huxley 1969). With respect to the exact mechanism through which tropomyosin works, recent data suggests that it may act as an allosteric switch as opposed to a steric blocker (reviewed in Gunning *et al.* 2008). In the latter, strong actomyosin interactions are sterically blocked by tropomyosin, until it shifts and permits myosin to bind actin with strong affinity (Bacchiocchi and Lehrer 2002). However, whether the tropomyosin shift actually causes myosin to bind actin with strong affinity has yet to be established and, furthermore, there is no evidence that tropomyosin alone is able to inhibit actomyosin interactions (Patchell *et al.* 2002, Patchell *et al.* 2005). It appears that troponin-I alters actomyosin binding through its interaction with myosin, while tropomyosin enhances this interaction while also regulating the conformation of actin monomers in the filament (see Gunning *et al.* 2005). Therefore, it appears that the role of tropomyosin in striated muscle may be more related to the actin filaments as opposed to myosin binding.

Actomyosin based mechanisms are also responsible for generating contractile force in smooth muscles, although smooth muscle is not arranged in sarcomeres (Huxley 1958) and troponin is not involved. Rather, actomyosin interactions are regulated

by calmodulin and caldesmon (Graceffa 1987). These proteins are parts of the thin filaments, along with actin and tropomyosin, and are regulated by Ca^{2+}. Briefly, calmodulin binds to Ca^{2+}, which causes myosin light chain kinase (MLCK) to phosphorylate and activate the myosin light chain (MLC) subunits embedded in the thick filaments (reviewed in Kamm and Stull 1985). Caldesmon mediates actomyosin binding affinity by inhibiting phosphate release from HMM heads (Alahyan *et al.* 2006). Caldesmon therefore controls the affinity with which actin and myosin bind, permitting or inhibiting muscular contractions. Although the data is not yet solid, tropomyosin is thought to propagate the signal from caldesmon to the actin filaments.

The structural and functional mechanisms of force production in striated and smooth muscle demonstrate that actomyosin interactions responsible for producing contractile force are mediated by tropomyosin and other regulatory proteins. If actomyosin interactions are responsible for producing force in other motile systems, then tropomyosin may also be involved (Huxley 1973). With respect to the spindle, actin and myosin are involved with force production for chromosome movement (reviewed in Forer *et al.* 2003, Sheykhani *et al.* 2013). Furthermore, recent data has shown that another muscle protein, titin, which is responsible for elasticity, colocalizes with microtubules

along kinetochore fibres during metaphase and anaphase in crane-fly and locust spermatocytes (Fabian *et al.* 2007). It is therefore worthwhile investigating whether tropomyosin also plays a role in this system, which is what I did in my thesis research. If tropomyosin functions in the spindle as it does in muscle, then it may serve as a mediator of actomyosin interactions, thereby affecting force production. However, tropomyosin may also function in ways other than mediating actomyosin force production (Lazarides 1976). These will be discussed in the next section.

F.2 Complementary systems: Tropomyosin in non-muscle cells

Since its discovery in muscle (Bailey 1946) tropomyosin has been characterized in various non-muscle cells, demonstrating a diverse array of structural and functional properties. Tropomyosins make up a large family of alpha-helical rod-like dimers whose isoform diversity is generated from multiple genes as well as alternative RNA processing. Vertebrate tropomyosins are encoded by four genes that produce over 40 different isoforms (reviewed in Gunning *et al.* 2005, Schevzov *et al.* 2011). This tropomyosin gene family is thought to have arisen through duplication of an ancestral gene (Lees-Miller and Helfman 1991). Currently, these genes include TMP1 (α-Tm), TPM2 (β-Tm), TPM3 (γ-Tm) and TPM4 (δ-Tm) (Figure 7). Isoform

diversity is generated from sequence divergence amongst alternative exons within the same gene and the same exons in different genes (Schevzov *et al.* 2011). In general, tropomyosin isoforms can be categorized into one of two groups, namely high molecular weight (HMW) and low molecular weight (LMW) tropomyosins. HMW tropomyosins are made up of 281-284 amino acid residues and contain the 1a and either the 2a or 2b exons, while LMW tropomyosins are made up of 245-251 amino acid residues and contain the 1b exon (Schevzov *et al.* 2011). Typically, muscle tropomyosins, including α and β tropomyosins, belong to the HMW group and are encoded by TPM1 and TPM2 respectively. Non-muscle tropomyosins show greater isoform diversity (Pittenger *et al.* 1994).

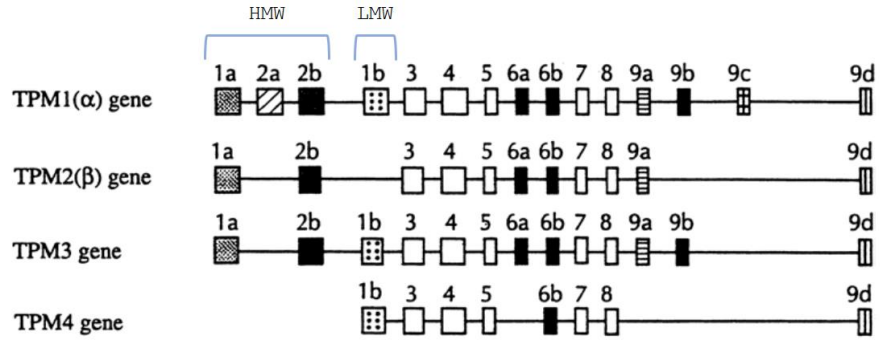

Figure 7 – Intron-exon organization of the mammalian tropomyosin genes. TPM1 (α) and TPM2 (β) correspond to the muscle tropomyosins α and β, and TPM3 (also known as γ-Tm) and TPM4 (also known as δ-Tm) correspond to non-muscle tropomyosins. HMW tropomyosins include the 1a and either the 2a or 2b exons, while LMW tropomyosins include the 1b exon. Image modified from Perry (2001). Originally published in *Journal of Muscle Research and Cell Motility*. DOI: 10.1023/A:1010303732441.

Tropomyosin isoforms display unique functional properties and their expression is both spatially and temporally regulated. Firstly, tropomyosin isoforms are tissue specific (reviewed in Gunning *et al.* 2005). For example, various mouse-derived tissues show differential isoform expression profiles observed via isoform-specific antibodies (Schevzov *et al.* 2005). Secondly, tropomyosin isoforms are expressed during specific developmental periods (reviewed in Gunning *et al.* 2008). For example, the digestive tissues of chicken display either different isoform specificity or quantitatively different isoform compositions between embryonic and adult tissues (Xie *et al.* 1991). These data suggest that tropomyosin isoforms perform specific functions and that their expression is highly regulated. Other organisms such as yeast and *Drosophila* contain fewer tropomyosin encoding genes. Yeast contains two tropomyosin genes, namely TPM1 and TPM2, whose gene products are structurally and functionally distinct (Drees *et al.* 1995). *Drosophila* also contains two tropomyosin genes that encode all of the muscle and non-muscle tropomyosin isoforms (Karlik and Fyrberg 1986).

In the cytoskeletons of non-muscle cells, tropomyosins serve various functions associated with the actin filaments to which they are bound. Tropomyosin molecules lie head-to-tail along the major groove of polar actin filaments with each

molecule spanning approximately 6-7 actin monomers (Gunning *et al.* 2005). Many of the functions conferred by tropomyosin are attributed to the nature of this binding. Specifically, tropomyosin-bound actin filaments display altered stability, polymerization and actin-binding protein interactions.

Tropomyosin provides stability to actin filaments and alters actin filament polymerization and branching (reviewed in Cooper 2002). LMW non-muscle tropomyosin isoforms, for example, slow depolymerization at the pointed ends of actin filaments, possibly through the binding interaction between tropomyosin and actin (Broschat *et al.* 1989). In yeast, genetic experiments have indicated that tropomyosin provides actin filament stability (Liu and Bretscher 1989). Briefly, cytoplasmic actin cables containing tropomyosin were more prominent in TPM1 overexpression mutants while they disappeared in TPM1 disruption mutants. On the other hand, actin structures that did not contain tropomyosin were unaffected. Furthermore, temperature sensitive mutants in which tropomyosin function was diminished and then enhanced showed a corresponding disappearance and reappearance of the actin cables. These results are consistent with the idea that tropomyosin confers actin filament stability. Tropomyosin also affects actin filament branching by the Arp2/3 complex (Blanchoin *et al.* 2001). Briefly, the LMW cytoskeletal

tropomyosin, Tm5a, reduced the frequency of actin filament branching by the Arp2/3 complex, although it did not completely inhibit branching. In addition, the LMW tropomyosin inhibited branching more frequently than either of two HMW tropomyosins, suggesting that branch inhibition by tropomyosin is isoform specific. Although the mechanism was not determined, tropomyosin was thought to inhibit branching by binding actin filaments and potentially blocking Arp2/3 binding. Tropomyosin also alters barbed-end dynamics of actin filaments (Wawro *et al.* 2007). Different formin proteins were shown to inhibit barbed-end elongation of actin filaments. However, three tropomyosin isoforms, including Tm5a, were able to relieve this inhibition in an isoform-specific manner. These results suggest that tropomyosins and formin proteins function antagonistically at the barbed-ends of actin filaments. As well, they demonstrate the isoform specificity of different tropomyosins and their functions. Lastly, tropomyosins can promote stress fibre formation by recruiting myosin II into stress fibres (Bryce *et al.* 2003). Specifically, incorporation of the LMW cytoskeletal tropomyosin Tm5NM1 recruited myosin heavy chain IIA and phosphorylated myosin light chain into the stress fibres, which supports active contractility of these stress fibres. Overall, tropomyosins play several roles in the cytoskeletons of non-

muscle cells. These roles predominately involve altering actin filament stability and dynamics which have implications for microfilament functioning. Tropomyosin may play similar roles in the spindle and alter spindle actin dynamics relating to stability, polymerization or actin-binding protein interactions.

G. Tropomyosin inhibition

Tropomyosin can be inhibited by upstream kinase inhibition or by direct binding inhibition. In general, successful tropomyosin inhibition results in the loss of actin filament integrity in cytoskeletal systems. Two anti-tropomyosin drugs, PD 098059 (PD) (Houle *et al.* 2003, Houle *et al.* 2007) and TR100 (Stehn *et al.* 2013), act through entirely different mechanisms but they both ultimately (after several hours) result in degraded F-actin organization. These drugs will be discussed in the following section.

G.1 Upstream kinase inhibition of tropomyosin

PD is a synthetic, non-competitive inhibitor that specifically inhibits the activation and phosphorylation of inactive MAPKK (Alessi *et al.* 1995, Figure 8). A series of experiments (Alessi *et al.* 1995) showed that PD inhibits the inactive form of MAPKK and, furthermore, it prevents MAPKK activation and phosphorylation by the MAPKK kinases, c-Raf or MEK kinase. PD

was also tested against several other protein kinases including MLCK and the results suggest that this drug does not significantly lower their activity. The activity of these serine/threonine kinases following treatment with PD ranged from 87±5 - 109±7 % of control activity, with MLCK functioning at 88±2 % activity (Alessi *et al.* 1995). For comparison, MAPKK activity following PD treatment was lower than 20% of control activity. Taken together these data suggest that PD is specific for MAPKK and that kinases in other phosphorylation pathways are less affected or even unaffected.

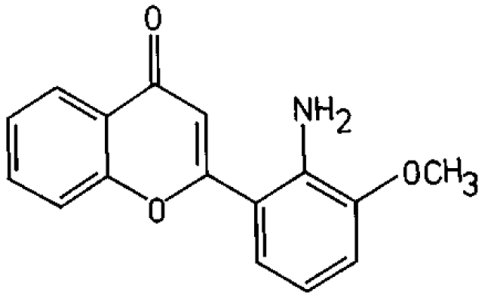

Figure 8 – Structure of PD 098059 (PD) (2′-amino-3′-methoxyflavone). PD inhibits inactive MAPKK which prevents downstream phosphorylation of tropomyosin. Image from Alessi *et al.* (1995). Originally published in *Journal Biological Chemistry*. DOI: 10.1074/jbc.270.46.27489.

Investigations into the effects of PD on actin filament organization have shown that PD disrupts proper F-actin formation by inhibiting MAPKK, which has the downstream effect of preventing tropomyosin phosphorylation (Houle *et al.* 2003,

Houle *et al.* 2007). Tropomyosin is not phosphorylated by either Phosphorylase kinase or Protein kinase A (reviewed in Perry 2001). However, tropomyosin 1 is phosphorylated by DAP kinase-I (Houle *et al.* 2007) downstream of ERK (MAPK) (*Houle et al.* 2003, Figure 9). Briefly, H_2O_2 promotes F-actin assembly into stress fibres in non-muscle cells. PD treatment inhibits H_2O_2 induced stress fibre formation and promotes membrane blebbing and focal adhesion missassembly which are associated with actin filaments. Tropomyosin 1, a HMW cytoskeletal TPM2 gene product (Schevzov *et al.* 2011) was shown to be phosphorylated after exposure to H_2O_2 but not in the presence of PD. These results demonstrate that tropomyosin 1 phosphorylation is necessary for F-actin to assemble into stress fibres and to display proper function. However, PD inhibits tropomyosin 1 phosphorylation which prevents F-actin assembly into stress fibres and impairs actin filament function.

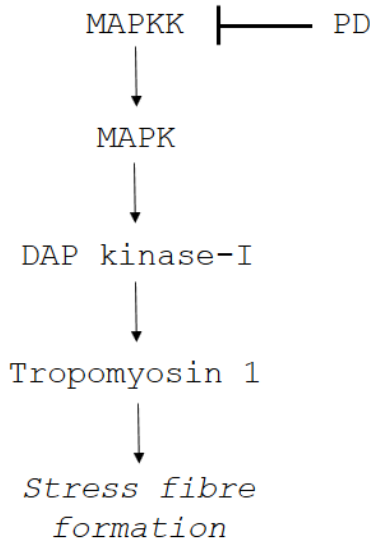

Figure 9 – Sequence of events leading to tropomyosin 1 phosphorylation by DAP kinase-I in the MAPKK pathway. PD inhibits MAPKK which prevents tropomyosin 1 phosphorylation. Tropomyosin 1 phosphorylation is required for F-actin to assemble into stress fibres. Schematic derived from data in Houle *et al.* (2003) and Houle *et al.* (2007).

G.2 Direct binding inhibition of tropomyosin

Tropomyosin can also be inhibited directly, by the anti-tropomyosin drug TR100 (Figure 10). Briefly, TR100 was identified in a screen against the tropomyosin isoforms Tm5NM1/2, that were shown to be the most abundant isoforms present in tumor cells and potentially necessary for tumor cell survival (Stehn *et al.* 2013). The screen was conducted by showing that, firstly, F-actin depolymerization (as a ratio of G:F actin) decreased with increasing Tm5NM1/2 saturation and, secondly, TR100 negates the ability of Tm5NM1/2 to confer F-

actin stability. F-actin and Tm5NM1/2-coated F-actin, treated with TR100, showed similar rates of depolymerization. These results demonstrate that tropomyosin promotes actin stability and that directly inhibiting tropomyosin with TR100 reduces this stability. The effects of TR100 were shown to be dose dependent and most robust for Tm5NM1/2 containing actin filaments. However, TR100 works by binding to the 9d exon sequence of tropomyosins, at the protein level, and this sequence is present in other tropomyosin isoforms (Schevzov *et al.* 2011). Therefore, while TR100 shows selectivity for Tm5NM1/2, it can affect other tropomyosins as well. Indeed, while TR100 showed an initial preferential loss for Tm5NM1/2 containing F-actin, actin filaments containing other LMW and HMW tropomyosins were also unable to bundle into stress fibres at higher concentrations of TR100 or for longer incubation periods. In general, these results were observed after 24-hour incubation periods. Overall, this suggests that TR100 has the potential to inhibit various tropomyosins expressing the 9d exon sequence and that this inhibition results in actin filament disorganization and improper F-actin functioning.

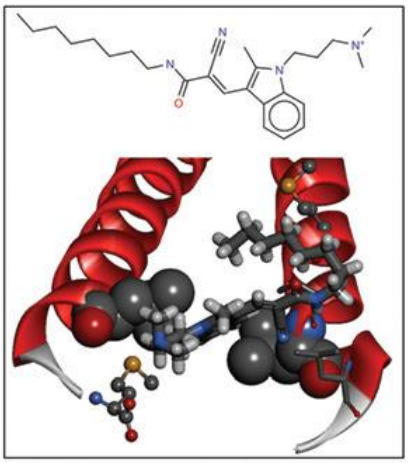

Figure 10 – Structure of TR100 and predicted modelling for interaction with 9d exon sequence of tropomyosin. Image from Stehn *et al.* (2011). Originally published in *Cancer Research*. DOI: 10.1158/0008-5472.CAN-12-4501.

Tropomyosin can therefore be inhibited in two ways, by preventing its phosphorylation with PD or by directly binding it with TR100. Both anti-tropomyosin drugs affect tropomyosin-bound actin filaments and result in improper F-actin functioning, actin filament disorganization and a loss of F-actin stability. Actin filaments are affected because tropomyosin is inhibited. With respect to TR100, it was not shown whether actin filaments free of tropomyosin were affected by this drug (Stehn *et al.* 2013). However, due to the binding of TR100 with tropomyosin, it is presumed that actin filament disorganization occurs because tropomyosin is inhibited. Within the spindle, actin localizes to kinetochore fibres where it contributes force production for chromosome movement during anaphase. If tropomyosin is present

in the spindle, inhibiting it with either PD or TR100 may affect spindle actin and therefore affect chromosome movement during anaphase or other actin associated functions in the spindle.

H. Tropomyosin in the spindle

Tropomyosin has recently been localized in the mitotic spindle of *Drosophila* S2 cells (Goins and Mullins 2015). Briefly, these cells expressed three cytoskeletal tropomyosin isoforms including the isoform Tm1J, which is a HMW TPM1 gene product (Schevzov *et al.* 2011). Successfully transformed cells expressing eGFP-TM1J, showed Tm1J localization to specific regions of the mitotic spindle (Figure 11). Briefly, Tm1J localized to centrosomes during prophase and throughout metaphase. It also localized to kinetochores during metaphase and through early anaphase, where it remained as kinetochores moved poleward. During mid to late anaphase, Tm1J localized to the spindle midzone and central spindle areas. Although this was not discussed by the authors, faint outlines of the spindle and kinetochore fibres could also be seen in some images.

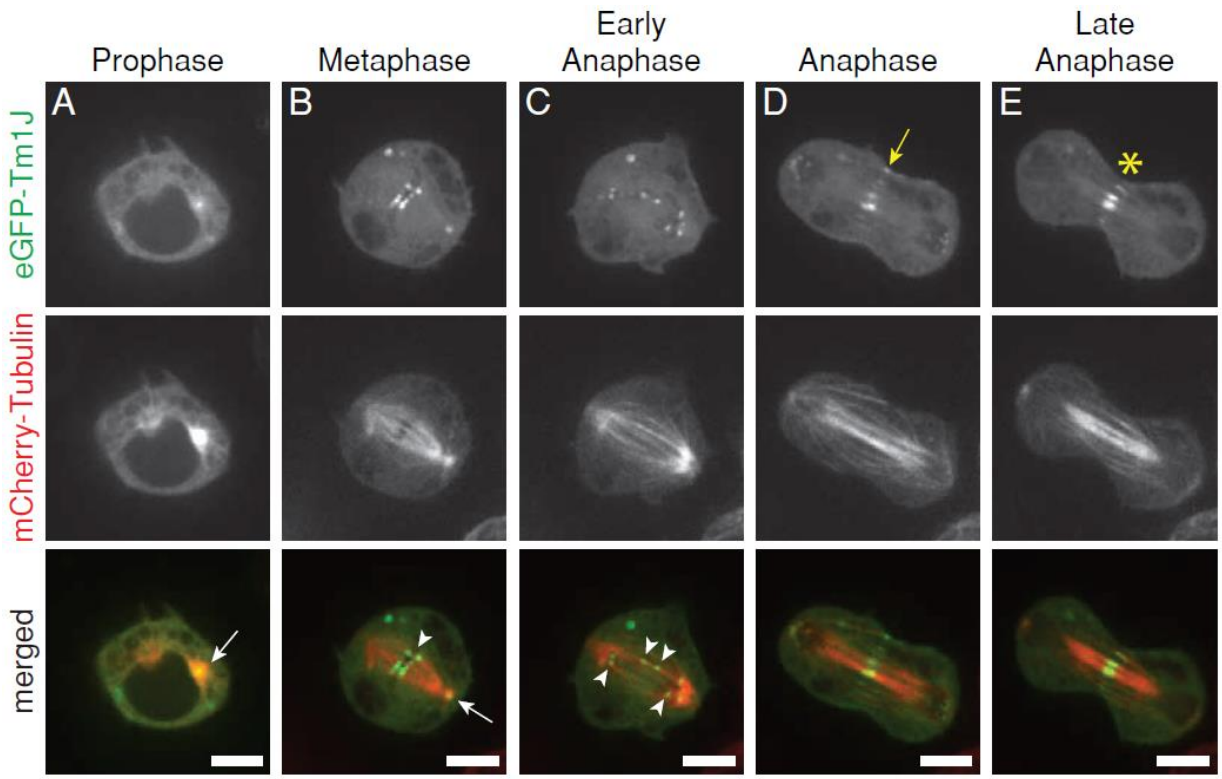

Figure 11 – Tropomyosin localization to the spindle in *Drosophila* S2 cells during mitosis. Tropomyosin Tm1J localizes to centrosomes (white arrow) and kinetochores (white arrow heads) during metaphase and remains at the kinetochores during early anaphase. In later anaphase, Tm1J localizes to the spindle midzone (yellow arrow) and central spindle (yellow arrow) areas. Image from Goins and Mullins (2015). Originally published in *Molecular Biology of the Cell*. DOI: 10.1091/mbc.E14-12-1619.

In trying to elucidate the functional mechanism of Tm1J, two mutant proteins were generated to test whether troponin or phosphorylation are involved. Firstly, two residues were mutated in the putative troponin-T binding site. These mutants had similar localization of wild-type expressing cells; however, they had abnormal mitoses with kinetochore attachment defects,

unfocused spindle poles, delayed anaphase progression and missegregated chromosomes. Secondly, mutating the phosphorylation site on Tm1J, so that it could no longer be phosphorylated, did not affect Tm1J localization or proper spindle functioning. Together, these data suggest that tropomyosin localizes to the spindle, in particular to centrosomes and kinetochores during metaphase through early anaphase, and that it may function through a mechanism involving troponin.

I. Crane-fly spermatocytes provide an excellent model for studying meiotic processes and cytoskeletal components

Crane-fly (*Nephrotoma suturalis* (Loew)) primary spermatocytes provide an excellent model for studying the spindle and for illustrating chromosome movement. There are several reasons for choosing crane-flies to study the events of meiosis (Forer 1982b) and these will be discussed here briefly. Firstly, crane-flies can be easily reared in lab and cells can be obtained from suitable animals at any time throughout the year. Secondly, the cells within a single testis are synchronous, meaning that they enter the same divisional stage at more or less the same time. This is beneficial for studying the spindles at particular stages of division such as metaphase or anaphase. Thirdly, because there are small numbers of chromosomes, movements of

individual chromosomes can be easily followed throughout division under phase-contrast light microscopy.

Primary spermatocytes are obtained from the testes of fourth-instar male larvae. The cells are comprised of three autosomal bivalents and two univalent sex chromosomes that undergo a reductional meiosis-I division (Forer 1980). The anaphase movements of the bivalents and univalents occur sequentially. During anaphase A, autosomal bivalents separate and move toward their respective spindle poles as spindle fibres shorten. During anaphase B, the spindle elongates and each of the sex-chromosome univalents moves toward a spindle pole (Yin and Forer 1996). The sex chromosomes exhibit amphitelic orientation, with kinetochore fibres extending to each pole, and display distance segregation, meaning that they are unpaired and unconnected and yet separate to opposite spindle poles (Forer *et al.* 2013). Several distinct measurements including kinetochore-to-pole, kinetochore-to-equator, inter-kinetochore and inter-polar distances can be plotted as functions of time. Therefore, chromosome movement can be well characterized. In addition, various experiments have been performed in crane-fly primary spermatocytes which have helped to elucidate the mechanisms of chromosome movement. For example, actin and myosin have been implicated as force producers for chromosome movement in crane-

fly primary spermatocytes (reviewed in Forer *et al.* 2003). Therefore, these cells provide a good model for investigating other actomyosin associated proteins, such as tropomyosin. To my knowledge, no prior attempts have been made to localize or test the possible roles of tropomyosin during anaphase chromosome movement.

Possible Roles for Tropomyosin During Anaphase Chromosome Movement

Introduction

The mitotic or meiotic spindle assembles during cell division in order to partition replicated or homologous chromosomes of a single cell into two daughter cells (Gadde and Heald 2004). Ensuring the proper segregation of genetic material is essential for producing viable daughter cells that contain the correct type and amount of DNA needed to carry out their functions. Understanding the mechanisms involved in chromosome movement during cell division contributes to understanding how genetic material is properly distributed into two daughter cells.

Microtubules are the major structural components of the spindle. Since their discovery in kinetochore fibres, many functional models have proposed that microtubules, along with microtubule associate proteins, produce the force for chromosome movement (Forer *et al.* 2003). Currently, the Flux and the Pac-Man models are the most commonly described mechanisms of force production for chromosome movement. These models differ with respect to how microtubules produce force; however, they both propose that microtubules and their motor proteins alone are responsible for moving chromosomes (e.g. Cassimeris *et al.* 1987, Mitchison 1988, Sharp *et al.* 2000, Rogers 2005). In general, these models suggest that microtubule depolymerization at the

pole (the Flux model) or at the kinetochore (the Pac-Man model) generate the force that moves chromosomes during cell division.

However, other functional proteins, such as actin and myosin, have also been identified in the spindle and they have been implicated as force producers for chromosome movement. Actin and myosin are structural components of both mitotic and meiotic spindles (reviewed in Forer *et al.* 2003, Sheykhani *et al.* 2013). In particular, these proteins, as well as the muscle protein titin (Fabian *et al.* 2007), are present along the kinetochore fibres where they colocalize with microtubules and are involved in chromosome movement during anaphase. For example, anti-actin drugs such as cytochalasin D (CD) and latrunculin (Lat) as well as anti-myosin drugs such as 2,3-butanedione 2-monoxime (BDM) and ML-7 have all been shown to slow or stop chromosome movement when added during anaphase (Forer and Pickett-Heaps 1998, Silverman-Gavrila and Forer 2001, Xie and Forer 2008, Sheykhani *et al.* 2013). This suggests that actin and myosin contribute to producing the force that moves chromosomes during anaphase. The mechanism through which spindle actin and myosin produce force has yet to be determined. In order to elucidate how actin and myosin may function in the spindle, it is helpful to understand how these proteins function in other cytoskeletal systems.

Actin and myosin produce contractile force in muscle cells (Huxley 1969). Briefly, actin filaments slide past myosin filaments by cross-bridge cycling which generates the force that causes muscles to contract. In striated muscle, the actomyosin interactions are regulated by tropomyosin and troponin (reviewed in Squire 1997). By binding along actin filaments, tropomyosin mediates the actomyosin interactions and thereby mediates force production. Tropomyosin also binds along actin filaments in non-muscle cells where it confers structural and functional properties to actin filaments (reviewed in Cooper 2002, Gunning *et al.* 2015). In non-muscle cells, tropomyosin provides actin filament stability, alters actin filament polymerization and regulates actin-binding protein interactions. For example, tropomyosin localizes to the leading edges of lamellipodia where it is proposed to alter actin-binding protein interactions and thereby regulate actin filament polymerization (Hillberg *et al.* 2006). In yeast, tropomyosin is associated with actin filament stability and genetic manipulation studies have shown that actin requires tropomyosin to form actin cables (Liu and Bretscher 1989). Generally, tropomyosin is thought to confer these functions to actin filaments through the nature in which it binds along the actin filaments. In consideration that tropomyosin plays a role in both muscle and non-muscle cells,

where it is associated with actin filaments, it is worthwhile investigating whether tropomyosin is also involved in the spindle.

A recent study has shown that tropomyosin localizes to the spindle of *Drosophila* S2 cells (Goins and Mullins 2015). An isoform of tropomyosin, known as Tm1J, was observed predominantly at the centrosomes and at the kinetochores during metaphase and early anaphase, as well as at the central spindle and mid-body during late anaphase. These data are evidence that tropomyosin localizes to the spindle. Furthermore, when putative troponin binding sites on tropomyosin were mutated, cells displayed abnormal mitoses, with respect to chromosome division. This suggests that tropomyosin may function in the spindle through a tropomyosin-troponin mechanism similar to striated muscle. However, the exact functional mechanism of spindle tropomyosin has not been determined and whether tropomyosin is present in other spindles has not been investigated.

The purpose of my thesis was to test the possible roles of tropomyosin during anaphase chromosome movement in crane-fly primary spermatocytes. Actin and myosin are involved in anaphase chromosome movement in these cells; therefore, they provide good models to investigate tropomyosin. The objectives of my research were to localize spindle tropomyosin and test whether it plays a

role during anaphase chromosome movement. Briefly, this was accomplished by treating live cells with inhibitory drugs against tropomyosin as well as by staining for tropomyosin at various stages of cell division. Two inhibitory drugs against tropomyosin were tested. Firstly, cells were treated with PD 098059 (PD). PD is a selective inhibitor against MAPKK, which prevents the downstream phosphorylation of tropomyosin (Houle *et al.* 2013, Houle *et al.* 2007). Cells were also treated with TR100. TR100 is a selective inhibitor against tropomyosin, that binds directly to different tropomyosin isoforms containing the 9d exon sequence (Schevzov *et al.* 2011, Stehn *et al.* 2013). Tropomyosin inhibition by either PD or TR100, generally after incubation periods of one hour, result in disrupted actin filament organization and degraded actin filament function. Two different antibodies were used to stain for tropomyosin, since the isoform specificity of spindle tropomyosin was not known. TM311 is specific for the 1a exon sequence of high molecular weight tropomyosins (Schevzov *et al.* 2011) and shares antigen sequence homology with *Drosophila* tropomyosins. TM311 binds to tropomyosin in the spindles of *Drosophila* S2 cells (Goins and Mullens 2015). TM5NM1/2 is specific for the 9d exon sequence of low molecular tropomyosins (Schevzov *et al.* 2011). TR100 and TM5NM1/2 may share antigen specificity. Briefly, PD altered

movement in approximately 70% of the chromosomes followed during anaphase while TR100 altered movement in approximately 33% of the chromosomes followed during anaphase. Tropomyosin was also observed at the centrosomes and along the kinetochore fibres with both TM311 and TM5NM1/2. Overall, the results suggest that tropomyosin localizes to the meiotic spindle of crane-fly primary spermatocytes where it may serve functional roles during anaphase chromosome movement.

Future experiments should investigate the levels of tropomyosin phosphorylation along kinetochore fibres as well as treating cells prior to anaphase onset. For example, it would be worthwhile to test the level of tropomyosin phosphorylation following PD treatment, to see whether chromosome movement is altered when phosphorylation levels are reduced. Furthermore, treating cells prior to anaphase onset may allow more time for the drugs, specifically TR100, to permeate the cell and inhibit tropomyosin along the kinetochore fibres. There is indication from other cytoskeletal effects of TR100 that suggest the drug may take a few minutes to affect actin-containing filaments in crane-fly primary spermatocytes. Treating cells prior to anaphase onset may allow more time for the drug to inhibit tropomyosin along kinetochore fibres before chromosomes reach the spindle poles.

Materials and Methods

Crane fly stock

Crane flies (*Nephrotoma suturalis* (Loew)) were reared in lab according to the methods described in Forer (1982b). Briefly, adult crane flies were kept in a Plexiglass cage where they copulated. Females laid their eggs onto small plastic petri dish bottoms lined with moist papier-mâché which were collected every 3-4 days. Lightly toasted nettle leaves were pulverized by hand into a fine powder and sprinkled onto the papier-mâché with the eggs. The petri dishes were then covered with lids. Larvae hatched approximately 6-8 days later. They were kept in the small petri dishes for approximately 9-10 days before being transferred to larger petri dishes. Larvae were fed with toasted nettle leaves every 3-4 days. Pupae began to appear approximately one month after hatching. They were collected, rinsed with water and transferred to a crystallizing dish lined with moist papier-mâché which was placed in the Plexiglass cage. Adults emerged approximately 5-6 days later. Pupae dehydrated and died if the papier-mâché was not kept moist.

Larval selection

Fourth-instar male larvae were chosen for dissections. Male and female larvae have no external features to distinguish them

(Forer 1982b) so males could not be chosen with complete accuracy. However, within any given dish, males tended to be shorter and/or thinner than females, so they could be chosen with reasonable accuracy. Fourth-instar males were chosen based on fat-body content, which is a good indicator of developmental stage (Forer 1982b). I found that testes with the greatest number of dividing spermatocytes came from fourth-instar males whose body fat was opaque and disguised almost all of the digestive tract.

Solutions

Insect Ringer's solution [0.13 M NaCl, 5 mM KCl, 1.5 mM $CaCl_2$ and 3 mM buffer (KH_2PO_4 and $Na_2HPO_4 \cdot 7H_2O$, pH 6.8); final pH 6.8] was used at room temperature. This Ringer's solution was originally made for *Drosophila* (Ephrussi and Beadle 1936) but is used for crane-flies with the addition of buffer. It was stored in the refrigerator and prepared every few weeks from 10X and 20X stock solutions which were all kept frozen. Fibrinogen solution was prepared daily by dissolving bovine fibrinogen (MP Biomedicals, LLC) in Insect Ringer's (10 mg: 1 mL). Thrombin solution was prepared by dissolving thrombin (Sigma) in Insect Ringer's at a concentration of 100 units per 2 mL stored in aliquots of approximately 70 µL at -80˚C. One aliquot was used for a few weeks, during this time it would be stored at -4˚C after use.

Prior to use, the aliquot was allowed to thaw and, like the fibrinogen solution, it was kept on the work bench and used at room temperature. PD 098059 (PD) (LC Laboratories) was dissolved in dimethyl sulfoxide (DMSO) at a concentration of 85 mM and stored in aliquots of 3 µL and 6 µL at -30˚C. Prior to use, an aliquot of PD was allowed to thaw and then diluted in 5 mL of IR to give final concentrations of 50 µM (from 3 µL) or 100 µM (from 6 µL). TR100 (Sigma) was dissolved in DMSO at a concentration of 10 mM and stored at -4˚C. Prior to use, different volumes ranging from 12 µL to 50 µL were diluted in 5 mL of IR to give final concentrations ranging from 25 µM to 100 µM. Phosphate buffered saline (PBS) 10X stock [1.31 M NaCl, 0.051 M Na_2HPO_4, 0.016 M KH_2PO_4; final pH 7.0] was made every few weeks and stored in the refrigerator. Before use, PBS was diluted in ddH_2O to 1X concentration.

Live cell preparations

Living primary spermatocytes were obtained from crane flies as described in Forer and Picket-Heaps (1998). Briefly, testes were dissected out of fourth-instar male larvae and placed under Halocarbon oil. An individual testis was then rinsed in three drops of Insect Ringer's that were placed on a plastic petri dish lid. In the last drop of Insect Ringer's, any remaining fat attached to the testis was removed with stainless steel

forceps. A drop of approximately 2-3 µL of fibrinogen solution was placed on a flamed coverslip and the testis was transferred to the drop of fibrinogen, pierced with a stainless-steel needle and the cells that emerged were spread around the coverslip so that the cells were evenly distributed. Shortly after, an equal volume of thrombin solution was spread over the fibrinogen and a fibrin clot was allowed to form for about 20 seconds under a petri dish lid to prevent evaporation. The coverslip was then inverted onto a stainless-steel perfusion chamber that was filled with Insect Ringer's and the chamber was sealed with a molten mixture of 1:1:1 Vaseline, lanolin and paraffin. The perfusion chamber was connected to input and output tubes which allowed solutions of Insect Ringer's, DMSO or diluted drugs to be perfused through.

Phase-contrast light microscopy and data analysis

Prometaphase-I or metaphase-I cells were chosen. Stage was determined by the chromosome shape and alignment, as well as the spindle shape. As cells approached anaphase, chromosomes aligned at the equator and the spindle became outlined by highly refractive mitochondria. A few minutes after anaphase onset, as separating half-bivalents moved toward opposite spindle poles, a solution containing diluted PD or TR100 or an equal volume of DMSO was perfused into the chamber and bathed all of the cells

held in the fibrin clot. The highest concentration of DMSO was 0.5%. Control cells were perfused regularly with Insect Ringer's.

Cells were observed and recorded with phase-contrast light microscopy using a Nikon 100x oil immersion objective (NA, 1.3). Images were recorded on DVD discs in real time and time-lapsed avi files were generated with VirtualDub freeware (www.virtualdub.org). Kinetochore-to-pole, kinetochore-to-equator and interkinetochore distances were measured using Winimage software and movement graphs were generated by plotting the distances versus time (SlideWrite).

Lysing and fixation

The lysing, fixing and staining procedures were based on those described by Fabian and Forer (2005). Briefly, cells that were recorded during anaphase were lysed [100 mM piperazineN,N-bis(2-ethanesulfonic acid) [PIPES], 10 mM EGTA, 5mM $MgSO_4$, NP40 2%, DMSO 5%] and then fixed with 0.2% glutaraldehyde in PBS. Cells were lysed by perfusing lysis buffer into the chamber and then removing and submerging the coverslip in more lysis buffer or by directly removing and submerging the coverslip in lysis buffer from the perfusion chamber. After variable amounts of time in lysis buffer (between approximately 20-60 minutes) the cells

were then fixed for 6 minutes [0.2% glutaraldehyde in PBS], washed in PBS (three times for 5 minutes each), kept for 10 minutes in sodium borohydride [1mg/ml in PBS] and then washed in PBS (once quickly and then twice for 5 minutes each). The fixed preps were then stored at 4˚C in PBS-glycerol 1:1 (v/v) until they were ready to be stained.

Antibody staining

Preps were double stained for tubulin and tropomyosin. The best results were obtained when tropomyosin was stained first. Microtubules were stained with YL ½ rat monoclonal antibody against tubulin (1:100) (Invitrogen) followed by Alexa 594 goat-anti-rat immunoglobulin IgG (1:200) (Invitrogen). Tropomyosin was stained with TM311 mouse monoclonal antibody against tropomyosin (1:200, 1:100 or 1:50) (Abcam Canada) followed by Alexa 488 goat-anti-mouse immunoglobulin IgM (1:150 or 1:100) (Invitrogen). TM311 is specific for the 1a exon sequence of high molecular weight tropomyosins (Schevzov *et al.* 2011) which shares sequence homology with *Drosophila* isoforms (amino acid sequence of antibody immunogen: LDKENALDRAEQAEADKKAA). Tropomyosin was also stained with TM5NM1/2 sheep polyclonal antibody against tropomyosin (1:100 or 1:50) (EDM Millipore) followed by reconstituted Alexa 488 donkey-anti-sheep immunoglobulin IgG (H&L) (1:50 or 1:100) (Cedarlane: Novus

Biologicals). TM5NM1/2 is specific for the 9d exon sequence of low molecular tropomyosins (Schevzov *et al.* 2011). All antibodies were diluted in PBS. The incubation time for each antibody was 1 hour at room-temperature, except for primary antibodies against tropomyosin which were incubated for 2 hours. Prior to adding an antibody, preps were washed with 0.1% Triton X-100 to facilitate flow. Preparations were kept in the dark during the incubation periods to prevent light inactivation of the fluorochromes. Coverslips were mounted in Mowiol (Calbiochem) solution (Osborn and Weber 1982) containing paraphenylene diamine as antifading agent (Fabian and Forer 2005), and stored at 4 °C in the dark until viewed in the confocal microscope.

Some preps were also triple stained for tubulin, actin and tropomyosin. Microtubules were stained with YL ½ rat monoclonal antibody against tubulin (1:100) (Invitrogen) followed by Alexa 633 goat-anti-rat immunoglobulin IgG (1:200) (Invitrogen). Actin was stained with 0.43 µM or 0.66 uM Alexa 568 phalloidin (Invitrogen). Tropomyosin was stained with TM311 mouse monoclonal antibody against tropomyosin (1:100 or 1:50) (Abcam Canada) followed by Alexa 488 goat-anti-mouse immunoglobulin IgM (1:150 or 1:100) (Invitrogen). Tropomyosin was also stained with TM5NM1/2 sheep polyclonal antibody against tropomyosin (1:100 or

1:50) (EDM Millipore) followed by reconstituted Alexa 488 donkey-anti-sheep immunoglobulin IgG (H&L) (1:50 or 1:100) (Cedarlane: Novus Biologicals). The same staining procedure was followed for triple staining as it was for double staining, except that preps were incubated with phalloidin for 1 hour after staining for tubulin and tropomyosin.

Confocal microscopy and image processing

Cells were observed with different confocal microscopes. Firstly, the Olympus Fluoview 300 confocal microscope, with argon laser at 488 nm and HeNe laser at 543 and 660 nm, using an Olympus Plan Apo 60X oil immersion objective (NA, 1.4). Secondly, the LSM 700 Zeiss Observer Z.1 confocal microscope, with lines at 488, 555 and 639, using a Zeiss EC Plan-NEOFLUAE 40X oil immersion objective (NA, 1.3). Lastly, some images were collected on an Olympus Fluoview 3000 confocal microscope using a 60X oil immersion objective (NA, 1.35) which was temporarily available at York University (Toronto, Canada). The images were further processed using Image J software (available at http://rsb.info.nih.gov/ij/).

Triple stained images have not been included because we were unable to resolve issues with the LSM 700 Zeiss Observer Z.1 confocal microscope. Negative controls showed images in

channels for which there were no fluorescent antibodies or phalloidin. For example, images appeared in the Alexa 568 channel when no Alexa 568 phalloidin had been added. This cannot be explained by secondary antibody cross reaction. I sought help from different confocal microscope technicians but was unable to solve the problem. Therefore, only double stained images have been included.

Results

Control divisions

Crane-fly primary spermatocytes have three autosomal bivalents and two univalent sex chromosomes (Forer 1980, Forer 1982b, Yin and Forer 1996). During anaphase-I, the autosomal bivalents separate into two half-bivalents that move toward opposite spindle poles as their kinetochore fibres shorten. Once the autosomal half-bivalents reach the spindle poles, the sex-chromosome univalents move toward opposite spindle poles as the spindle elongates. My experiments focused on autosomal half-bivalent movement.

Chromosome movement was analyzed by plotting the kinetochore to pole or kinetochore to equator distances over time (Figure 12) or the interkinetochore distance over time (Figure 13). Anaphase speeds were then calculated from the slopes of the movement graphs. In order to calculate the speeds of individual kinetochores in which the interkinetochore distance was measured over time, the separation speed was divided by two. Speeds varied considerably between pairs of autosomal half-bivalents, within the same cell and between cells (Dietz 1972). On average, kinetochores moved poleward with a speed of 0.5±0.2µm/min (Figure 14). Sometimes, as kinetochores

approached the spindle poles they slowed down to approximately 25% of their initial anaphase speed (n=13/47).

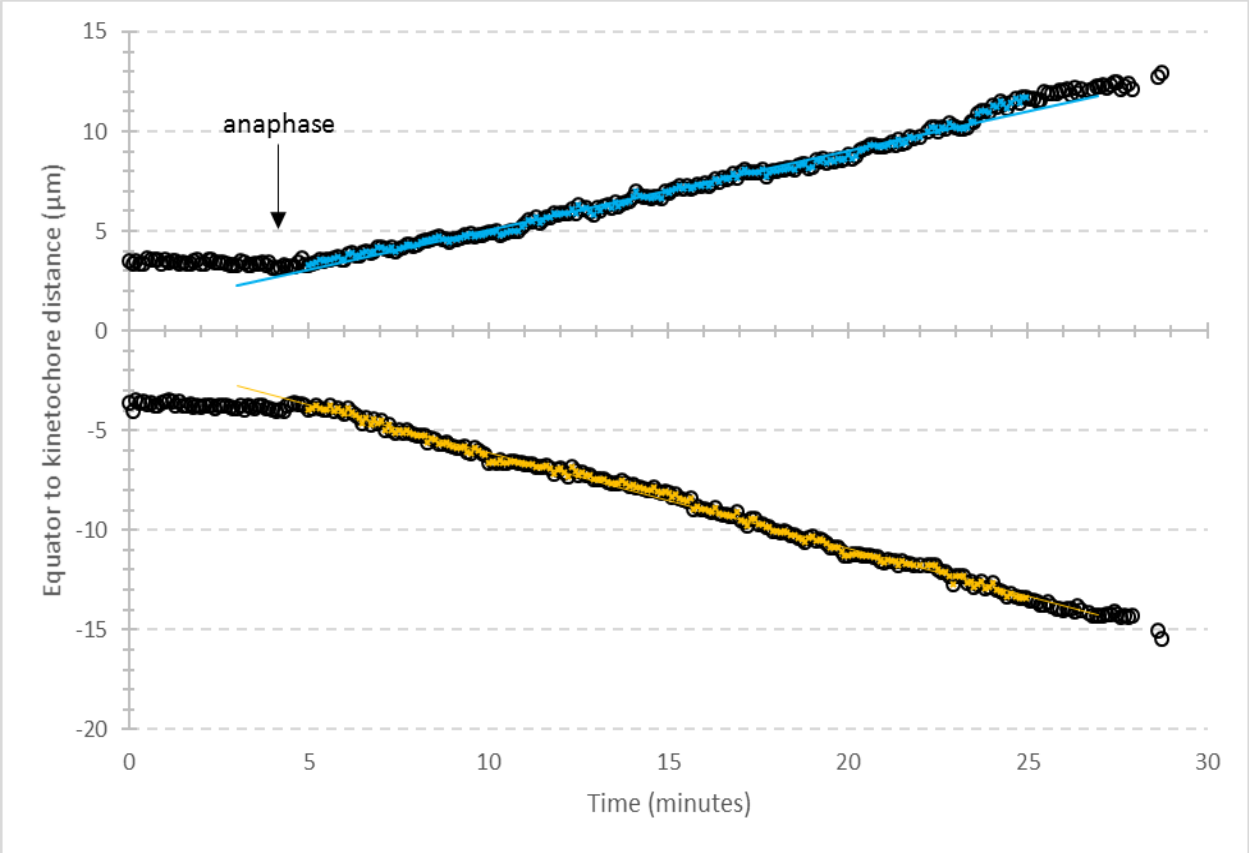

Figure 12 – Illustrating constant poleward velocity during anaphase in Insect Ringer's. Kinetochore to equator distances were plotted over time for a pair of separating half-bivalents. The top kinetochore (blue) moves poleward at 0.4µm/min and the bottom kinetochore (yellow) moves poleward at 0.5µm/min. This graph is an example of one of the many control divisions that were observed in Insect Ringer's.

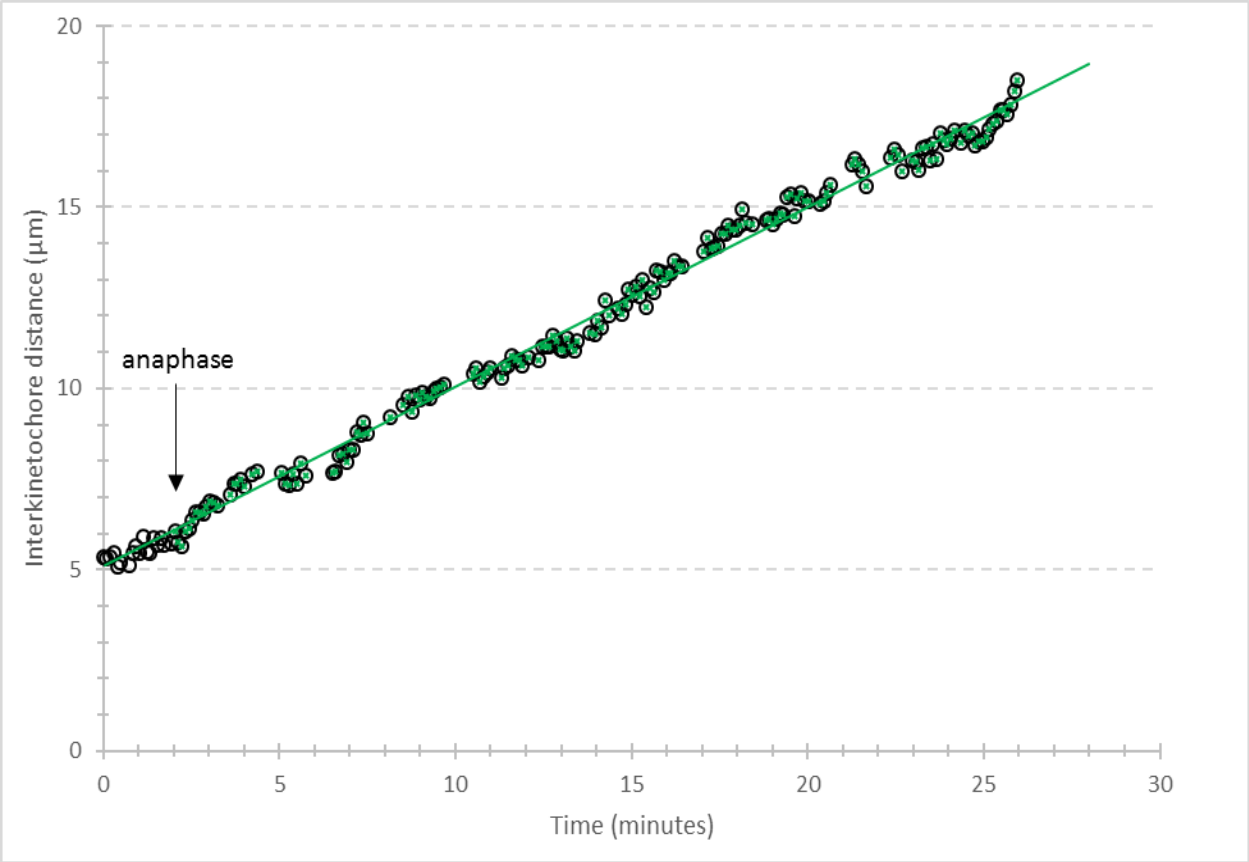

Figure 13 – Illustrating constant poleward velocity during anaphase in Insect Ringer's. The interkinetochore distance was plotted over time for a pair of separating half-bivalents. The kinetochores move poleward with a separation speed of 0.5µm/min. This graph is an example of one of the many control divisions that were observed in Insect Ringer's.

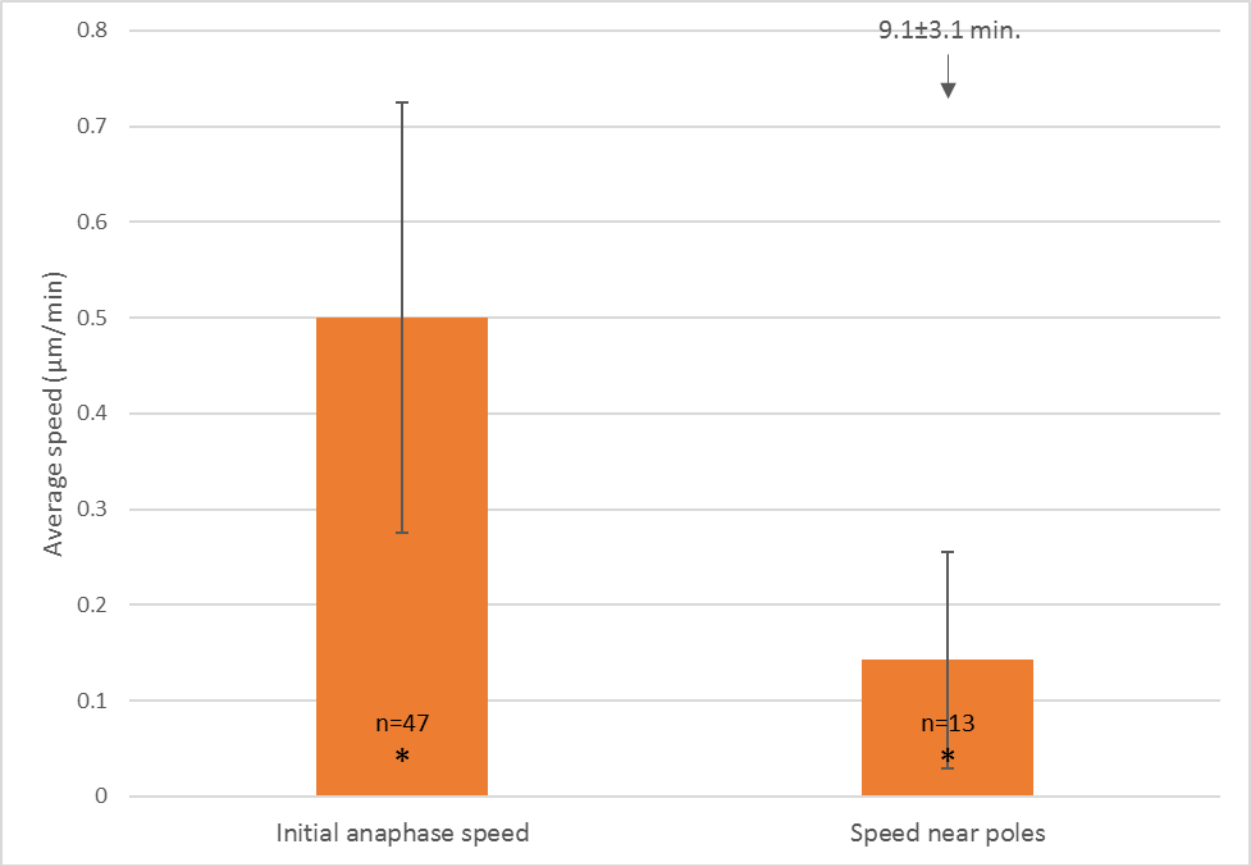

Figure 14 – Average control speeds during anaphase in Insect Ringer's. Kinetochores moved poleward with an average initial speed of 0.5±0.2µm/min (n=47). Sometimes, as kinetochores approached the spindle poles, they slowed down to approximately 28% of their initial anaphase speed (n=13/47). Time indicates minutes after anaphase onset. Asterisks indicate significant differences in speed (*, $p<0.05$). Error bars represent SD. [n=number of kinetochores].

Anaphase chromosome movement following treatment

To test whether tropomyosin is involved in anaphase chromosome movement, live cells were treated with inhibitory drugs against tropomyosin during anaphase and chromosome movement was analyzed with movement graphs. Similar methods have been used in crane-fly primary spermatocytes to test the roles of actin and myosin during anaphase chromosome movement (Forer and Pickett-Heaps 1998, Silverman-Gavrila and Forer 2001, Xie and Forer 2008, Sheykhani *et al.* 2013). When added during anaphase, these drugs slow, stop or slow and then stop chromosome movement. It was predicted that if tropomyosin is also involved in anaphase chromosome movement, then inhibitory drugs against tropomyosin would alter chromosome movement.

Briefly, cells were chosen in the prometaphase-I to metaphase-I stage of division. Stage was determined by the chromosome shape and alignment as well as the spindle shape. After anaphase onset, as autosomal half-bivalents moved toward their respective spindle poles, cells were treated with PD, TR100 or an equal volume of DMSO. Movement graphs were then generated by plotting the kinetochore to pole or kinetochore to equator distances over time or the interkinetochore distance over time. Anaphase speeds for individual kinetochores both

prior to and following treatment were calculated from the slopes of the movement graphs.

Table 1 provides a summary of the average relative anaphase speeds following DMSO, PD and TR100 treatment and Table 2 provides a summary of the number of kinetochores showing different effects following DMSO, PD and TR100 treatment. Data were combined for the different concentrations within each treatment because the kinetochores reacted similarly between concentrations. Overall, over approximately 70% of the kinetochores followed during anaphase were altered following PD treatment, while approximately 33% of the kinetochores followed during anaphase were altered by TR100 treatment. In general, kinetochores that were affected by PD or TR100 treatment either slowed, slowed and then stopped or stopped following treatment.

Table 1 – Average relative anaphase speeds following DMSO, PD and TR100 treatments. Relative speeds for individual kinetochores were calculated as percentages of the initial anaphase speed of the kinetochore prior to treatment (Tx). Some kinetochores were analyzed after washing out PD (speed after wash out). Times indicate minutes after anaphase onset. [n=number of kinetochores].

Treatment	Chromosome movement	Number of kt.		Average relative speed (% initial speed)			
				Speed following Tx	Second speed in Tx	Resumed speed in Tx	Speed after wash out
DMSO [0.25% - 0.5%]	No effect	19		102.6± 50.5			
			Time (min)	3.8±2.1			
PD [50 µM and 100 µM] n=63	No effect	18		99.4±24.6			97.8±89.8 [n=7]
			Time (min)	4.8±1.3			13.8±0.5
	Slowed	19		47.9±13.4		114.7 [n=2]	60.7±13.2 [n=5]
			Time (min)	3.5±0.8		17	10.6± 1.3
	Slowed then stopped	9		53.4±15.1	Stopped	53.6±37.4 [n=6]	
			Time (min)	1.9±0.3	6.6±4.8	11.8±22.2	
	Stopped	17		Stopped		123.0± 92.2 [n=14]	132.3± 105.2 [n=7]
			Time (min)	4.3±2.1		15.6± 5.4	21.8± 3.95
TR100 [25 µM – 100 µM] n=81	No effect	54		114.3± 49.2			
			Time (min)	3.8±1.6			
	Slowed	20		43.5±14.3		91.8±17.9 [n=7]	
			Time (min)	3.4±1.5		9.2±2.7	
	Stopped	3		Stopped		196.5± 134.8	
			Time (min)	3.7±0.6		22±11.3	
	Delayed stop	4		165.4± 69.2	Stopped	208.2± 67.5	
			Time (min)	4.5±0.6	8.8±0.5	20.2±2.6	

Table 2 – Summary of chromosome movements after control (DMSO) and drug treatments (PD and TR100) added during anaphase. The numbers of kinetochores having different effects following DMSO, PD and TR100 treatment have been included as well as their relative percentages (in brackets). The relative percent of kinetochores were calculated for each treatment, by dividing the number of kinetochores having a particular effect over the total number of kinetochores following that treatment.

Treatment	Total number of kinetochores	Chromosome movement following treatment [number of kinetochores]				
		No effect	Slowed	Slowed then stopped	Stopped	Delayed stop
DMSO [0.25% - 0.5%]	19	19 (100%)				
PD [50 µM and 100 µM]	63	18 (28.6%)	19 (30.2%)	9 (14.3%)	17 (27%)	
TR100 [25 µM - 100 µM]	81	54 (66.7%)	20 (24.7%)		3 (3.7%)	4 (4.9%)

DMSO treatment

In total, ten cells were treated with DMSO [0.25% to 0.5%] and 19 kinetochores were followed during anaphase. DMSO did not affect chromosome movement when added during anaphase (Tables 1 and 2). An example graph following DMSO treatment has been included (Figure 15). Previous studies in crane-fly primary spermatocytes have also shown that Insect Ringer's solution, containing up to 0.2% DMSO, had no effect on chromosome movement during anaphase (reviewed in Xie and Forer 2008).

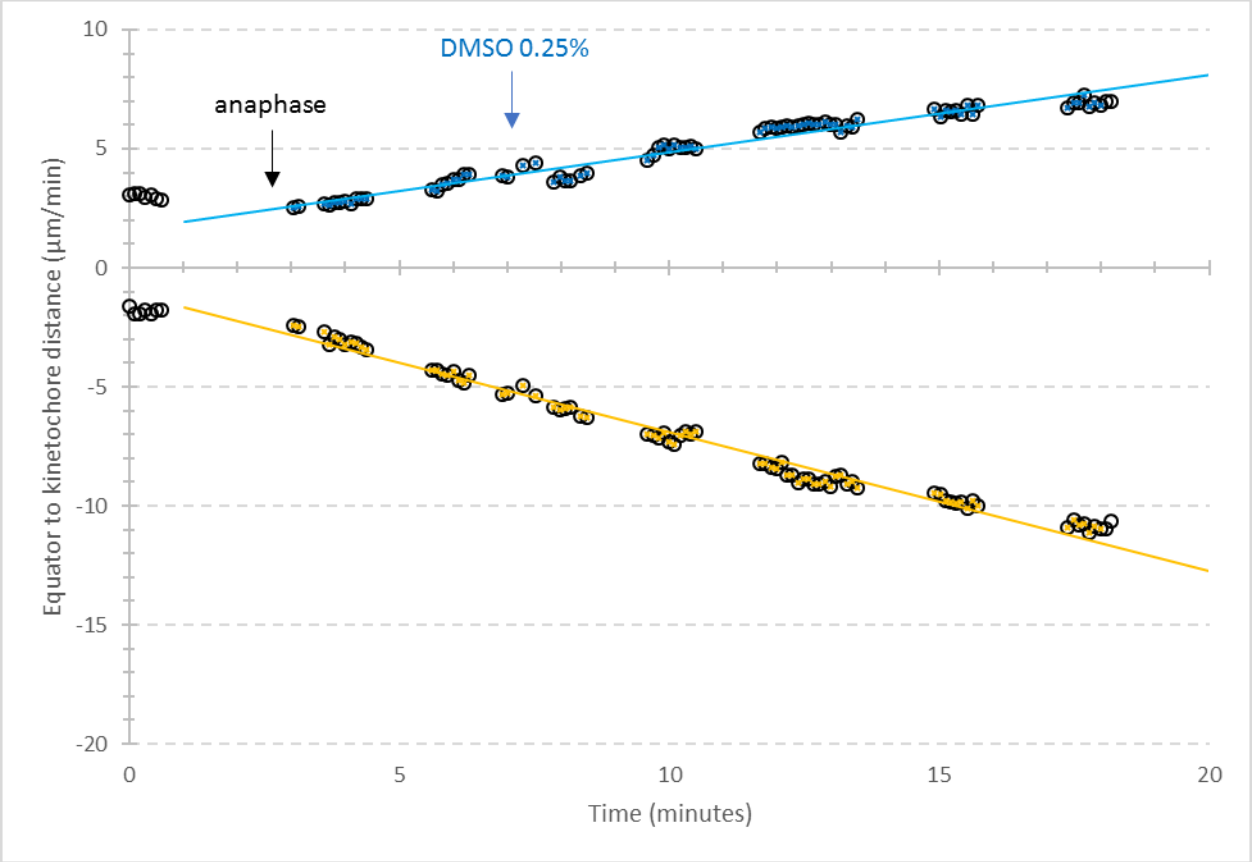

Figure 15 – Illustrating chromosome movement following DMSO treatment. DMSO [0.25%] was added approximately 4 minutes after anaphase onset. Following treatment, chromosomes continued moving poleward with no observable change in speed.

PD treatment

Cells were treated with PD at both low [50 µM] and high [100 µM] concentrations. In total, eighteen cells were treated with PD during anaphase and 63 kinetochores were followed. PD altered anaphase chromosome movement in over 70% of the kinetochores followed during anaphase (Table 2). Some kinetochores slowed to approximately 48% of their initial anaphase speed (n=19/63) (Figure 16). A graph illustrating slowed movement following PD treatment has been included (Figure 17). Kinetochores sometimes slowed and then stopped moving following PD treatment (n=9/63). These kinetochores slowed to approximately 53% of their initial anaphase speed before stopping (Figure 18). Most of these kinetochores resumed poleward movement while still in PD (n=6/9) with an average speed of approximately 54% of their initial anaphase speed. A graph illustrating slowed and then stopped movement following PD treatment has been included (Figure 19). Lastly, some kinetochores stopped moving following PD treatment (n=17/63) (Figure 20). Most of these kinetochores resumed movement while still in PD, with an average speed of approximately 123% of their initial anaphase speed (n=14/17). After wash out, the kinetochores continued moving poleward with an average speed of approximately 132% of their initial anaphase speed (n=9/17). A graph illustrating stopped movement following

PD treatment has been included (Figure 21). Overall, between cells and within the same cell, bivalents reacted differently to PD treatment. However, most partner half-bivalents reacted the same (n=50/63 kinetochores). In addition, many kinetochores increased in speed or resumed poleward movement while still in PD after slowing or stopping (n=22/45).

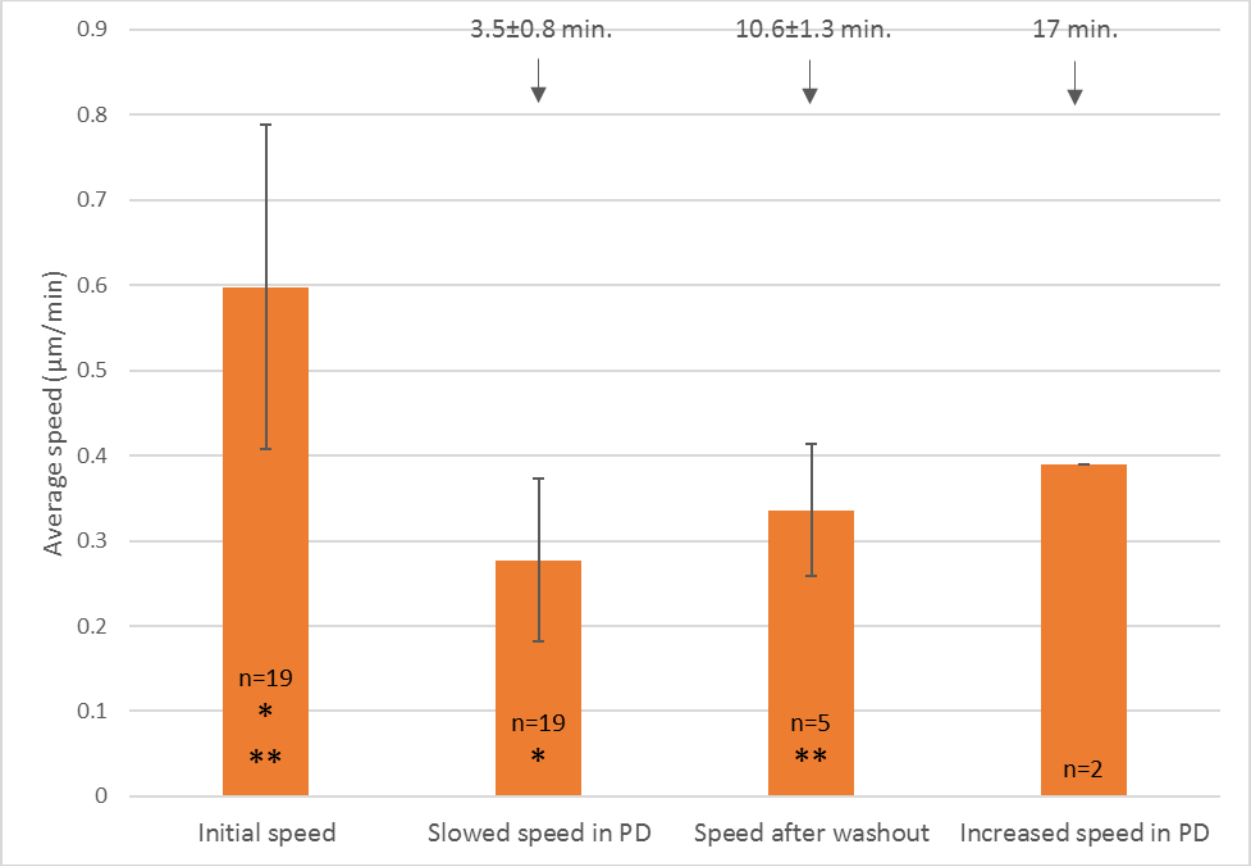

Figure 16 – Average speeds following PD treatment that slowed anaphase movement. Kinetochores moved with an average initial speed of 0.6±0.2µm/min (n=19). Following PD treatment [50 µM and 100 µM] kinetochores slowed on average to 48% of their initial anaphase speed. After wash out, kinetochores moved with an average speed of approximately 61% of their initial anaphase speed (n=5). After slowing, one pair of partner kinetochores increased in speed while still in PD. Times indicate minutes after anaphase onset. Asterisks indicate significant differences in speed (*, $p<0.05$; **, $p<0.05$). Error bars represent SD. [n=number of kinetochores].

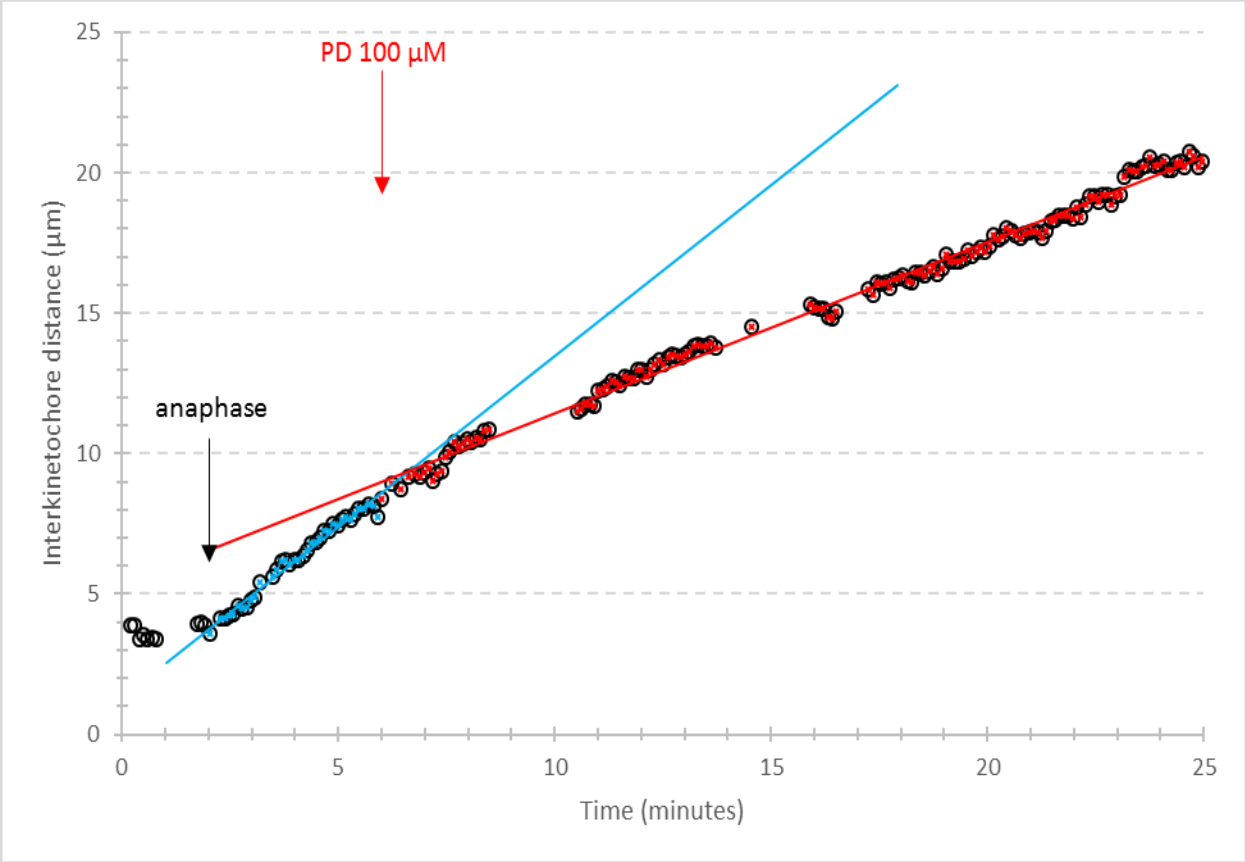

Figure 17 – Illustrating slowed chromosome movement following PD treatment. PD [100 µM] was added approximatley 4 minutes after anaphase onset. Immediately following PD treatment, kinetochore movement slowed. Prior to PD treatment, the kinetochores moved poleward with a separation speed of 1.2µm/min. Following PD treatment, the kinetochores moved poleward with a separation speed of 0.6µm/min.

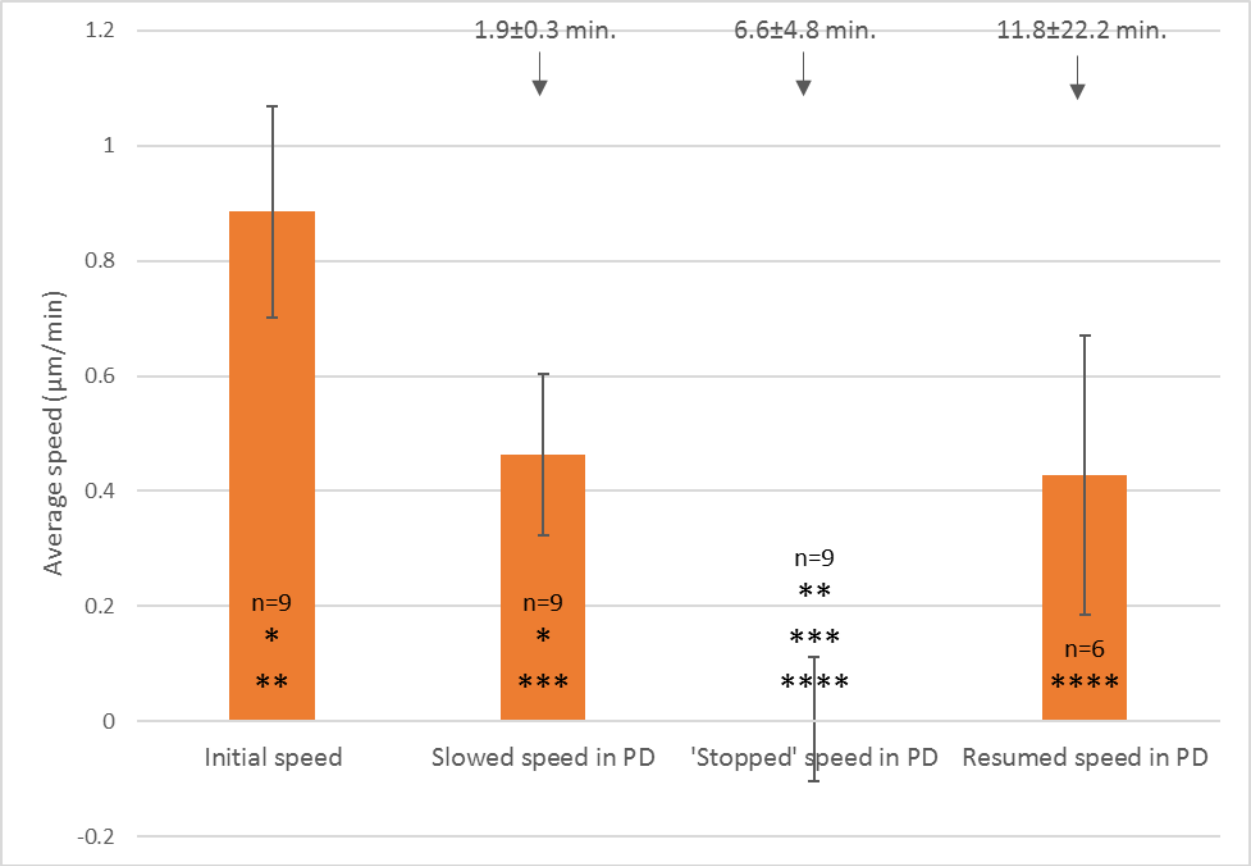

Figure 18 – Average speeds following PD treatment that slowed and then stopped anaphase movement. Kinetochores moved with an average initial speed of 0.88±0.2µm/min (n=9). Following PD treatment [50 µM and 100 µM] kinetochores slowed on average to 53% of their initial anaphase speed and then stopped moving poleward. Some of these kinetochores then resumed poleward movement with an average speed of 54% of their initial anaphase speed (n=6/9). Times indicate minutes after anaphase onset. Asterisks indicate significant differences in speed (*, $p<0.05$; **, $p<0.05$; ***, $p<0.05$; ****, $p<0.05$). Error bars represent SD. [n=number of kinetochores].

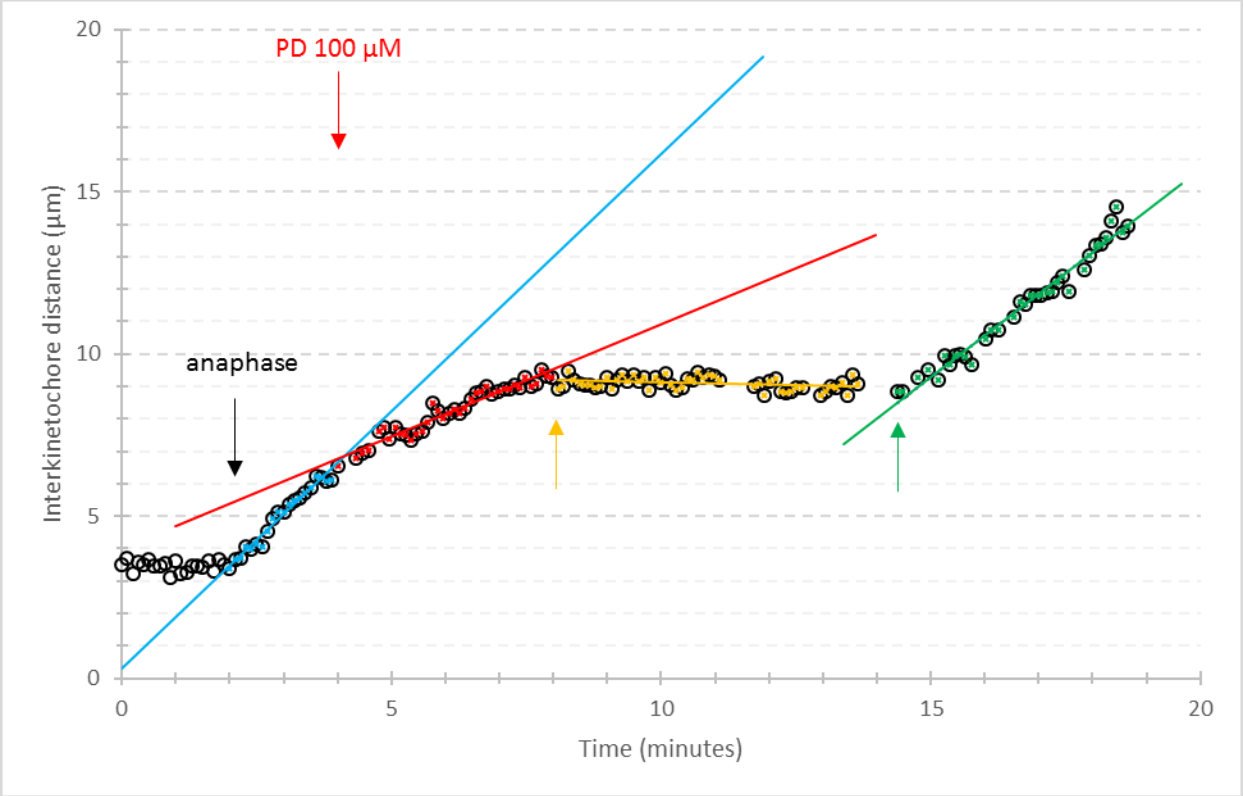

Figure 19 – Illustrating slowed and then stopped chromosome movement following PD treatment. PD [100 µM] was added approximately 2 minutes after anaphase onset. Immediately following PD treatment, kinetochore movement slowed. Prior to PD treatment, the kinetochores moved poleward with a separation speed of 1.6µm/min. Following PD treatment, the kinetochores moved poleward with a separation speed of 0.7µm/min. Approximately 4 minutes after PD treatment, the kinetochores stopped moving poleward (yellow arrow). The kinetochores resumed movement approximately 10 minutes after PD treatment with a speed of 1.3µm/min (green arrow).

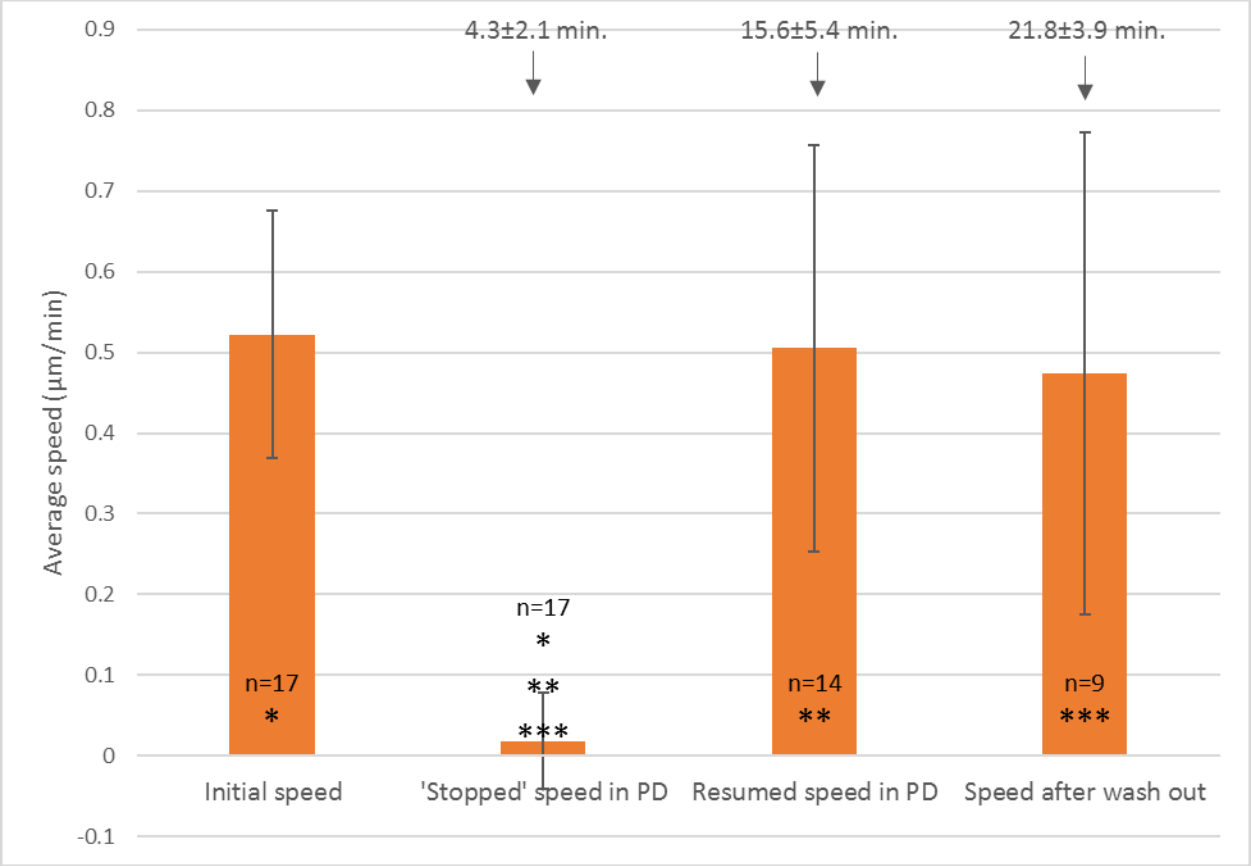

Figure 20 – Average speeds following PD treatment that stopped anaphase movement. Kinetochores moved with an average initial speed of 0.52±0.2µm/min (n=17). Following PD treatment [50 µM and 100 µM] kinetochores stopped moving poleward. Most of these kinetochores resumed poleward movement while still in PD, with an average speed of approximately 123% of their initial anaphase speed (n=14/17). After wash out, kinetochores moved with an average speed of approximately 132% of their initial anaphase speed. Times indicate minutes after anaphase onset. Asterisks indicate significant differences in speed (*, $p<0.05$; **, $p<0.05$; ***, $p<0.05$; ***, $p<0.05$). Error bars represent SD. [n=number of kinetochores].

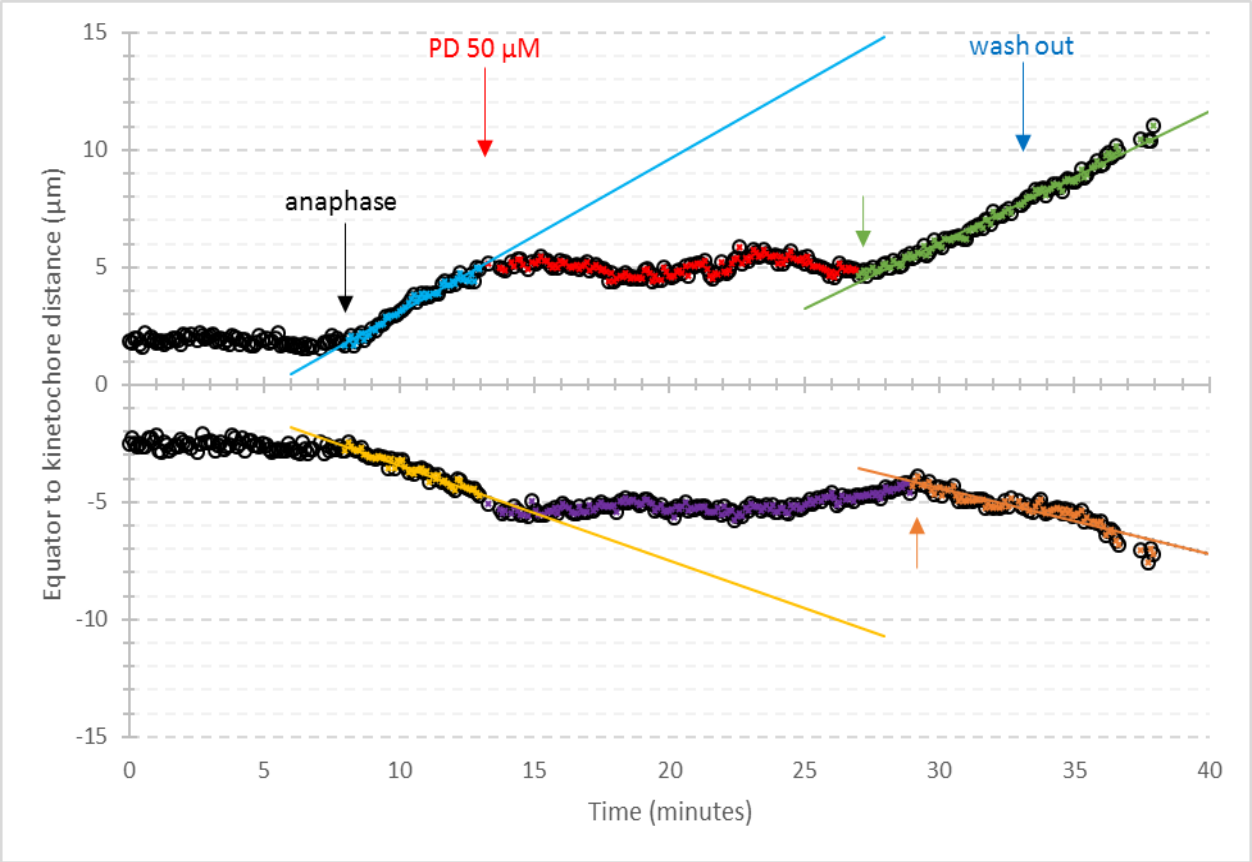

Figure 21 – Illustrating stopped chromosome movement following PD treatment. PD [50 µM] was added approximatley 5 minutes after anaphase onset. Immediately following PD treatment, kinetochores stopped moving poleward. The top kinetochore resumed poleward movement approximately 15 minutes after PD was added (green arrow) and the bottom kinetochore resumed poleward movement approximately 17 minutes after PD was added (orange arrow). Kinetochores resumed poleward movement before PD was washed out.

TR100 treatment

Cells were treated with variable concentrations of TR100 ranging from 25 µM to 100 µM. In total, thirty-four cells were treated with TR100 during anaphase and 81 kinetochores were followed. In 66% of the kinetochores followed during anaphase, TR100 did not affect chromosome movement (Table 2, Figure 22). A graph illustrating chromosome movement following TR100 treatment in which movement was unaffected has been included (Figure 23). In 33% of the kinetochores following during anaphase, movement slowed or stopped following TR100 treatment (Table 2). Some kinetochores slowed to approximately 44% of their initial anaphase speed immediately following TR100 treatment (n=20/81) (Figure 24). Some of these kinetochores (n=7/20) then subsequently increased in speed while still in TR100 to approximately 92% of their initial anaphase speed. A graph illustrating slowed movement following TR100 treatment has been included (Figure 25). Some kinetochores stopped moving poleward immediately following TR100 treatment (n=3/81) (Figure 26). After stopping, these kinetochores resumed poleward movement while still in TR100, with an average speed of approximately 196% of their initial anaphase speed. A graph illustrating stopped movement following TR100 treatment has been included (Figure 27). Lastly, some kinetochores continued moving poleward

after TR100 treatment but then stopped moving approximately 4 minutes after treatment (n=4) (Figure 28). These kinetochores then resumed poleward movement with an average speed of approximately 208% of their initial anaphase speed. A graph illustrating this type of movement following TR100 treatment has been included (Figure 29). In general, partner half-bivalents reacted the same (n=68/81). TR100 did not consistently slow or stop chromosome movement at any concentration in which it was used.

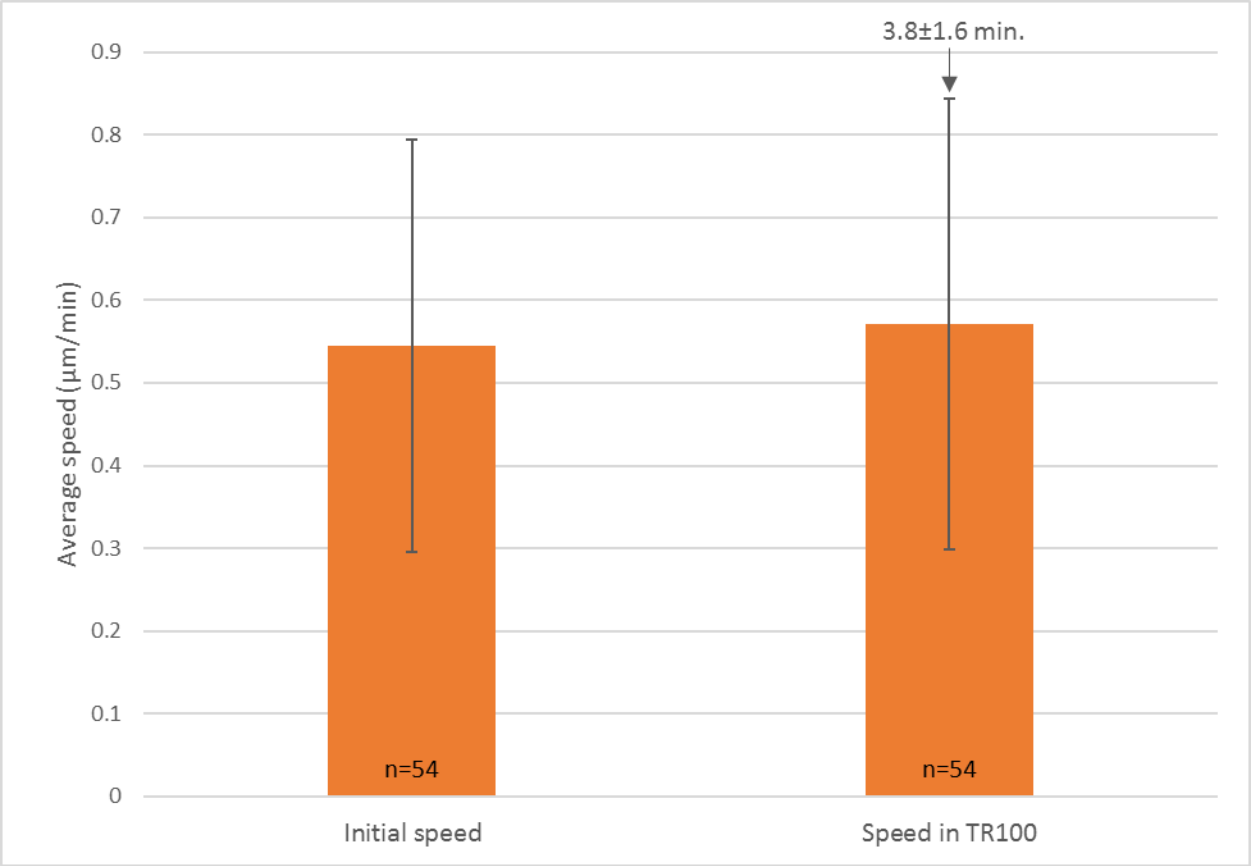

Figure 22 – Average speed following TR100 treatment in which chromosome movement was unaffected. Kinetochores moved with an average initial speed of 0.54±0.2µm/min (n=54). Following TR100 treatment [25 µM to 100 µM] kinetochores moved poleward with an average speed of approximately 114% of their initial anaphase speed. Time indicates minutes after anaphase onset. Error bars represent SD. [n=number of kinetochores].

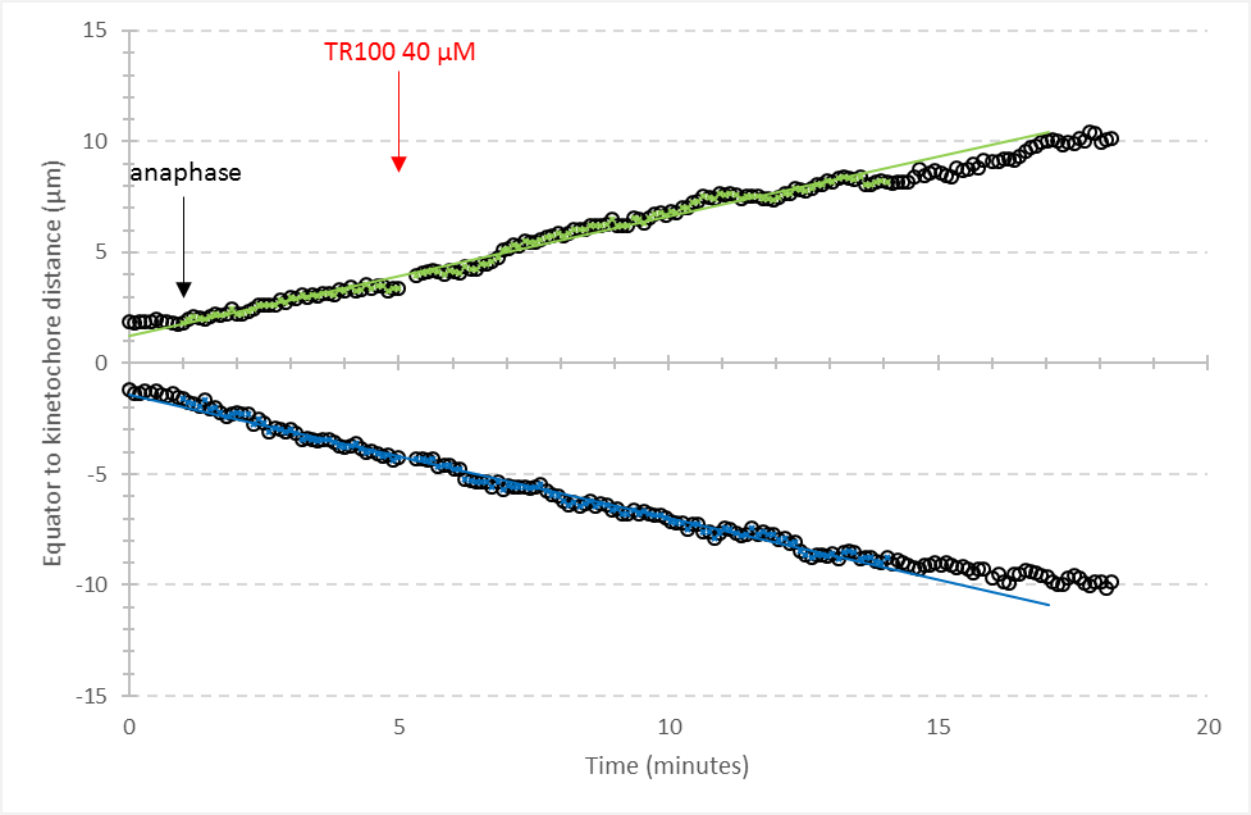

Figure 23 – Illustrating chromosome movement that was unaffected following TR100 treatment. TR100 [40 µM] was added approximatley 4 minutes after anapahse onset. Following treatment, chromosomes continued moving poleward with no observable change in speed.

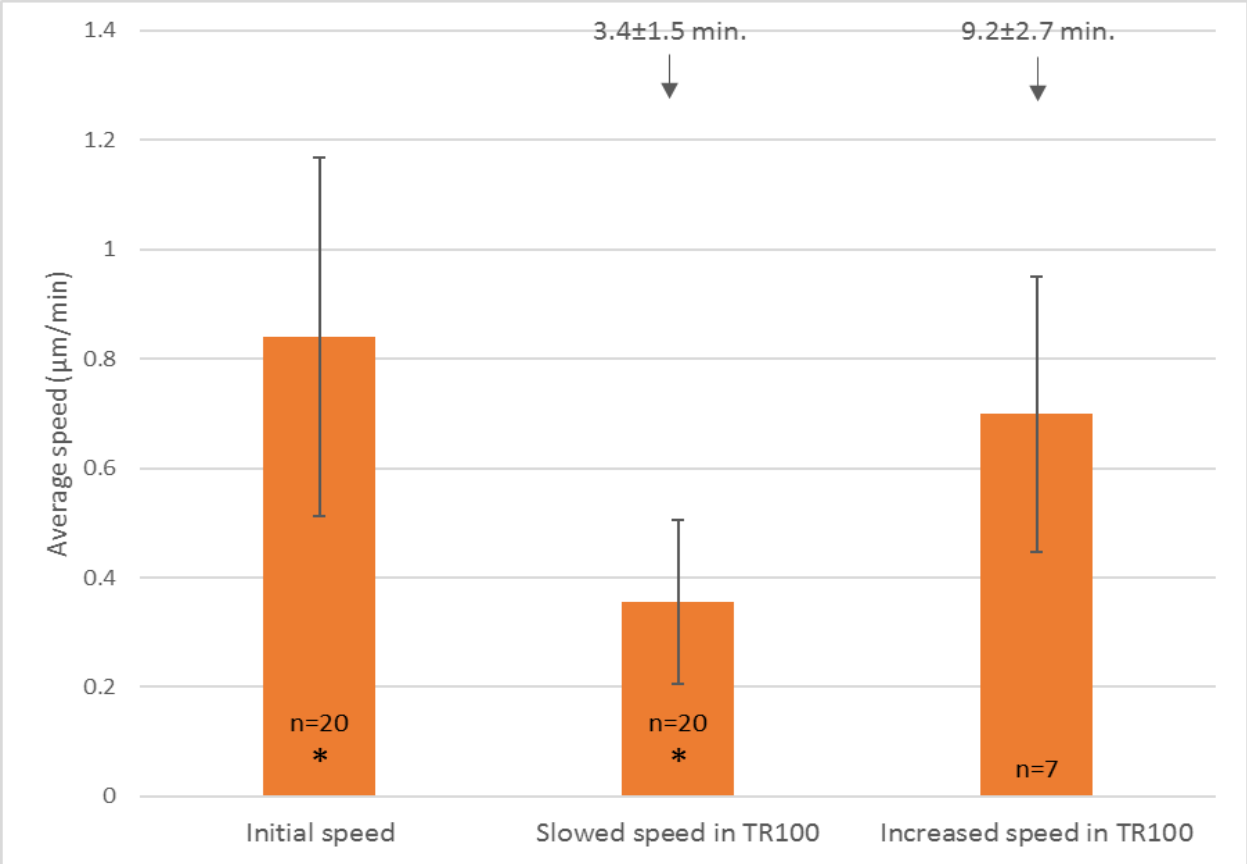

Figure 24 – Average speeds following TR100 treatment that slowed anaphase movement. Kinetochores moved with an initial average speed of 0.84±0.3µm/min (n=20). Following TR100 [25 µM to 50 µM] kinetochores slowed on average to 44% of their initial anaphase speed. Some kinetochores then increased in speed to approximately 92% of their initial anaphase speed (n=7/20). Times indicate minutes after anaphase onset. Asterisks indicate significant differences in speed (*, $p<0.05$). Error bars represent SD. [n=number of kinetochores].

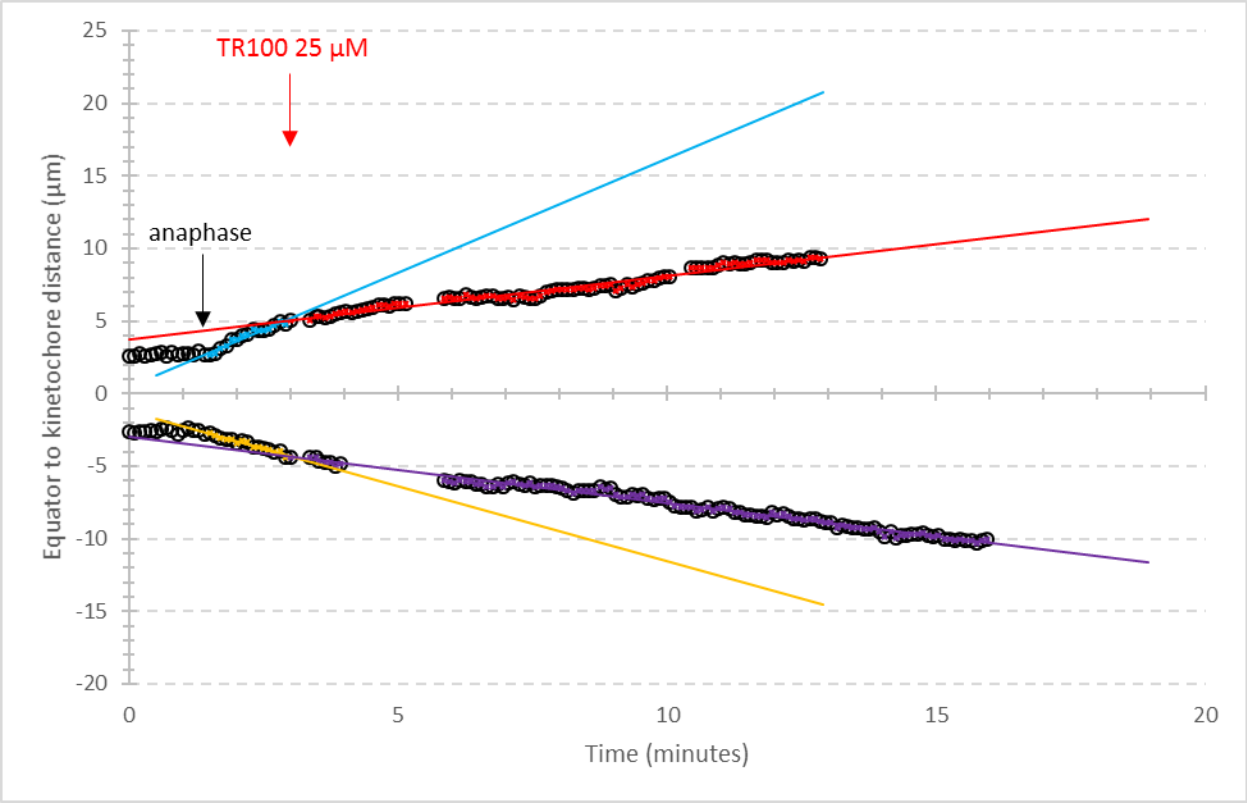

Figure 25 – Illustrating slowed chromosome movement following TR100 treatment. TR100 [25 µM] was added approximately 1.5 minutes after anaphase onset. Following treatment, kinetochore movement slowed. Prior to TR100 treatment, the top kinetochore moved with a speed of 1.5µm/min (blue) and the bottom kinetochore moved with a speed of 1.0µm/min (yellow). Following TR100 treatment, the top (red) and bottom (purple) kinetochores slowed to 0.4µm/min.

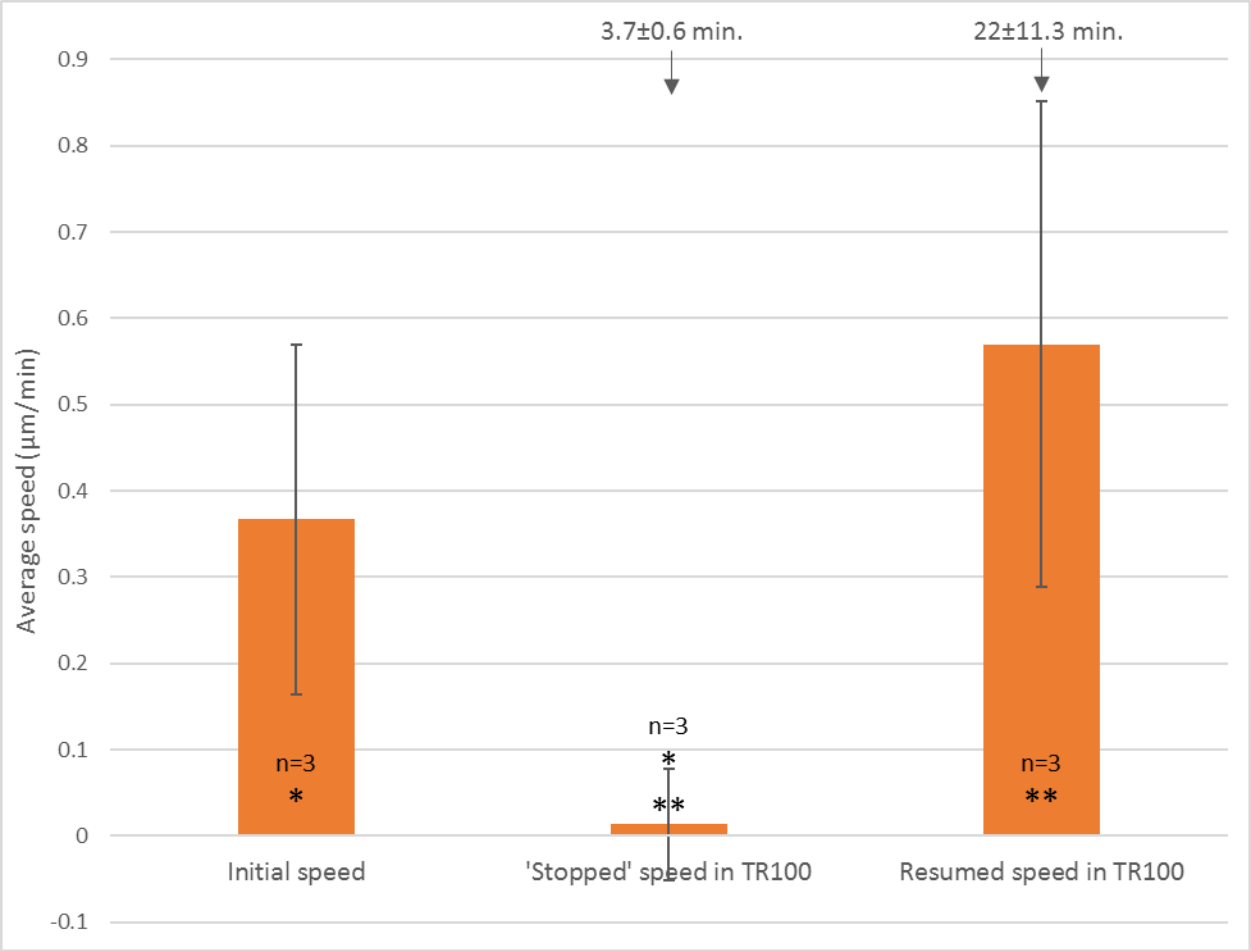

Figure 26 – Average speeds following TR100 treatment that stopped anaphase movement. Kinetochores moved with an initial average speed of 0.37±0.2µm/min (n=3). Following TR100 treatment [40 µM and 50 µM] the kinetochores stopped moving poleward. They resumed poleward movement with an average speed of 196% of their initial anaphase speed. Times indicate minutes after anaphase onset. Asterisks indicate significant differences in speed (*, $p<0.05$; **, $p<0.05$). Error bars represent SD. [n=number of kinetochores].

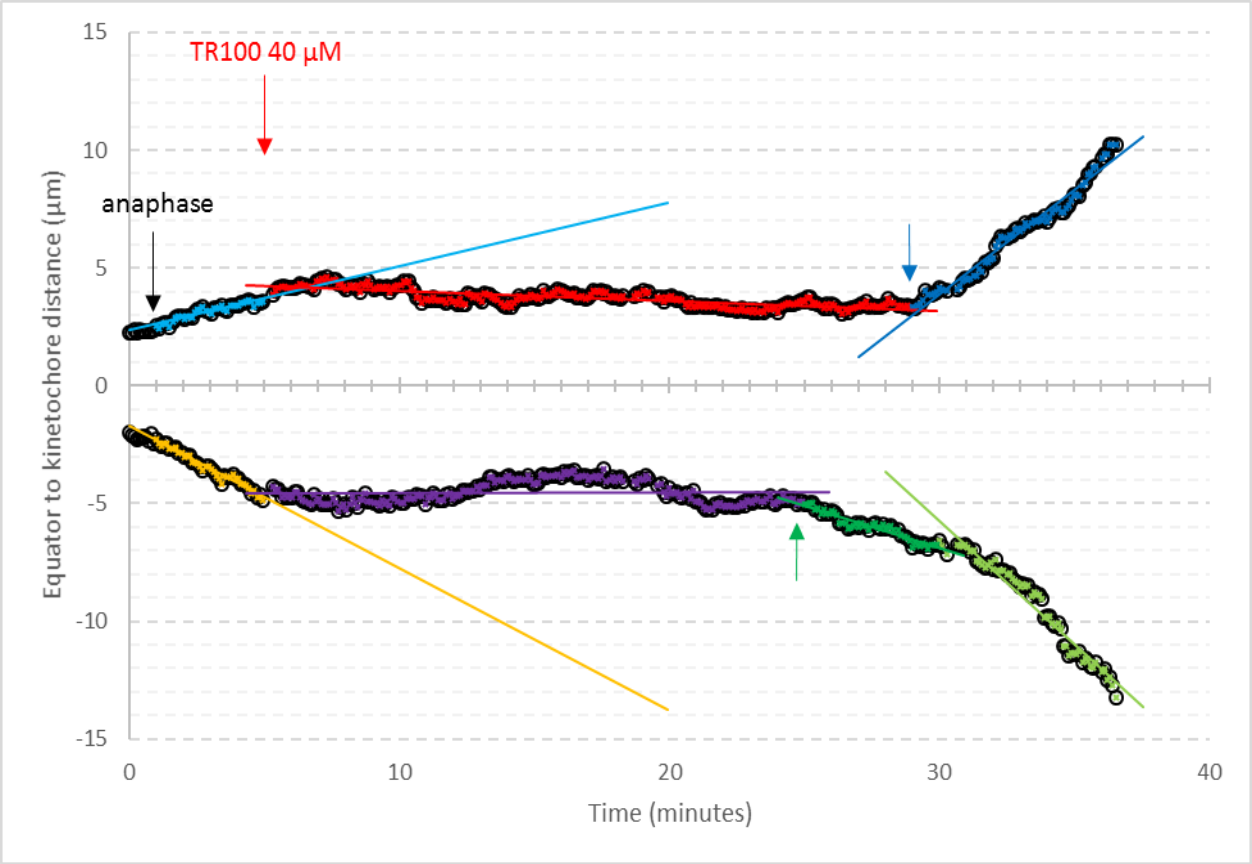

Figure 27 – Illustrating stopped chromosome movement following TR100 treatment. TR100 [40 µM] was added approximately 4 minutes after anaphase onset. Following treatment, kinetochores stopped moving poleward. The top kinetochore resumed movement approximately 24 minutes after TR100 treatment (blue arrow). The bottom kinetochore resumed movement approximately 20 minutes after anaphase onset (green arrow). The top kinetochore moved with an initial speed of 0.3µm/min (light blue) and resumed speed of 0.9µm/min (dark blue). The bottom kinetochore moved with an initial speed of 0.6µm/min (yellow) and resumed movement of 1.0µm/min (light green).

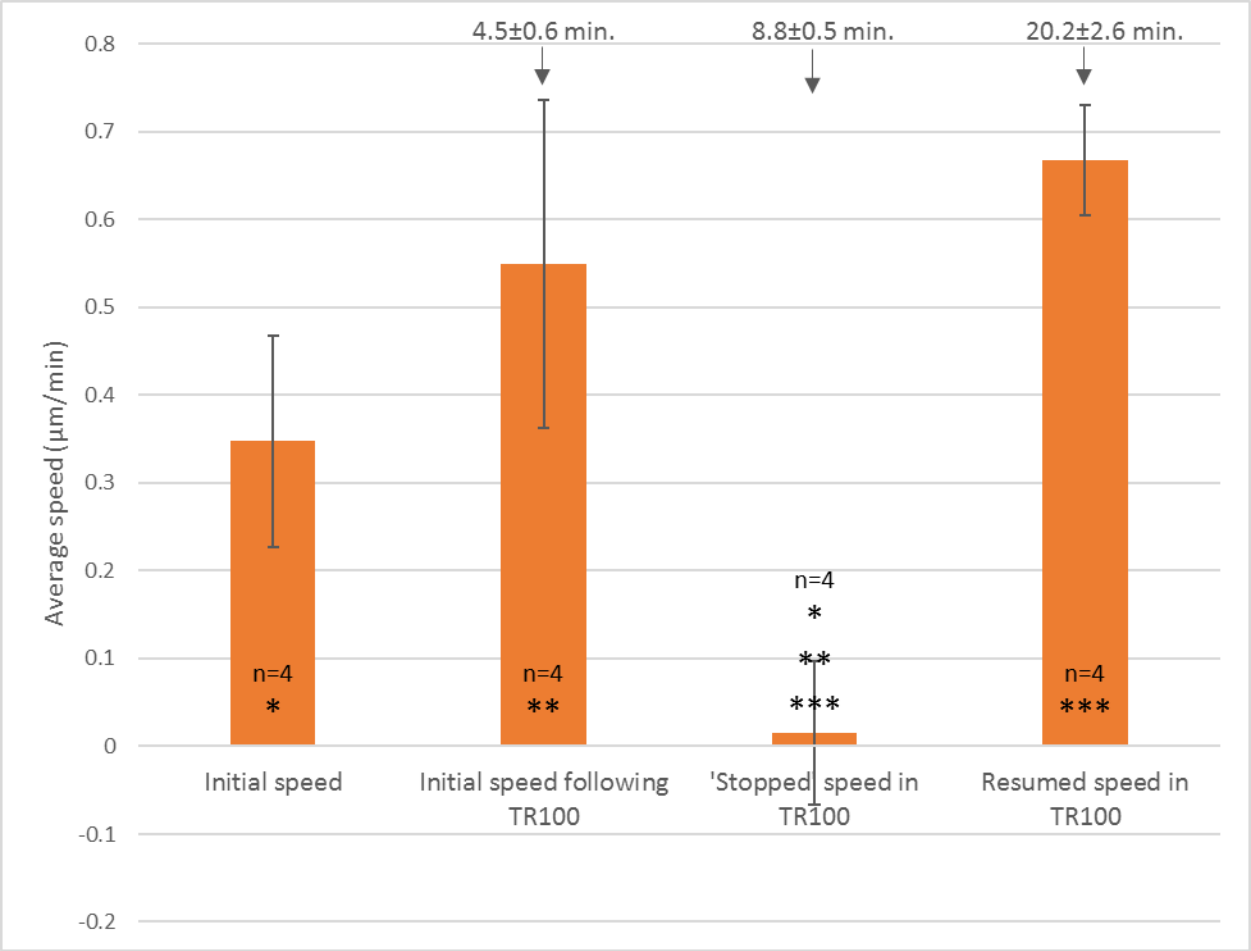

Figure 28 – Average speeds following TR100 treatment that had a delayed effect. Kinetochores moved with an initial average speed of 0.35±0.1µm/min (n=4). Immediately following TR100 treatment [25 µM to 50 µM] the kinetochores moved poleward with an average speed of 0.55±0.2µm/min. Approximately 4 minutes after treatment, the kinetochores stopped moving poleward. The stopped kinetochores then resumed poleward movement with an average speed of approximately 208% of their initial anaphase speed. Times indicate minutes after anaphase onset. Asterisks indicate significant differences in speed (*, $p<0.05$; **, $p<0.05$; ***, $p<0.05$). Error bars represent SD. [n=number of kinetochores].

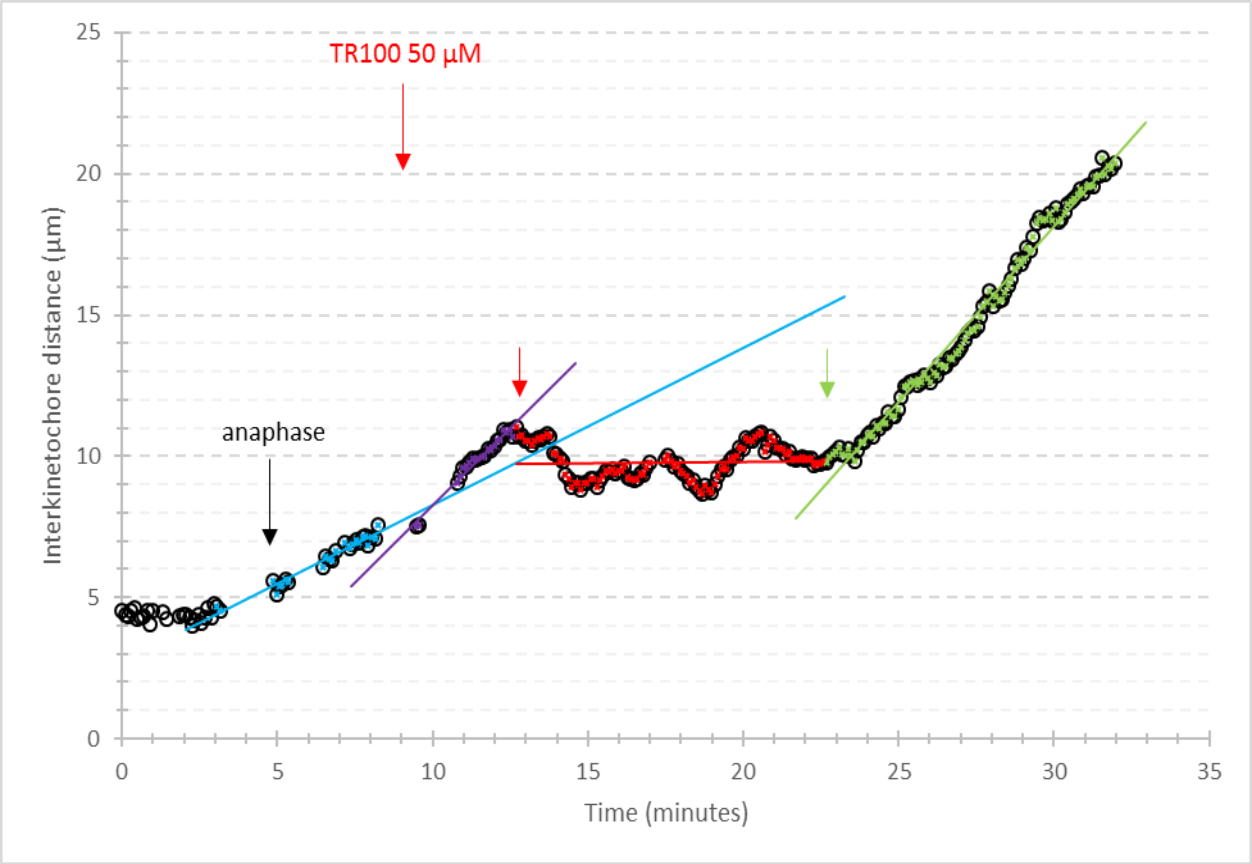

Figure 29 – Illustrating chromosome movement that showed a delayed effect following TR100 treatment. TR100 [50 µM] was added approximatley 4 minutes after anaphase onset. Immediately following treatment, the kinetochores continued moving poleward. Approximately 3.5 minutes after TR100 treatment, the kinetochores stopped moving poleward and moved toward each other. The kinetochores resumed poleward movement approximately 14 minutes after TR100 treatment.

Cytoskeletal effects following treatment

Cytoskeletal effects including membrane blebbing, inhibition of cleavage furrow ingression and loss of actin fingers, were observed following treatment with TR100. In general, these effects were observed after chromosomes were near or at the spindle poles and they occurred in cells in which chromosome movement was either affected or unaffected.

Membrane blebbing

Membrane blebs occasionally appeared in cells after chromosomes reached the spindle poles, following treatment with 25 µM TR100 (n=4/34) (Figure 30). Membrane blebs did not appear in control cells (n=35) or cells treated with PD (n=18).

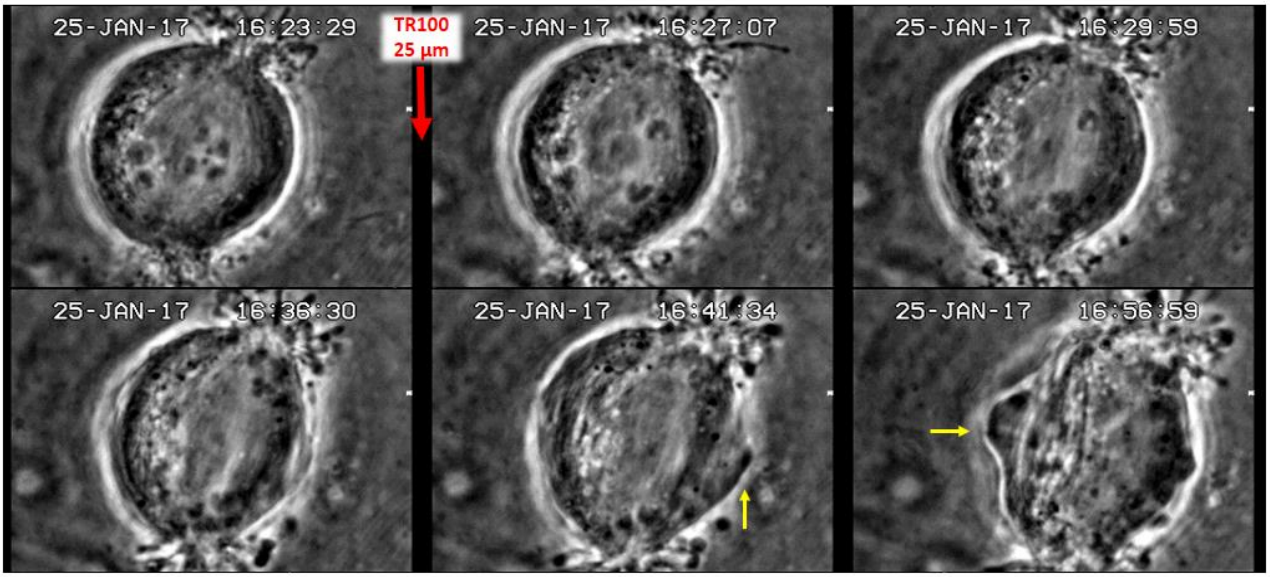

Figure 30 – Membrane blebbing following TR100 treatment. This cell was treated with TR100 [25 µM] 2 minutes after anaphase onset (red arrow). Membrane blebbing was observed approximately 15 minutes following TR100 treatment (yellow arrows). This cell did not cleave.

Cleavage furrows

The contractile ring forms and cleavage furrows begin to ingress after autosomal half-bivalents reach the spindle poles in crane-fly primary spermatocytes. In general, cleavage furrows ingress from both sides of the cell; however, unilateral cleavage furrows may appear in some cells in which ingression occurs from one side (Silverman-Gavrila and Forer 2001). Both symmetrical and asymmetrical cleavage furrow ingressions were counted here. In control conditions (Insect Ringer's and DMSO), cleavage furrows were observed in over 77% (n=27/35) of the cells (Figure 31). They were also observed in 60% (n=3/5) of cells in PD treatment and 85% (n=11/13) of cells following PD treatment but after wash out. In TR100 treatment, cleavage furrows were observed in only 21% (n=7/34) of cells.

To account for the possibility that cleavage furrow initiation may have been delayed, as opposed to being inhibited, cells in which cleavage furrows were not observed following TR100 treatment were recorded, on average, for longer periods of time than the average time required for cleavage furrows to appear in control conditions (IR and DMSO) or in TR100 (Figure 32). In one cell treated with 25 µM TR100, an asymmetric cleavage furrow appeared and ingressed for approximately 1.5-2 minutes, before regressing (Figure 33).

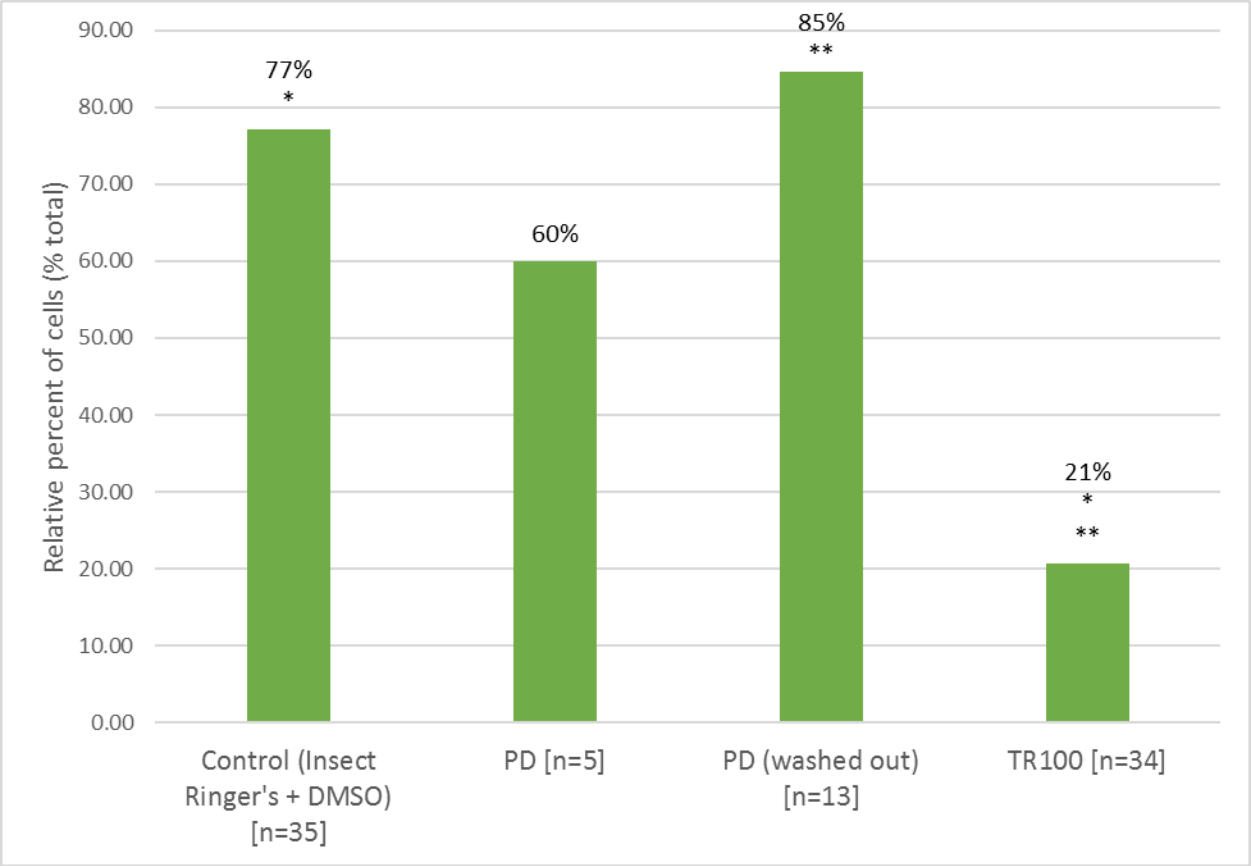

Figure 31 – Relative percent of cells with cleavage furrow ingression in different treatments. Relative percentages were calculated as the number of cells showing cleavage furrow initiation divided by the total number of cells in each treatment. In control conditions, cleavage furrows appeared in 77% of control cells (Insect Ringer's and DMSO). While in PD [50 µM and 100 µM], 60% of cells showed cleavage furrows. After washing out PD [50 µM and 100 µM], 84% of cells showed cleavage furrows. Cleavage furrows appeared on only 21% of cells in TR100 [25 µM to 100 µM]. Asterisks indicate significant differences (*, $p<0.05$; **, $p<0.05$) calculated with Fisher's exact test. [n=number of cells].

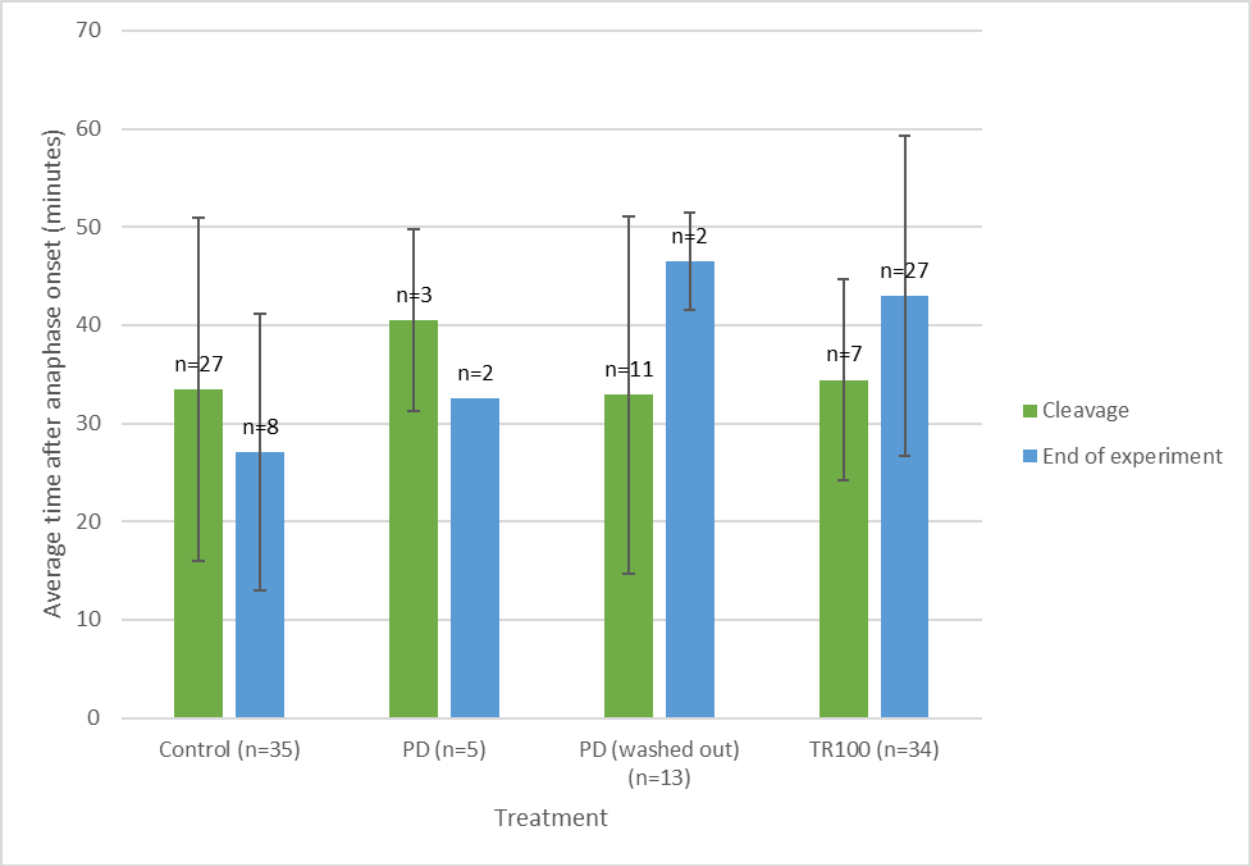

Figure 32 – Average time after anaphase onset that cleavage furrows begin to ingress (minutes). Bars represent the average time for cleavage furrows to appear after anaphase onset (green) or the average length of time that cells were recorded after anaphase onset where no cleavage furrow appeared (blue). Cleavage furrows appeared approximately 33.5±14.9 minutes after anaphase onset in control conditions (Insect Ringer's and DMSO). In TR100, cleavage furrows appeared 34.4±11.5 minutes after anaphase onset. Cells treated with TR100, in which no cleavage furrows were observed, were recorded, on average, for 43±19.1 minutes after anaphase onset. Error bars represent SD. [n=number of cells].

(a)

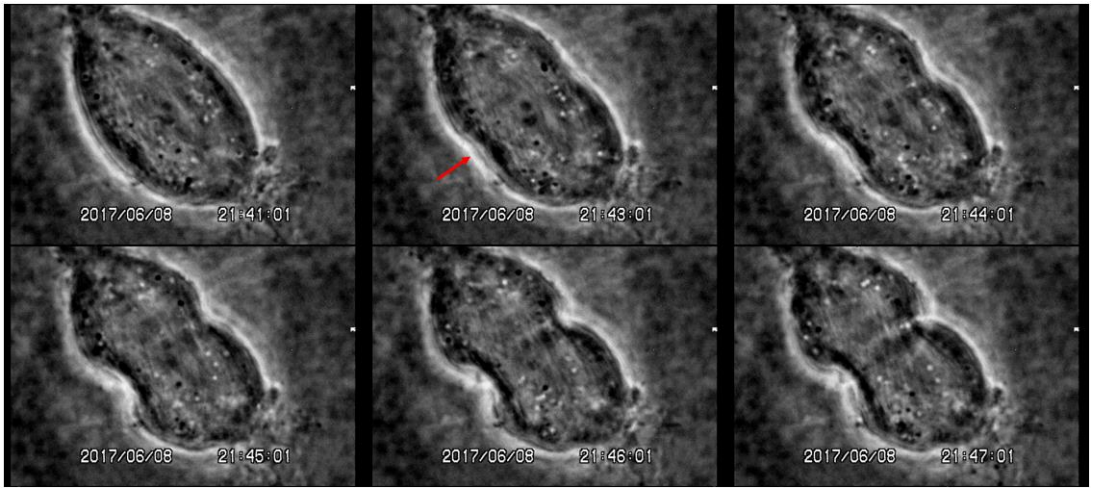

(b)

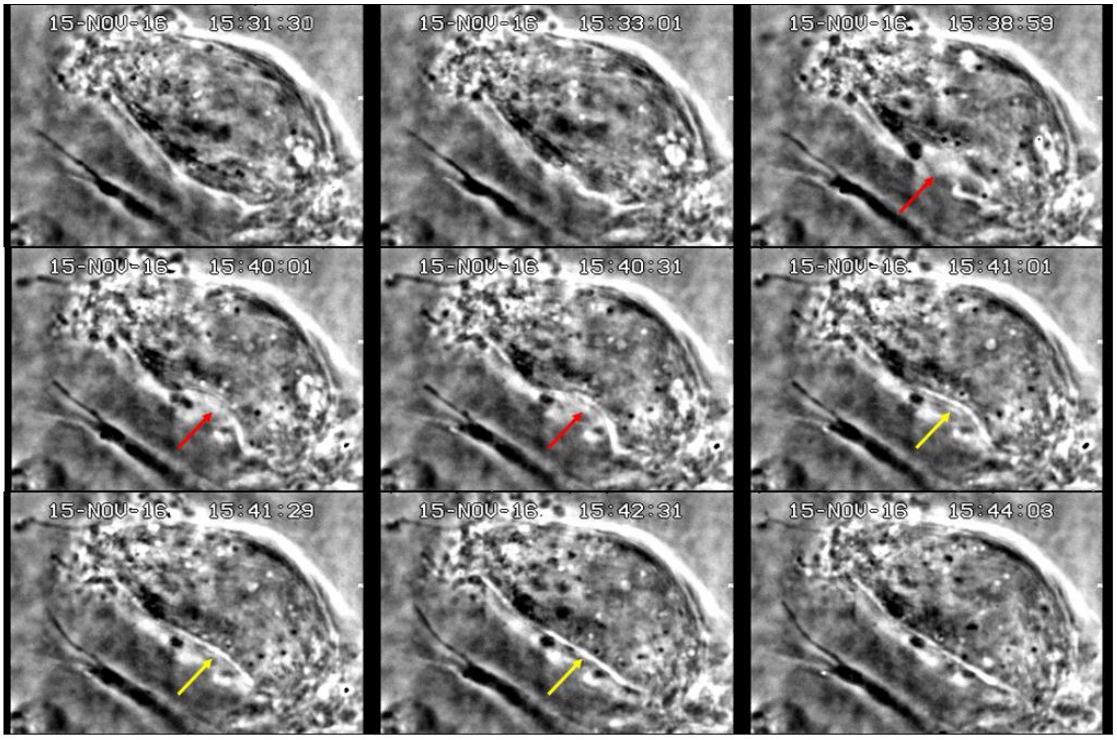

Figure 33 – Cleavage furrow attempt in TR100. (a) Typical cleavage furrow ingression in control conditions. This cleavage furrow appeared approximately 20 minutes after anaphase onset (red arrow) and continued to ingress for several (>4) minutes. (b) This cell was treated with TR100 [25 µM] 4 minutes after anaphase onset. Approximately 50 minutes after anaphase onset a cleavage furrow appeared (red arrow). The cleavage furrow ingressed for approximately 1.5-2 minutes before regressing (yellow arrow). The cell was recorded for 60 minutes after anaphase onset and did not cleave.

Actin fingers

In crane-fly primary spermatocytes, bunches of actin filaments are often seen protruding at the spindle poles and these are referred to as "actin fingers" (Xie and Forer 2008). Following TR100 treatment, at various concentrations [25 µM to 100 µM], actin fingers often changed shape and eventually disappeared (Figure 34). After variable amounts of time following TR100 treatment, actin fingers began to appear thicker and shorter. The actin fingers became progressively compact and eventually disappeared at the spindle poles. This occurred in 25/29 cells treated with TR100, in which actin fingers were visible. Changes in the actin fingers could be seen as early as 2-3 minutes following TR100 treatment and gross changes appeared approximately 19.3±13 minutes after TR100 treatment. Actin fingers did not change in shape or lose integrity throughout cell division in control conditions (Insect Ringer's and DMSO). Actin fingers were present in 4 cells treated with PD, and they did not change shape following PD treatment.

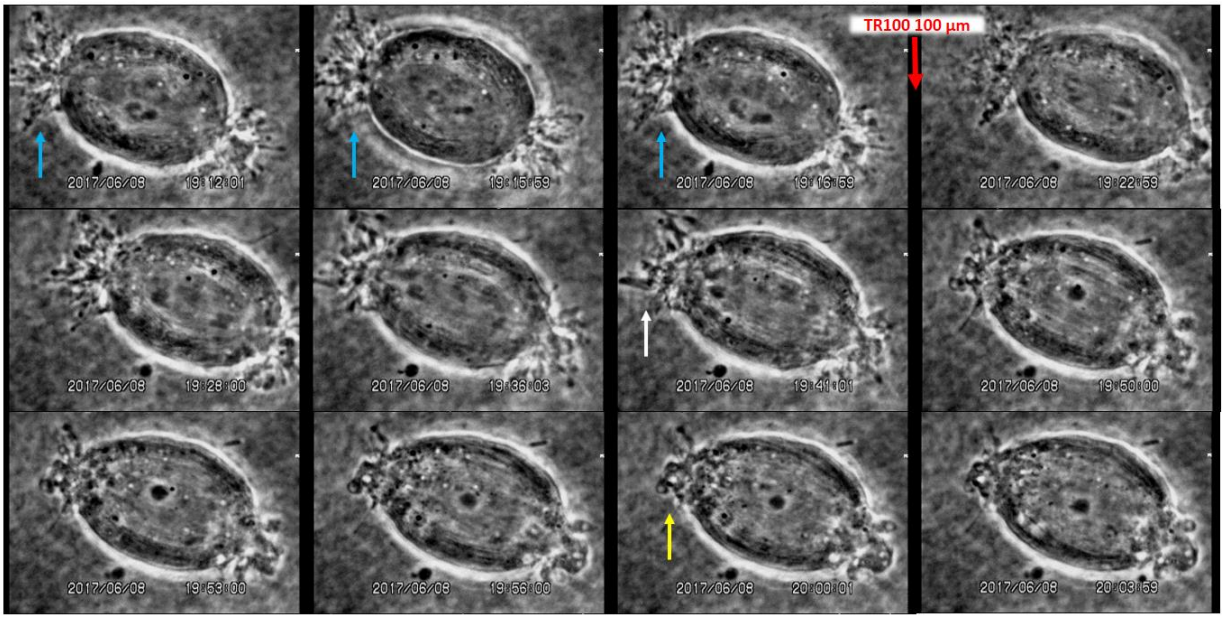

Figure 34 – Loss of actin fingers following TR100 treatment. This cell was treated with TR100 [100 µM] 6 minutes after anaphase onset (red arrow). Actin "fingers" at the spindle poles (blue arrows, Xie and Forer 2008) gradually changed shape and then disappeared following TR100 treatment. The "fingers" became more compact or thicker (white arrow) and then progressively shrunk or disappeared (yellow arrow). Chromosome movement was not significantly affected following TR100 treatment and the cell did not cleave.

Tropomyosin localization in the spindle

Tropomyosin was stained with two different antibodies against different isoforms. To test for a range of possible tropomyosins in the spindle, two antibodies were chosen that have different isoform specificity, TM311 and TM5NM1/2. Tropomyosin localized at the spindle poles and along the kinetochore fibres of crane-fly primary spermatocytes, as observed with both the TM311 and TM5NM1/2 antibodies. During prometaphase-I to anaphase-I, tropomyosin was observed at the spindle poles and along the kinetochore fibres (Figure 35, Figure 36 and Figure 37). In anaphase-I, tropomyosin was observed along kinetochore fibres attached to autosomal half-bivalents as well as the sex chromosome univalents. These data show that tropomyosin localizes to the meiotic spindles of crane-fly primary spermatocytes, particularly to the spindle poles and along kinetochore fibres closer to anaphase-I.

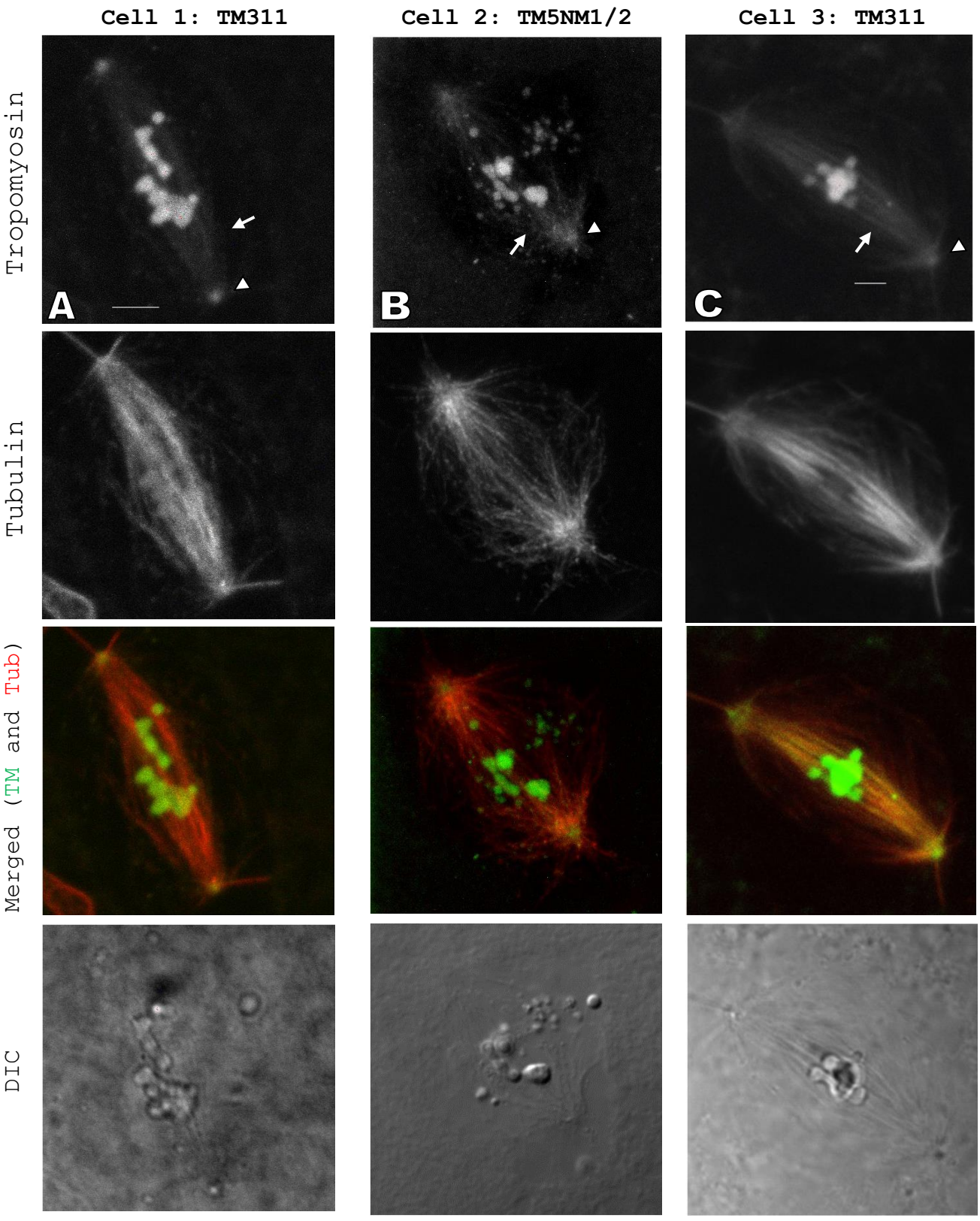
Cell 1: TM311
Cell 2: TM5NM1/2
Cell 3: TM311
Tropomyosin
Tubulin
Merged (TM and Tub)
DIC
A
B
C

Figure 35 – Three different cells stained for tropomyosin in prometaphase-I to metaphase-I stages of cell division. Spindle microtubules have been stained with YL ½ rat monoclonal antibody against tubulin followed by Alexa 594 goat-anti-rat immunoglobulin IgG. (A) cell 1: tropomyosin was stained with TM311 mouse monoclonal antibody against tropomyosin (1:200) followed by Alexa 488 goat-anti-mouse immunoglobulin IgM (1:150). (B) cell 2: tropomyosin was stained with TM5NM1/2 sheep polyclonal antibody against tropomyosin (1:100) followed by reconstituted Alexa 488 donkey-anti-sheep immunoglobulin IgG (H&L) (1:50). (C) cell 3: tropomyosin was stained with TM311 mouse monoclonal antibody against tropomyosin (1:100) followed by Alexa 488 goat-anti-mouse immunoglobulin IgM (1:100). Images of cells 1 and 3 were taken with Olympus Fluoview 300 confocal microscope (60X oil immersion objective; NA, 1.4). Images of cell 2 were taken with Olympus Fluoview 3000 confocal microscope (60X oil immersion objective; NA, 1.35). Tropomyosin localizes to the spindle, along kinetochore fibres (white arrow) and at the spindle poles (arrowhead). Bars, 5 µm.

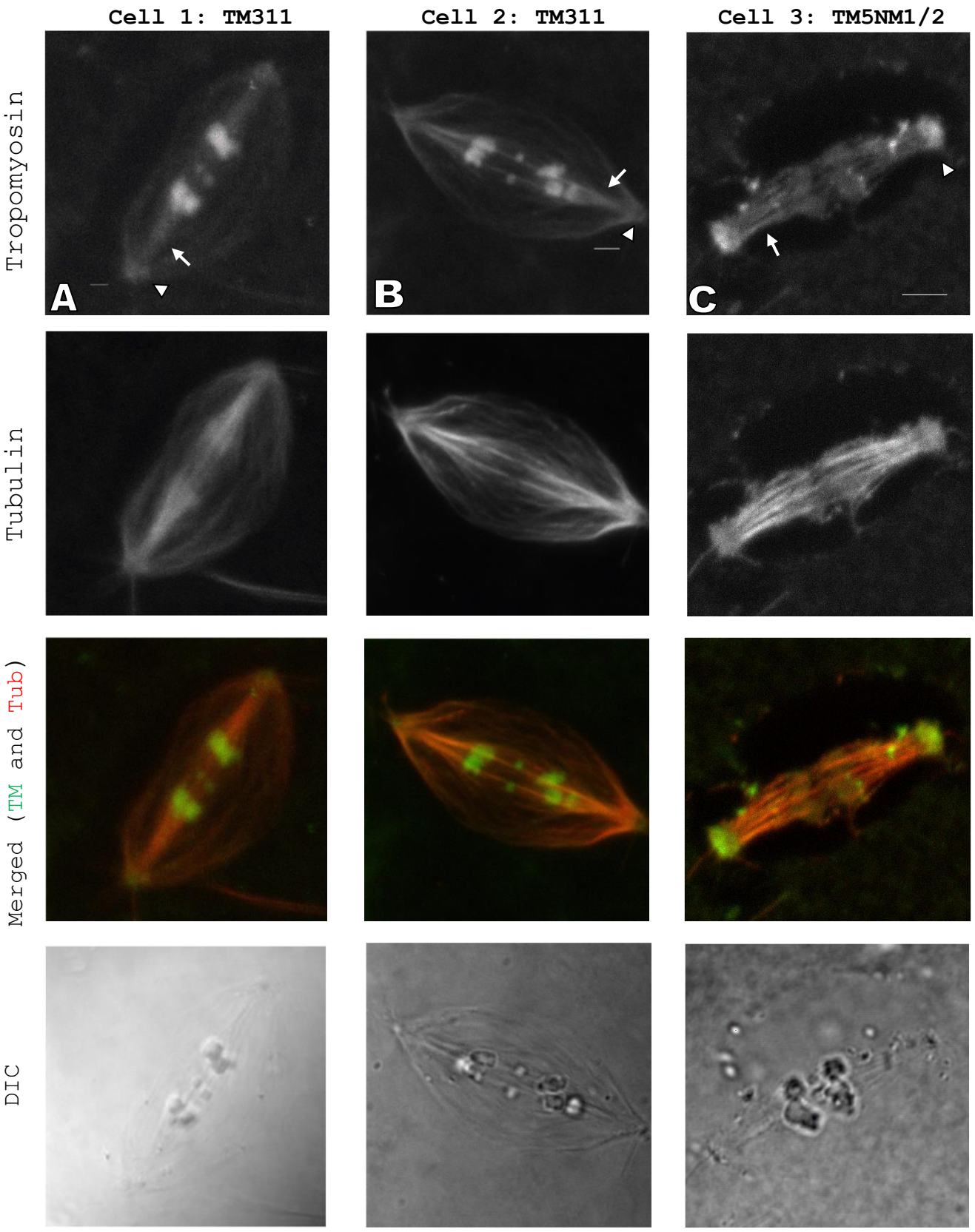
Cell 1: TM311
Cell 2: TM311
Cell 3: TM5NM1/2
Tropomyosin
Tubulin
Merged (TM and Tub)
DIC
A
B
C

Figure 36 – Three different cells stained for tropomyosin in anaphase-I, as autosomal half-bivalents move toward spindle poles. Spindle microtubules have been stained with YL ½ rat monoclonal antibody against tubulin followed by Alexa 594 goat-anti-rat immunoglobulin IgG. (A) cell 1 and (B) cell 2: tropomyosin was stained with TM311 mouse monoclonal antibody against tropomyosin (1:100) followed by Alexa 488 goat-anti-mouse immunoglobulin IgM (1:100). (C) cell 3: tropomyosin was stained with TM5NM1/2 sheep polyclonal antibody against tropomyosin (1:100) followed by reconstituted Alexa 488 donkey-anti-sheep immunoglobulin IgG (H&L) (1:50). Images were taken with Olympus Fluoview 300 confocal microscope (60X oil immersion objective; NA, 1.4). Tropomyosin localizes to the spindle, along kinetochore fibres (white arrow) and at the spindle poles (arrowhead). Bars, 5 µm.

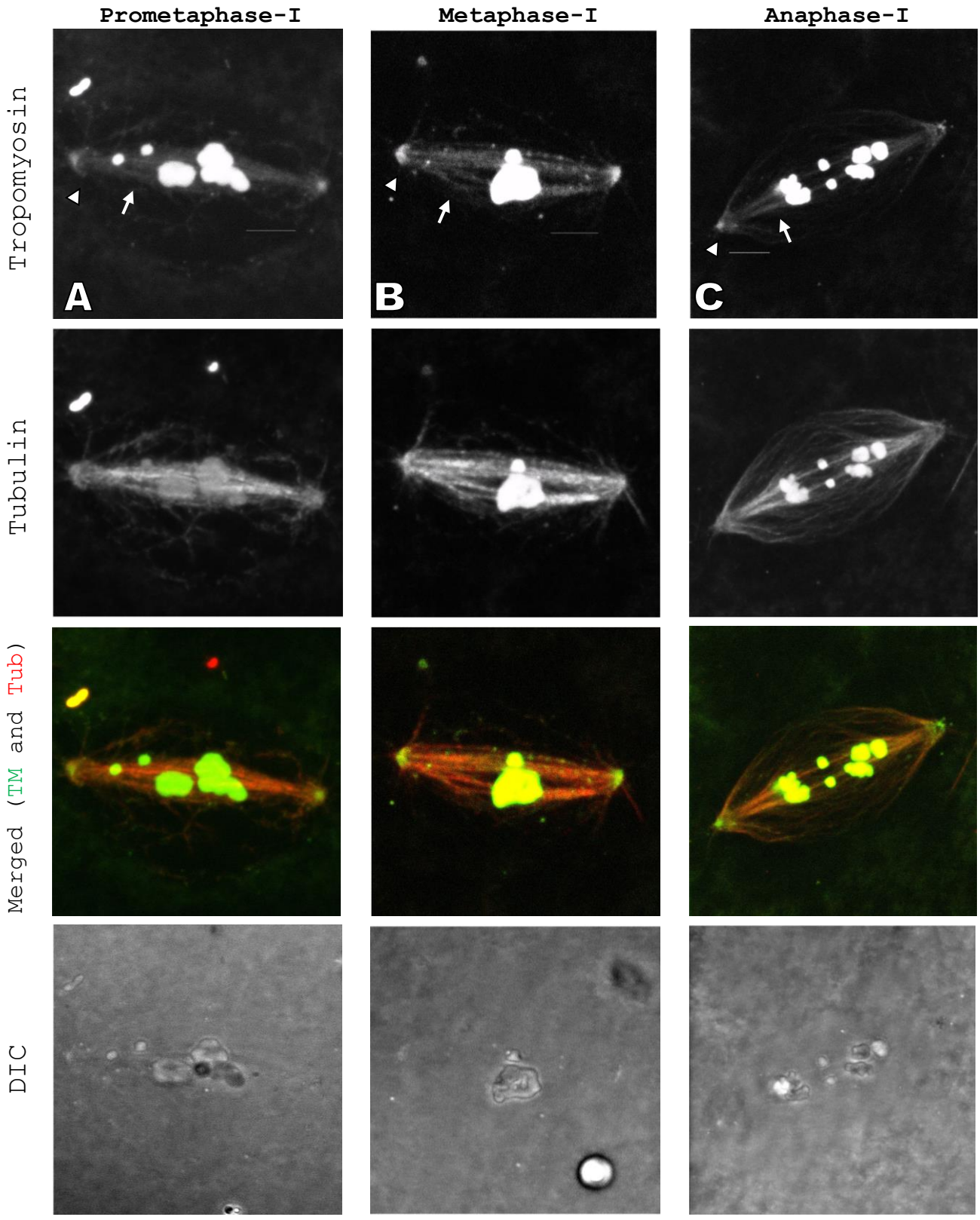
Prometaphase-I
Metaphase-I
Anaphase-I
Tropomyosin
Tubulin
Merged (TM and Tub)
DIC
A
B
C

Figure 37 – Three different cells stained for tropomyosin in prometaphase-I to anaphase-I stages of cell division. Spindle microtubules have been stained with YL ½ rat monoclonal antibody against tubulin followed by Alexa 594 goat-anti-rat immunoglobulin IgG. Tropomyosin was stained with TM311 mouse monoclonal antibody against tropomyosin (A, 1:200) (B, 1:200) (C, 1:100) followed by Alexa 488 goat-anti-mouse immunoglobulin IgM (A, 1:150) (B, 1:150) (C, 1:100). Images of were taken with LSM 700 Zeiss Observer Z.1 confocal microscope (40X oil immersion objective; NA, 1.3). Tropomyosin localizes to the spindle, along kinetochore fibres (white arrow) and at the spindle poles (arrowhead). Bars, 5 µm.

Non-constant poleward velocity during anaphase

In the cells of some testes, autosomal half-bivalents moved with non-constant poleward velocity during anaphase in Insect Ringer's. This occurred on a per animal, per testis basis, meaning that all of the cells within a single testis displayed non-constant poleward velocity. These kinetochores began anaphase with normal poleward velocities and after variable amounts of time, but before reaching the spindle poles, the kinetochores either slowed (n=13/72) or stopped moving (n=12/72) (Figure 38). After slowing, some kinetochores subsequently increased in speed to approximately 88% of their initial anaphase speed (n=11/13) or, after stopping, kinetochores resumed poleward movement at approximately 109% of their initial anaphase speed (n=12/12). A movement graph illustrating temporarily stopped movement during anaphase in Insect Ringer's has been included (Figure 39). Table 3 provides a summary of the average anaphase speeds in Insect Ringer's.

In order to account for this 'abnormality', control cells were recorded in testes prior to adding drug treatments. Only testes in which cells displayed constant poleward velocity during anaphase in Insect Ringer's were used for drug treatments.

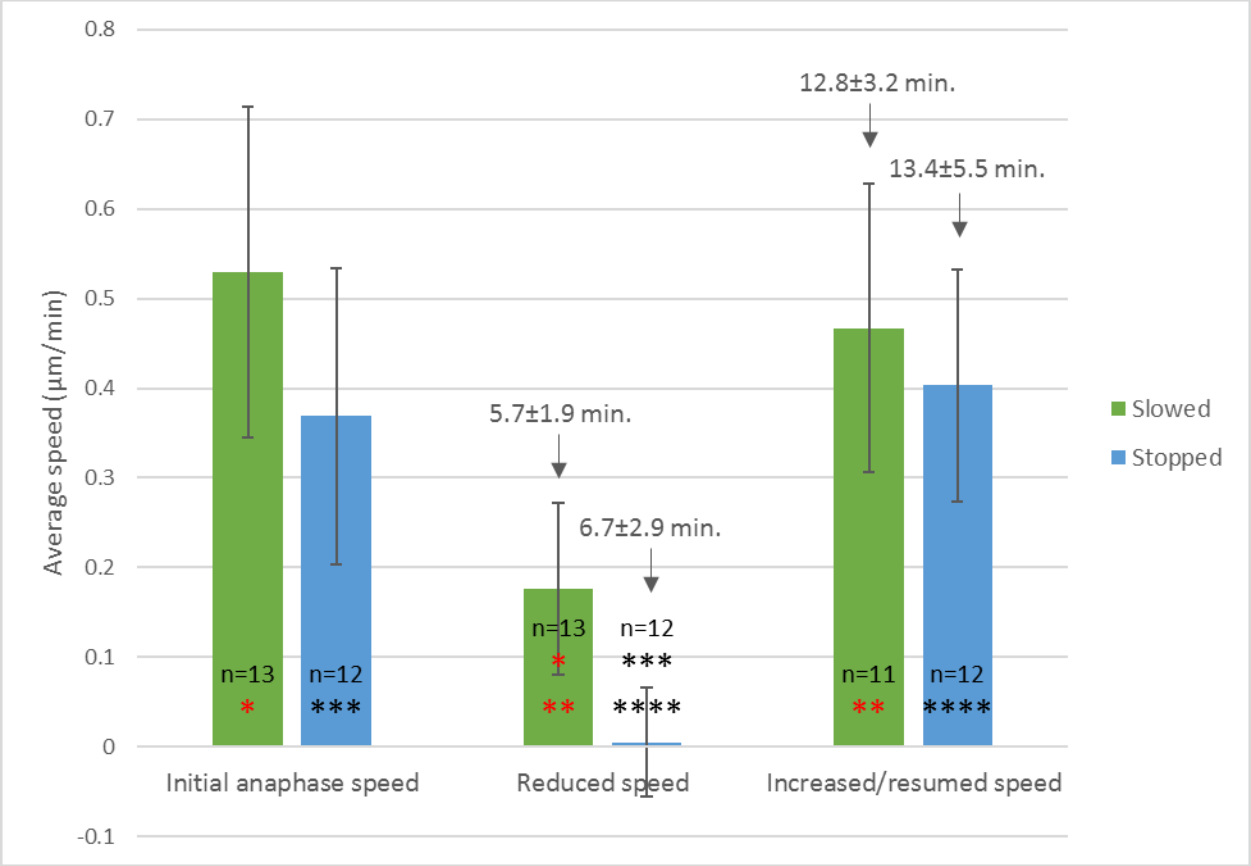

Figure 38 – Average speeds for kinetochores with non-constant poleward velocity in Insect Ringer's. Kinetochores sometimes slowed during anaphase in Insect Ringer's (n=13/72) (green). These kinetochores moved with an average initial speed of 0.53±0.2µm/min and then slowed to approximately 33% of their initial anaphase speed. Most of these kinetochores then increased in speed to approximately 88% of their initial anaphase speed (n=11/13). Kinetochores sometimes stopped during anaphase in Insect Ringer's (n=12/72) (blue). These kinetochores moved with an average initial speed of 0.37±0.2µm/min before stopping. After variable amounts of time, these kinetochores resumed poleward movement with an average speed of approximately 109% of their initial anaphase speed. Times indicate minutes after anaphase onset. Asterisks indicate significant differences in speed (*, $p<0.05$; **, $p<0.05$; ***, $p<0.05$; ****, $p<0.05$). Error bars represent SD. [n=number of kinetochores].

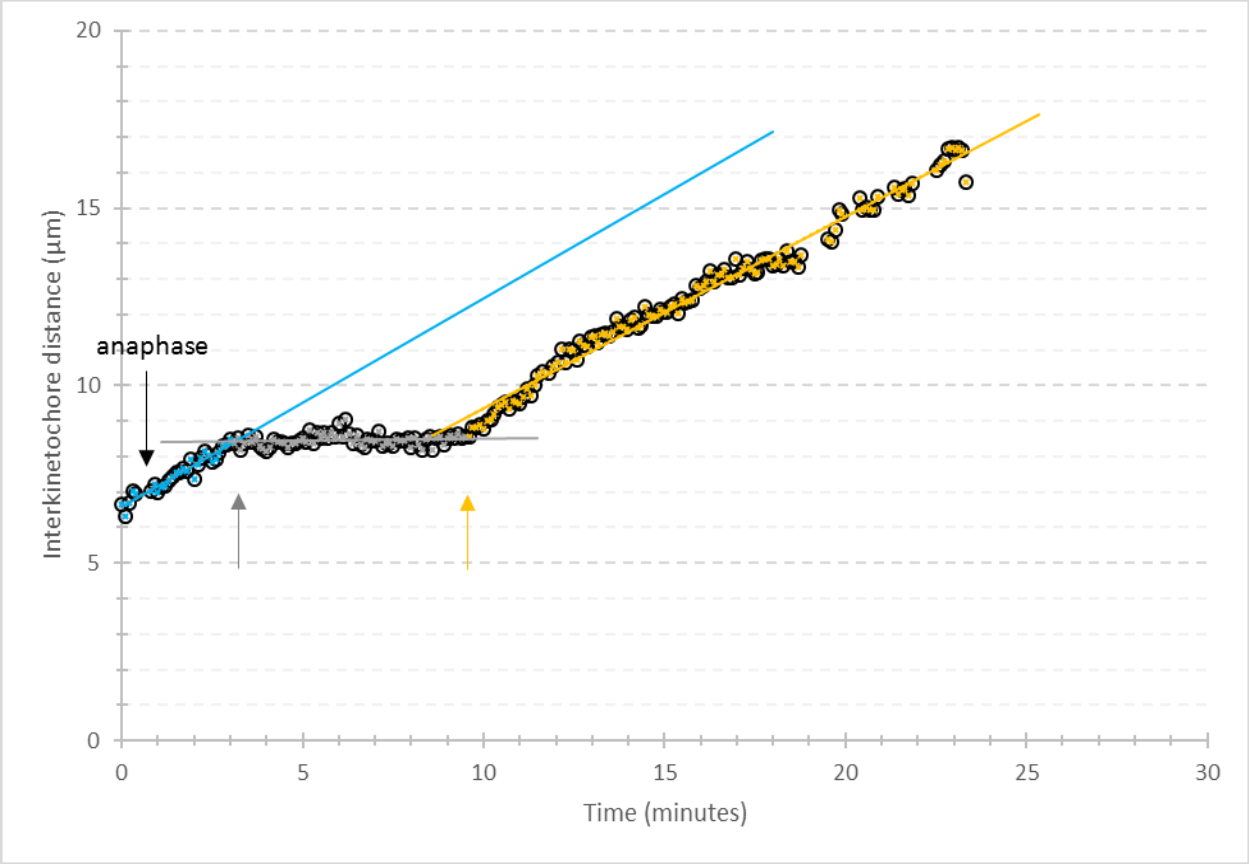

Figure 39 – Illustrating non-constant poleward velocity during anaphase in Insect Ringer's. The kinetochores move toward opposite spindle poles with an initial separation speed of 0.6µm/min. Approximately 2.5 minutes after anaphase onset, the kinetochores stop moving poleward (grey arrow). Approximately 6.5 minutes later, the kinetochores resumed poleward movement (yellow arrow) with a separation speed of 0.5µm/min. Chromosome arms stretched between these separating half-bivalents and then retracted within one minute of resumed poleward movement.

Table 3 – Average speeds during anaphase in Insect Ringer's for kinetochores with constant and non-constant poleward velocity. Times indicate minutes after anaphase onset. [n=number of kinetochores].

Treatment	Chromosome movement	Number of kt.		Speed (µm/min)		
				Initial anaphase speed (µm/min)	Reduced speed	Increased/ resumed speed
Insect Ringer's	Constant	47		0.50±0.22		
			Time (min)			
	Non-constant: slowed	13		0.53±0.18	0.18±0.096	0.47±0.16 [n=11/13]
			Time (min)		5.68±1.87	12.78±3.22
	Non-constant: stopped	12		0.37±0.16	Stopped	0.40±0.13
			Time (min)		6.72±2.94	13.39±5.51

Within the testis in which cells displayed non-constant poleward velocity during anaphase, chromosome arms were often seen stretching between pairs of separating half-bivalents. Each half-bivalent has four chromosome arms, that typically trail behind the kinetochore as it moves poleward. Of the trailing chromosome arms, one arm, from either one or both of the half-bivalents within a pair, often stretched between the half-bivalents as they moved toward opposite spindle poles. Most of these chromosome arms then retracted toward the kinetochore. Table 4 summarizes the occurrence of chromosome arm extension and retraction during anaphase chromosome movement in Insect Ringer's. A cell in which a chromosome arm can be seen stretching and retracting has also been included (Figure 40). In general, between pairs of separating half-bivalents in which one of both of the chromosomes moved with non-constant poleward velocity, at least one of the half-bivalents displayed chromosome arm extension (n=18/25) and retraction (n=13/25). Chromosome arms typically retracted within 3 minutes of resumed poleward movement (Table 5) and most kinetochores resumed movement within the same minute that chromosome arms retracted (n=8/12).

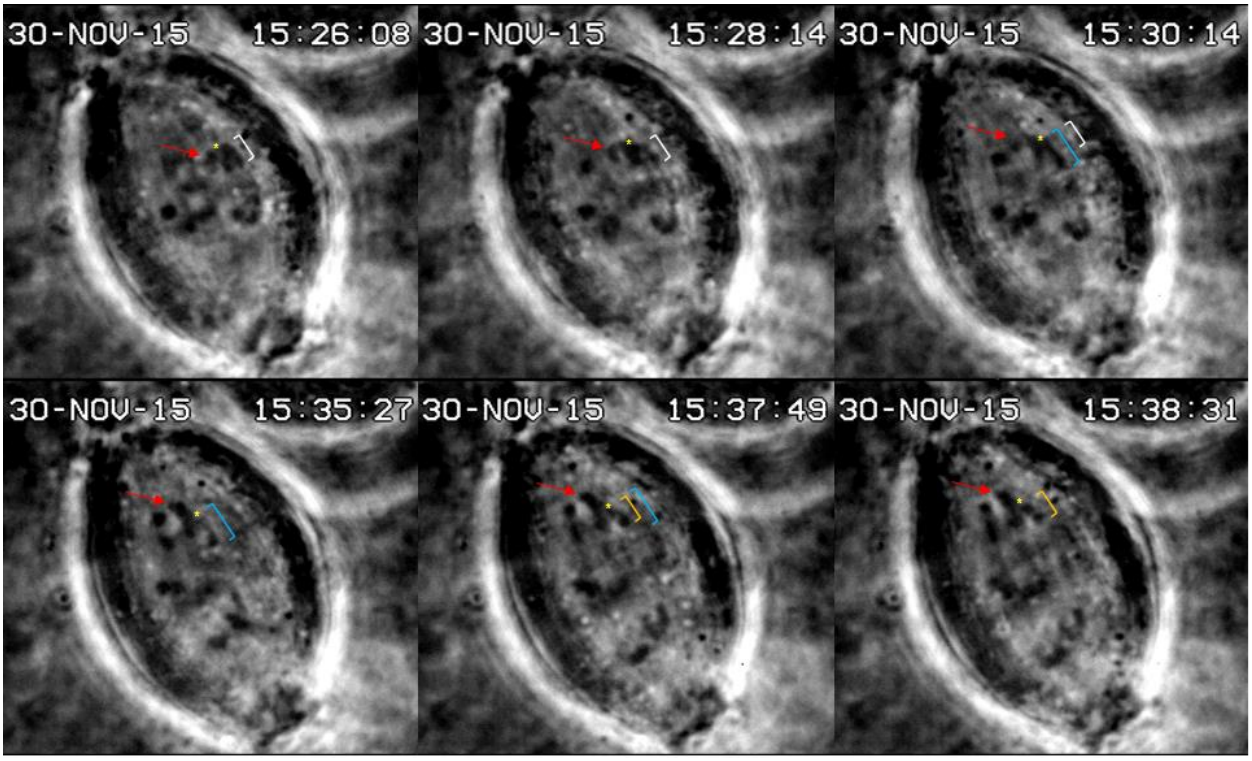

Figure 40 – Chromosome arm extension and retraction during non-constant anpahase movement in Insect Ringer's. Chromosome arms sometimes appeared to stretch between separating half-bivalents and then retract. In this cell, a chromosome arm (white bracket) of the top right half-bivalent can be seen stretching (blue bracket) and then retracting (orange bracket). This half-bivalent slowed down and then increased in speed during anaphase in IR. The chromosome arm retracted within the same minute that the half-bivalent increased in speed. The yellow asterisk represents the kinetochore and the red arrow points to a chromosome arm that moves ahead of the kinetochore during anaphase.

Table 4 – Summary of chromosome arm extensions and retractions for autosomal half-bivalents during anaphase in Insect Ringer's. A chromosome arm from one or both of the half-bivalents within a pair were seen stretching toward the opposite half-bivalent and then retracting during anaphase chromosome movement. Sometimes, chromosome arms could not be clearly seen stretching and retracting and have been included as "cannot conclude".

Anaphase movement	**Total number of kt.**	**Number of kinetochores**				
		No arm extension or retraction	Arm extension & retraction	Arm extension (retraction not visible)	Partner half-bivalent's arm extension & retraction	Cannot conclude
Constant	47	45	2			
Non-constant: slows or stops and then resumes	23	3	9	5	3	3
Non-constant: slows	2		1			1

Table 5 – Absolute difference in time between chromosome arm retraction and resumed poleward movement during anaphase in Insect Ringer's.

	Absolute difference in time between arm retraction and resumed movement (minutes) [n=12]					
	0 min.	0.5 min.	1 min.	1.5 min.	2 min.	3 min.
Number of kinetochores (with resumed movement)	5	1	2	2	1	1

Discussion

The purpose of my thesis was to investigate possible roles for tropomyosin during anaphase chromosome movement. This was accomplished by treating cells with inhibitory drugs against tropomyosin during anaphase and by localizing tropomyosin in the spindle. Overall, my results suggest that tropomyosin is present in the spindle and there is indication from inhibitors that tropomyosin might be involved. This was one of the first attempts to characterize spindle tropomyosin and test whether it plays a role during anaphase chromosome movement. With the exception of a recent study conducted in *Drosophila* S2 cells (Goins and Mullens 2015), tropomyosin has not been localized in the spindle or tested for functional roles during mitosis or meiosis.

Anaphase chromosome movement following drug treatments

Cells were treated with two different inhibitory drugs against tropomyosin during anaphase. These drugs, PD and TR100, inhibit tropomyosin through different mechanisms; however, they both ultimately result in actin filament disorganization and degraded actin filament function (Houle *et al.* 2003, Houle *et al.* 2007, Stehn *et al.* 2013). Previous experiments involving PD and TR100 showed their inhibitory effects after long incubation periods.

For example, cells with altered actin filament dynamics were incubated with PD for 1 hour (Houle *et al.* 2003, Houle *et al.* 2007) or were treated with TR100 for typically 24-hours, or at least 1 hour (Stehn *et al.* 2013). In my experiments, I tested the immediate (within several minutes) effects of these drugs on chromosome movement during anaphase.

PD treatment

PD inhibits tropomyosin phosphorylation and alters the actin microfilament system (Houle *et al.* 2003, Houle *et al.* 2007). Cells in anaphase were treated with PD at both low [50 µM] and high [100 µM] concentrations. PD altered movement in over 70% of the chromosomes studied. Immediately following PD treatment, affected kinetochores either slowed, slowed and then stopped, or stopped moving poleward. Usually, partner half-bivalents reacted the same (n=50/63 kinetochores). However, between cells and within the same cell, bivalent pairs reacted differently. The same pattern has been observed in crane-fly primary spermatocytes following treatment with inhibitory drugs against actin and myosin (Forer and Pickett-Heaps 1998, Silverman-Gavrila and Forer 2001, Sheykhani *et al.* 2013), in that, while partner half-bivalents typically react the same to anti-actin and anti-myosin drugs, different bivalent pairs may react differently. This variability may be accounted for by functional

differences amongst individual kinetochore fibres (reviewed in Xie and Forer 2008). For example, kinetochore microtubules within the same spindle may originate from either the kinetochore or the centrosome and individual kinetochore fibres display different rates of tubulin flux. Thus, individual kinetochore fibres within the same spindle display different dynamics and possibly different force generating mechanisms. These data suggest that different bivalent pairs may use different force generating mechanisms to move chromosomes and that different combinations of these mechanisms can be used within the same spindle (Forer and Pickett-Heaps 1998, Xie and Forer 2008). This explains why different bivalent pairs reacted differently to PD.

Furthermore, stopped kinetochores often resumed movement while still in PD (n=20/28). Kinetochores also resume movement after stopping in the presence of anti-actin and anti-myosin drugs (Forer and Pickett-Heaps 1998, Silverman-Gavrila and Forer 2001, Fabian and Forer 2005, Sheykhani *et al.* 2013). It appears that chromosomes are able to resume movement because crane-fly primary spermatocytes have redundant mechanisms for chromosome movement and, when one mechanism is inhibited, chromosomes can switch to another. This was tested by Fabian and Forer (2005) who showed that chromosomes normally use actin-based mechanisms

for anaphase movement but when actin is removed in early prometaphase, producing actin-free spindles, anaphase chromosome movement proceeds normally. This suggests while chromosomes normally may use actin-based mechanisms for anaphase movement, they can use alternative mechanisms when actin is not present or inhibited. Redundant mechanisms for chromosome movement are likely, considering the fundamental importance of chromosome motility during cell division, in which faithful chromosome segregation is necessary for cell survival.

Since PD inhibits tropomyosin phosphorylation (Houle *et al.* 2003, Houle *et al.* 2007) and it has been shown here to alter chromosome movement during anaphase, this suggests that tropomyosin phosphorylation is involved in anaphase chromosome movement. Tropomyosin phosphorylation seems to be involved in altering the actin-tropomyosin complex, which may have implications during anaphase chromosome movement. Specifically, tropomyosin phosphorylation stiffens the regions of head-to-tail overlap of tropomyosin molecules (Lehman *et al.* 2015). Rather than altering the binding capacity of tropomyosin for F-actin, tropomyosin phosphorylation therefore alters the head-to-tail binding of contiguous tropomyosin molecules along actin filaments. Furthermore, actin-activated myosin-ATPase activity is significantly higher in the presence of phosphorylated

tropomyosin compared to non-phosphorylated tropomyosin (Heeley *et al.* 1989). This may explain why chromosome movement was altered following PD treatment. If PD inhibited tropomyosin phosphorylation, then chromosome movement may have been affected because of reduced levels of actin-activated myosin-ATPase activity along kinetochore fibres. It is therefore worthwhile to investigate whether altered anaphase chromosome movement, following PD treatment, is due to inhibiting tropomyosin phosphorylation. This can be determined by measuring the levels of tropomyosin phosphorylation with antibodies specific to phosphorylated and non-phosphorylated forms of tropomyosin. Similar experiments have been conducted in crane-fly primary spermatocytes in which myosin phosphorylation levels along kinetochore fibres were reduced by ML-7 and Y 27632 (Sheykhani *et al.* 2013).

TR100 treatment

TR100 is a specific inhibitor against tropomyosin isoforms containing the 9d exon sequence expressed at the protein level (Stehn *et al.* 2013). It negates tropomyosin from conferring actin filament stability and disrupts the actin microfilament system by binding directly to tropomyosin. Cells in anaphase were treated with various concentrations of TR100, ranging from 25 µM to 100 µM. When added during anaphase, approximately 66%

of the chromosomes studied showed no effect following TR100 treatment. However, approximately 33% of chromosomes slowed, stopped or stopped after a few minutes. This data will be discussed in the following section with respect to and in consideration of other cytoskeletal effects following TR100 treatment.

Cells that were treated with TR100 showed additional cytoskeletal effects, indicating that this drug alters the actin microfilament system of crane-fly primary spermatocytes. Firstly, some cells exhibited membrane blebbing following TR100 treatment. Membrane blebbing is typically associated with a loss of microfilament integrity and apoptosis (Coleman *et al.* 2001). Membrane blebbing has also been observed following PD treatment (Houle *et al.* 2003, Houle *et al.* 2007) although this was not observed here. Membrane blebbing suggests that TR100 may affect the actin microfilament system in crane-fly primary spermatocytes by inhibiting tropomyosin.

Secondly, cleavage furrows were inhibited by TR100. In control conditions, cleavage furrows typically appeared after 34 minutes following anaphase onset. However, in 80% of cells treated with TR100, cleavage furrows did not appear. In one cell, a cleavage furrow appeared, ingressed for a few minutes but then quickly regressed and did not cleave. This suggests

that the contractile mechanism involved in cleavage furrow ingression is inhibited by TR100.

Cleavage furrows ingress during cytokinesis, through an actomyosin based contractile mechanism (Schroeder 1973, Fujiwara and Pollard 1976, Fujiwara *et al.* 1978, Sanger and Sanger 1980, Komatsu *et al.* 2000, Vavylonis *et al.* 2008). The data presented here suggests that cleavage furrow ingression may depend on tropomyosin and that TR100 inhibits tropomyosin from conferring actin filament function in the contractile ring. Similar results were obtained in crane-fly primary spermatocytes treated with anti-myosin drugs (Silverman-Gavrila and Forer 2001). Briefly, when added after cleavage furrow initiation, BDM inhibited further ingression. After wash out, the cleavage furrow began to ingress again but then quickly regressed. In general, BDM and ML-7, which reduce myosin phosphorylation, prevent cleavage furrow ingression (Silverman-Gavrila and Forer 2001).

Lastly, bunches of actin filaments were often seen protruding at the spindle poles prior to anaphase onset and are referred to as "actin fingers" (Xie and Forer 2008). As early as 2-3 minutes following TR100 treatment, these actin fingers began to change shape. They became progressively thicker and shorter, with gross changes in the actin fingers appearing approximately 20 minutes after treatment with TR100. Eventually, the actin

fingers disappeared from most of the cells in which fingers were present prior to TR100 treatment. Overall, these data suggest that TR100 affects the actin microfilament system in crane-fly primary spermatocytes, presumably by inhibiting tropomyosin and preventing tropomyosin from conferring actin filament stability.

Taken together, the data presented here suggest that TR100 affects the actin microfilament system of crane-fly primary spermatocytes and that anaphase chromosome movement may be largely unaffected because of timing constraints. In general, not all chromosomes studied during anaphase are affected by inhibitory drugs, such as those against actin and myosin, possibly because of redundant mechanisms for chromosome movement (Forer and Pickett-Heaps 1998, Silverman-Gavrila and Forer 2001, Fabian and Forer 2005, Xie and Forer 2008, Sheykhani *et al.* 2013). However, PD affects chromosome movement in over 70% of the chromosomes studied during anaphase. This suggests that tropomyosin is involved in anaphase chromosome movement.

In consideration that TR100 affected other cytoskeletal functions, especially those involving actin filaments, it seems likely that chromosome movement was unaffected in 66% of the chromosomes studied during anaphase because of time constraints. Cells were treated with TR100 after anaphase onset, as autosomal half-bivalents moved toward the spindle poles. By the time that

TR100 permeated the cell and inhibited tropomyosin, chromosomes may have reached or neared the spindle poles. Previous studies involving TR100 have shown that it affects actin filament dynamics after incubation periods of several hours, ranging from 1-24 hours (Stehn *et al.* 2013, Bonello *et al.* 2016). In my experiments, the immediate effects (within several minutes) of TR100 were tested. Furthermore, TR100 binds to free tropomyosin molecules that are not already bound actin filaments (Bonello *et al.* 2016). Therefore, tropomyosin molecules would have to be incorporated into the kinetochore fibres following TR100 treatment, in order to affect actin filaments along the kinetochore fibres. Together, this suggests that TR100 may not have robust effects on chromosome movement when added during anaphase, due to the limited time during which TR100 can affect tropomyosin along kinetochore fibres. In order to test this, TR100 can be applied in late prometaphase-I to metaphase-I. The data presented here, specifically changes in the actin fingers, suggest that TR100 may take several minutes to affect the actin filament integrity. Therefore, if TR100 is added before anaphase onset, there may be enough time for TR100 to bind to tropomyosin molecules before they are incorporated into kinetochore fibres. These chromosomes may display abnormal anaphase movement if they use a mechanism involving tropomyosin.

Tropomyosin localization in the spindle

Tropomyosin was localized in the spindles of crane-fly primary spermatocytes using two different antibodies against tropomyosin. Tropomyosin isoforms display varying degrees of reactivity toward different antibodies but, generally, antibodies can be classified as binding to low molecular weight (LMW) or high molecular weight (HMW) isoforms (Schevzov *et al.* 2005, Schevzov *et al.* 2011). TM311 binds to the 1a exon sequence of HMW tropomyosin isoforms and TM5NM1/2 binds to the 9d exon sequence of HMW and LMW tropomyosin isoforms (Schevzov *et al.* 2005, Schevzov *et al.* 2011).

From prometaphase-I to anaphase-I, tropomyosin localized at the spindle poles and along kinetochore fibres, as observed with both TM311 and TM5NM1/2. Tropomyosin was anticipated to colocalize with spindle actin. Although it might be possible to test this, I could not do so because of technical difficulties (see Materials and Methods). Nonetheless, tropomyosin localized in places where actin would be expected. For example, tropomyosin localized along kinetochore fibres, where actin has been shown to localize (e.g. Xie and Forer 2008). In addition, tropomyosin was observed at the spindle poles. During cell division, the centrosome replicates and one centrosome moves to each spindle pole (Wade 2009). The centrosome is a microtubule

organizing center; however, it also functions as an actin-filament organizing center (Farina *et al.* 2016). Briefly, isolated centrosomes, are able to polymerize filaments from actin monomers, similarly to how they polymerize microtubules from tubulin dimers. Tropomyosin affects actin filament polymerization (reviewed in Cooper 2002) so it would be likely that tropomyosin localizes to actin-organizing centers, such as the centrosomes at the spindle poles. Overall, the data suggests that tropomyosin is present in the spindle of crane-fly primary spermatocytes, including along kinetochore fibres, where it would be involved in anaphase chromosome movement.

Chromosome movement and tropomyosin function

Tropomyosin was hypothesized to be involved in chromosome movement during anaphase primarily because actin and myosin are involved in anaphase chromosome movement and tropomyosin mediates actomyosin interactions. A recent study has shown that tropomyosin localizes to spindle poles and to the kinetochores in the mitotic spindle of *Drosophila* S2 cells (Goins and Mullens 2015). When this tropomyosin isoform was mutated, so that it could no longer be phosphorylated, anaphase chromosome movement was unaffected. These results contradict the data presented here, which suggest that inhibiting tropomyosin phosphorylation affects anaphase chromosome movement. However, in the *Drosophila*

S2 cells, tropomyosin phosphorylation was inhibited by mutating specific amino acid residues that differed from those discussed in regard to PD (Houle *et al.* 2003, Houle *et al.* 2007). Furthermore, tropomyosin phosphorylation levels should be tested in order to determine whether anaphase chromosome movement is altered when tropomyosin phosphorylation is affected along kinetochore fibres. Conversely, when the tropomyosin isoform was mutated in putative binding sites for troponin, anaphase chromosome movement was altered (Goins and Mullens 2015). Although this mutated tropomyosin still localized to the spindle poles and to the kinetochores, chromosomes exhibited kinetochore fibre attachment defects, unfocused spindle poles, delayed anaphase progression and abnormal chromosome segregation, for example chromosomes often missegregated. These results suggest that tropomyosin may function in the spindle through a troponin-tropomyosin based mechanism. Potentially, this troponin-tropomyosin based mechanism may function in the spindle similarly to how troponin and tropomyosin function in striated muscle.

Future studies regarding the role of tropomyosin during anaphase chromosome movement should investigate tropomyosin phosphorylation levels along kinetochore fibres following PD treatment as well as treating cells with TR100 during

prometaphase-I to metaphase-I. This will test whether chromosomes segregate normally when tropomyosin is inhibited prior to anaphase onset. Furthermore, it may be worthwhile to investigate whether another muscle protein, troponin, is also involved in anaphase chromosome movement.

Chromosome arms and non-constant poleward velocity

In the testes of some animals, cells display non-constant poleward velocity during anaphase chromosome movement that is associated with chromosome arm stretching and retracting. These half-bivalents slow down or stop during anaphase and then, after variable amounts of time, resume poleward movement. Most of these half-bivalents have chromosome arms that appear to stretch or extend toward the partner half-bivalent and then retract toward the kinetochore. Chromosome arm retraction often occurs within the same minute that poleward movement resumes or, at most, within three minutes of resumed movement. This suggests that chromosome arm extension and retraction is associated with non-constant poleward velocity during anaphase chromosome movement. In particular, there may be a force being exerted between chromosome arms of separating half-bivalents that opposes poleward acting forces and that results in non-constant poleward velocity. A possible explanation for chromosome arm

stretching and retracting may be faulty "tethers" attaching chromosome arms of separating half-bivalents.

Elastic tethers extend between chromosome arms of separating half-bivalents and exert a backward force that opposes pole directed forces (LaFountain *et al.* 2002, Sheykhani *et al.* 2017, Forer *et al.* 2017). Normally, tethers do not affect constant poleward velocity; however, it may be possible that if the tether elasticity is somehow altered, then the chromosomes will move with non-constant velocity. This seems plausible considering that chromosome arms are often seen stretching and retracting in half-bivalents that slow or stop and then resume movement. The tether extending between chromosome arms is composed of titin, which is a muscle protein associated with sarcomere elasticity (see Fabian *et al.* 2007). Although this explanation is very speculative, it may explain why the cells of some animal testes have chromosomes that move with non-constant poleward velocity. As previously mentioned, in order to account for this 'abnormality', only testes in which cells displayed constant poleward velocity were used for drug treatments.

References

Alahyan M, Webb MR, Marston SB, El-Mexgueldi M. 2006. The mechanism of smooth muscle caldesmon-tropomyosin inhibition of the elementary steps of the actomyosin ATPase. *J Biol Chem* 281: 19433-19448.

Alessi DR, Cuenda A, Cohen P, Dudley DT, Saltie AR. 1995. PD 098059 is a specific inhibitor of the activation of mitogen-activated protein kinase kinase *in vitro* and *in vivo*. *J Biol Chem* 270: 27489-27494.

Bailey K. 1946. Tropomyosin: a new asymmetric protein component of muscle. *Nature* 157: 368-369.

Begg DA, Rodewald R, Rebhun LI. 1978. The visualization of actin filament polarity in thin sections - evidence for the uniform polarity of membrane-associated filaments. *J Cell Bio* 79: 846-852.

Blanchoin L, Pollard TD, Hitchcock-DeGregori. 2001. Inhibition of the Arp2/3 complex-nucleated actin polymerization and branch formation by tropomyosin. *Curr Biol* 11: 1300-1304.

Bonello TT, Janco M, Hook J, Byun A, Appaduray M, Dedova I, Hitchcock-DeGregori S, Hardeman EC, Stehn JR, Böcking T, Gunning PW. 2016. A small molecule inhibitor of tropomyosin dissociates actin binding from tropomyosin-directed regulation of actin dynamics. *Sci Rep* 6: 19816

Bracchiocchi C and Lehrer SS. 2002. Ca^{2+}-Induced movement of tropomyosin in skeletal muscle filaments observed by multi-site FRET. *Biophys J* 82: 1524-1536.

Broschat KO, Weber A, Burgess DR. 1989. Tropomyosin stabilizes the pointed end of actin filaments by slowing depolymerization. *Biochem* 28: 8501-8506.

Brown SW and Nelson-Rees WA. 1961. Radiation analysis of a lecanoid genetic system. *Genetics* 46: 983-1007.

Bryce NS, Schevzov G, Ferguson V, Percival JM, Lin JJ, Matsumura F, Bamburg JR, Jeffrey PL, Hardeman EC, Gunning P, Weinberger RP. 2003. Specification of actin filament

function and molecular composition by tropomyosin isoforms. *Mol Biol Cell* 14: 1002-1016.

Cassimeris LU, Walker RA, Pryer NK, Salmon ED. 1987. Dynamic instability of microtubules. *Bioessays* 7: 149-154.

Cassimeris L, Inoue S, Salmon ED. 1988. Microtubule dynamics in the chromosomal spindle fibre: analysis by fluorescence and high-resolution polarization microscopy. *Cell Motil Cytoskel* 10: 185-196.

Coleman ML, Sahai EA, Yeo M, Bosch M, Dewar A, Olson MF. 2001. Membrane blebbing during apoptosis results from caspase-mediated activation of ROCK I. *Nature Cell Biol* 3: 339-345.

Compton DA. 2007. Chromosome orientation. *J Cell Biol* 179: 179-181.

Cooper JA. 2002. Actin dynamics: tropomyosin provides stability. *Curr Biol* 12: R523- R525.

Dietz R. 1972. Anaphase behaviour of inversions in living crane-fly spermatocytes. *Chromosome Today* 3: 70-85.

Downing KH and Nogales E. 1998. Tubulin and microtubule structure. *Curr Opin Cell Biol* 10: 16-22.

Drees B, Brown C, Barrell, BG, Bretscher A. 1995. Tropomyosin is essential in yeast, yet the TPM1 and TPM2 products perform distinct functions. *J Cell Biol* 128: 383-392.

Ephrussi B and Beadle GW. 1936. A technique of transplantation for *Drosophila*. *Am Nat* 70: 218-25.

Fabian L, Forer A. 2005. Redundant mechanisms for anaphase chromosome movements: crane-fly spermatocyte spindles normally use actin filaments but can also function without them. *Protoplasma* 225: 169-184.

Fabian L, Troscianczuk J, Forer A. 2007. Calyculin A, an enhancer of myosin, speeds up anaphase chromosome movement. *Cell & Chromosome* 6:1

Fabian L, Xia X, Venkitaramani DV, Johansen KM, Johansen J, Andrew DJ, Forer A. 2007. Titin in insect spermatocyte spindle fibers associates with microtubules, actin, myosin and the matrix proteins skeletor, megator and chromator. *J Cell Sci* 120: 2190-2204.

Farina F, Gaillard J, Guerin C, Coute Y, Sillibourne J, Blanchoin L, Thery M. 2016. The centrosome is an actin-organizing centre. *Nature Cell Biol* 18: 65-77.

Fitts RH. 2008. The cross-bridge cycle and skeletal muscle fatigue. *J Apply Physiol* 104: 551-558.

Forer A. 1974. Actin filaments – their universal occurrence and association with cell motility. *J Int Res* 2: 12-13.

Forer A and Zimmerman AM. 1976. Spindle birefringence of isolated mitotic apparatus analyzed by treatments with cold, pressure, and diluted isolation medium. *J Cell Sci* 20: 329-339.

Forer A. 1980. Chromosome movements in the meiosis of insects, especially crane-fly spermatocytes. In Blackman RL, Hewitt GM, Ashburner M, editors: "Insect cytogenetics". Oxford; Boston: Published for the Royal Entomological Society by Blackwell Scientific Publications; pp. 85-95.

Forer A. 1982a. Actin localization within cells by electron microscopy. In Wilson L, editor: "Methods in cell biology". Vol. 25. London: Academic Press; pp. 131-142.

Forer A. 1982. Crane fly spermatocytes and spermatids: a system for studying cytoskeletal components. In Wilson L, editor: "Methods in cell biology". Vol. 25. London: Academic Press; pp. 227-252.

Forer A, Pickett-Heaps JD. 1998. Cytochalasin D and latrunculin affect chromosome behaviour during meiosis in crane-fly spermatocytes. *Chromosome Res* 120: 533-549.

Forer A, Spurck T, Pickett-Heaps JD, Wilson PJ. 2003. Structure of kinetochore fibres in crane-fly spermatocytes after irradiation with an ultraviolet microbeam: neither

microtubules nor actin filaments remain in the irradiated region. *Cell Motil Cytoskel* 56: 173-192.

Forer A, Spurk T, Pickectt-Heaps. 2007. Actin and myosin inhibitors block elongation of kinetochore fibre stubs in metaphase crane-fly spermatocytes. *Protoplasma* 232: 79-85.

Forer A, Ferraro-Gideon J, Berns M. 2013. Distance segregation of sex chromosomes in crane-fly spermatocytes studied using laser microbeam irradiations. *Protoplasma* 250: 1045-1055.

Forer A, Duquette ML, Paliulis LV, Fegaras E, Ono M, Preece D, Berns MW. 2017 Elastic 'tethers' connect separating anaphase chromosomes in a broad range of animal cells. *Eur J Cell Biol*: article in press

Fujiwara K and Pollard TD. 1976. Fluorescent antibody localization of myosin in the cytoplasm, cleavage furrow, and the mitotic spindle of human cells. *J Cell Biol* 71: 848-875.

Fujiwara K, Porter ME, Pollard TD. 1978. Alpha-actinin localization in the cleavage furrow during cytokinesis. *J Cell Biol* 79: 268-275.

Gadde S, Heald R. 2004. Mechanisms and molecules of the mitotic spindle. *Curr Biol* 14: R797-R805.

Goins LM, Mullins RD. 2015. A novel tropomyosin isoform functions at the mitotic spindle and golgi in *Drosophila*. *Molec Biol Cell* 26: 2491-2504.

Gorbsky GJ, Sammak PJ, Borisy GG. 1987. Chromosomes move poleward in anaphase along stationary microtubules that coordinately disassembly from their kinetochore ends. *J Cel Biol* 104: 9-18.

Graceffa P. 1987. Evidence for interaction between smooth muscle tropomyosin and caldesmon. *FEBS Letters* 218: 139-142.

Grego S, Cantillana V, Salmon ED. 2001. Microtubule treadmilling in vitro investigated by fluorescence speckle and confocal microscopy. *Biophys J* 66-78.

Gunning PW, Schevzov G, Kee AJ, Hardeman EC. 2005. Tropomyosin isoforms: divining rods for actin cytoskeleton function. *Trends Cell Biol* 15: 333-340.

Gunning P, O'Niell G, Hardeman E. 2008. Tropomyosin-based regulation of the actin cytoskeleton in time and space. *Physiol Rev* 88: 1-35.

Gunning PW, Hardeman EC, Lappalainen P, Mulvihill DP. 2015. Tropomyosin – master regulator of actin filament function in the cytoskeleton. *J Cell Sci* 128: 2965-2974.

Henderson SA. 1970. The time and pace of meiotic crossing-over. *Ann Rev Gen* 4: 295-324.

Heeley DH, Watson MH, Mak AS, Dubord P. 1989. Effect of phosphorylation on the interaction and functional properties of rabbit striated muscle αα-tropomyosin. *J Biol Chem* 264: 2424-2430.

Hillberg L, Zhao Rathje LS, Nyakern-Meazza M, Helfand B, Goldman RD, Schutt CE, Lindberg U. 2006. Tropomyosins are present in lamellipodia of motile cells. *Eur J Cell Biol* 85: 399-409.

Hitchcock SE. 1975. Regulation of muscle contraction: binding of troponin and its components to actin and tropomyosin. *Eur J Biochem* 52: 255-263.

Houle F, Rousseau S, Morrice N, Luc M, Mongrain S, Turner CE, Tanaka S, Moreau P, Huot J. 2003. Extracellular signal-related kinase mediates phosphorylation of tropomyosin-I to promote cytoskeleton remodeling in response to oxidative stress: impact on membrane blebbing. *Molec Biol Cell* 14: 1418-1432.

Houle F, Poirier A, Dumaresq J, Huot J. 2007. DAP kinase mediates the phosphorylation of tropomyosin-I downstream of the ERK pathway, which regulates the formation of stress fibres in response to oxidative stress. *J Cell Sci* 120: 3666-3677.

Hughes AF and Swann MM. 1948. Anaphase movement in the living cell. *J Exp Biol* 25: 45-70.

Huxley HE. 1953. Electron microscope studies of the organization of the filaments in striated muscle. *Biochemica et Biophysica Acta* 12: 387-395.

Huxley HE and Hanson J. 1957. Quantitative studies on the structure of cross-striated myofibrils. *Biochemica et Biophysica Acta* 23: 229-249.

Huxley HE. 1958. The contraction of muscle. *Sci Am* 199: 66-83.

Huxley HE. 1963. Electron microscope studies on the structure of natural and synthetic protein filaments from striated muscle. *J Mol Biol* 7: 281-308.

Huxley HE. 1969. The mechanism of muscular contraction. *Science* 164: 1356-1366.

Huxley HE. 1973. Muscular contraction and cell motility. *Nature* 243: 445-449.

Inoue S. 1953. Polarization of optical studies of the mitotic spindle I The demonstration of spindle fibres in living cells. *Chromosoma.* 5: 487-500.

Inoue S. 1988. The living spindle. *Zool Sci* 5: 529-538.

Ishikawa H, Bischoff R and Holtzer H. 1969. Formation of arrowhead complexes with heavy meromyosin in a variety of cell types. *J Cell Biol* 43: 321-328.

Kamm KE and Stull JT. 1985. The function of myosin and myosin light chain kinase phosphorylation in smooth muscle. *Ann Rev Pharmacol Toxicol* 25: 593-260.

Kapoor TM, Lampson MA, Hergert P, Cameron L, Cimini D, Salmon ED, McEwan BF, Khodjakov A. 2006. Chromosomes can congress to the metaphase plate before biorientation. *Science* 311: 388-391.

Karlik CC and Fyrberg EA. 1986. Two *Drosophila melanogaster* tropomyosin genes: structural and functional aspects. *Mol Cell Biol* 6: 1965-1973.

Kraft T, Mahlmann E, Mattei T, Brenner B. 2005. Initiation of the power stroke in muscle: insights from the phosphate analog AlF_4. Proc Natl Acad Sci USA 102: 13861-13866.

Komatsu S, Yano T, Shibata M, Tuft RA, Ikebe M. 2000. Effects of the regulatory light chain phosphorylation of myosin II on mitosis and cytokinesis of mammalian cells. *J Biol Chem* 275: 34512-34520.

LaFountain JR Jr., Cole RW, Rieder CL. 2002. Partner telomeres during anaphase in crane-fly spermatocytes are connected by an elastic tether than exerts a backward force and resists poleward motion. *J Cell Sci* 115: 1541-1549.

LaFountain JR Jr., Cohan CS, Siegel AJ, LaFountain DJ. 2004. Direct visualization of microtubule flux during metaphase and anaphase in crane-fly spermatocytes. *Molec Biol Cell* 15: 5724-5732.

Lazarides E. 1976. Actin, α-actinin, and tropomyosin interaction in the structural organization of actin filaments in nonmuscle cells. *J Cell Biol* 68: 202-219.

Lees-Miller JP and Helfman DM. 1991. The molecular basis for tropomyosin isoform diversity. *BioEssays* 13: 429-437.

Lehman W, Medlock G, Li XE, Suphamungmee W, Tu AY, Schmidtmann A, Ujfalusi Z, Fischer S, Moore JR, Geeves MA, Regnier M. 2015. Phosphorylation of Ser283 enhances the stiffness of the tropomyosin head-to-tail overlap domain. Arch Biochem Biophys 571: 10-15.

Liu H, Bretscher A. 1989. Disruption of the single tropomyosin gene in yeast results in the disappearance of actin cables from the cytoskeleton. *Cell* 57: 233-242.

Maddox P, Straight A, Coughlin P, Mitchison TJ, Salmon ED. 2003. Direct observation of microtubule dynamics at kinetochores in *Xenopus* extract spindles. *J Cell Biol* 162: 377-382.

Maiato H, Khodjakov A, Reider CL. 2005. *Drosophila* CLASP is required for the incorporation of microtubule subunits into fluxing kinetochore fibres. *Nat Cell Biol* 7: 42-47.

Mitchison TJ. 1988. Microtubule dynamics and kinetochore function in mitosis. *Ann Rev Cell Biol* 4: 527-549.

Mitchison TJ. 1989. Poleward microtubule flux in the mitotic spindle: evidence from photoactivation of fluorescnence. *J Cell Biol* 109: 637-652.

Mira A. 1998. Why is meiosis arrested. *K Theor Biol* 194: 275-287.

Miyamoto DT, Perlman ZE, Burbank KS, Groen AC, Mitchison TJ. 2004. The kinesin Eg5 drives poleward microtubule flux in *Xenopus laevis* egg extract spindles. *J Cell Biol* 5: 813-818.

Moore DH and Ruska H. 1957. Electron microscope study of mammalian cardiac muscle cells. *J Biophys Biochem Cytol* 3: 261-268.

Moore PB, Huxley HE, DeRosier DJ. 1970. Three-dimensional reconstruction of F-actin, thin filaments and decorated thin filaments. *J Mol Biol* 50: 279-295.

Naysmith K. 2002. Segregating sister genomes: the molecular biology of chromosome separation. *Science* 297: 559-565.

Nicklas BN. 1989. The motor for poleward chromosome movement in anaphase is in or near the kinetochore. *J Cell Biol* 109: 2245-2255.

Osborn M and Weber K. 1982. Immunofluorescence and immunocytochemical procedures with affinity purified antibodies: tubulin-containing structures. *Methods Cell Biol* 24: 97–132.

Patchell VB, Gallon CE, Hodgkin MA, Fattoum A, Perry SV, Levine BA. 2002. The inhibitory region of troponin-I alters the ability of F-actin to interact with different segments of myosin. *Eur J Biochem* 269: 5088–5100.

Patchell VB, Gallon CE, Evans JS, Gao Y, Perry SV, Levine BA. 2005. The regulatory effects of tropomyosin and troponin-I on the interaction of myosin loop regions with F-actin. *J Biol Chem* 280: 14469–14475.

Perry SV. 2001. Vertebrate tropomyosin: distribution, properties and function. *J Mus Res Cell Motil* 22: 5-49.

Pickett-Heaps JD and Forer A. 2001. Pac-Man does not resolve the enduring problem of anaphase chromosome movement. *Protoplasma* 215: 16-20.

Pittenger MF, Kazzaz JA, Helfman DM. 1994. Functional properties of non-muscle tropomyosin isoforms. *Curr Opin Cell Biol* 6: 96-104.

Ris H. 1943. A quantitative study of anaphase movement in the aphid *Tamalia*. *Biol Bull* 85: 164-178.

Ris H. 1949. The anaphase movement of chromosomes in the spermatocytes of the grasshopper. *Biol Bull* 96: 90-106.

Rogers GC, Rogers SL, Schwimmer TA, Ems-McClung SC, Walczak CE, Vale RD, Scholey JM, Sharp DJ. 2004. Two mitotic kinesins cooperate to drive sister chromatid separation during anaphase. *Nature* 427: 364-370.

Rogers GC, Rogers SL, Sharp DJ. 2005. Spindle microtubules in flux. *J Cell Sci* 118: 1105-1116.

Sanger JM and Sanger JW. 1980. Banding and polarity of actin filaments in interphase and cleaving cells. *J Cell Biol* 86: 568-575.

Schevzov G, Vrhivski B, Bryce NS, Elmir S, Qiu MR, O'Neill GM, Yang N, Verrills NM, Kavallaris M, Gunning PW. 2005. Tissue specific tropomyosin isoform composition. *J Histochem Cytochem* 53: 557-570.

Schevzov G, Whittaker SP, Fath T, Lin JJC, Gunning PW. 2011. Tropomyosin isoforms and Sareagents. *BioArchitecture* 1: 135-164.

Scholey JM, Brust-Mascher I, Mogliner A. 2003. Cell division. *Nature* 422: 746-752.

Schrader F. 1953. Mitosis The movements of chromosomes in cell division. Columbia University Press: New York.

Schroeder TE. 1973. Actin in dividing cells: contractile ring filaments bind heavy meromyosin. *Proc Nat Acad Sci* 70: 1688-1692.

Sharp DJ, Rogers GC, Scholey JM. 2000. Microtubule motors in mitosis. *Nature* 407: 41-47.

Sheykhani R, Shirodkar PV, Forer A. 2013. The role of myosin phosphorylation in anaphase chromosome movement. *Eur J Cell Biol* 92: 175-186.

Sheykhani R, Berns M, Forer A. 2017. Elastic tethers between separating anaphase chromosomes in crane-fly spermatocytes coordinate chromosome movement to the two poles. *Cytoskel* 74: 91-103.

Silverman-Gavrila RV and Forer A. 2000. Evidence that actin and myosin are involved in the poleward flux of tubulin in metaphase kinetochore microtubules of crane-fly spermatocytes. *J Cell Sci* 113: 597-609.

Silverman-Gavrila RV, Forer A. 2001. Effects of anti-myosin drugs on anaphase chromosome movement and cytokinesis in crane-fly primary spermatocytes. *Cell Motil Cytoskel* 50: 189-197.

Silverman-Gavrila RV, Forer A. 2003. Myosin localization during meiosis I of crane-fly spermatocytes gives indications about its role in division. *Cell Motil Cytoskel* 55: 97-113.

Squire JM. 1997. Architecture and function in the muscle sarcomere. *Curr Opin Stuct Biol* 7: 247-257.

Stehn JR, Haass NK, Bonello T, Desouza M, Kottyan G, Treutlein H, Zeng J, Nascimento PRRB, Sequeira VB, Butler TL, Allanson M, Fath T, Hill TA, McCluskey A, Schevzov G, Palmer SJ, Hardeman EC, Winlaw D, Reeve VE, Dixon I, Weninger W, Cripe TP, Gunning PW. 2013. A novel class of

anticancer compounds targets the actin cytoskeleton in tumor cells. *Cancer Res* 73: 5169-5182.

Sumner AT. 1991. Scanning electron microscopy of mammalian chromosomes from prophase to telophase. *Chromosoma* 100: 410-418.

Taylor EW. 1965. Brownian and saltatory movements of cytoplasmic granules and the movement of anaphase chromosomes. In Proceedings of the 4th International Congress on Rheology Part 4 Sympsium on Biorheology. Copley AL, editor, Interscience, New York 175-191.

Tyska MJ and Warshaw DM. 2002. The myosin power stroke. *Cell Motil Cytoskel* 51: 1-15.

Vavylonis D, Wu JQ, Hao S, O'Shaughnessy B, Pollard TD. 2008. Assembly mechanism of the contractile ring for cytokinesis by fission yeast. *Science* 4: 97-100.

Wade RH and Hyman AA. 1997. Microtubule structure and dynamics. *Curr Opin Cell Biol* 9: 12-17.

Wade RH. 2009. On and around microtubules: an overview. *Mol Biotechnol* 43: 177-191.

Wadsworth P and Salmon ED. 1986. Analysis of the treadmilling model during metaphase of mitosis using fluorescence redistribution after photobleaching. *J Cell Biol* 102: 1032-1038.

Wadsworth P, Sheldon E, Rupp G, Reider CL. 1989. Biotin-tubulin incorporates into kinetochore fibre microtubules during early but not late anaphase. *J Cell Biol* 109: 2257-2265.

Wakabayashi T, Huxley HE, Amos LA and Klug A. 1975. Three-dimensional image reconstruction of actin-tropomyosin complex and actin-tropomyosin-troponin T-troponin I complex. *J Mol Biol* 93: 477-497.

Watanabe Y. 2004. Modifying sister chromatid cohesin for meiosis. *J Cell Sci* 117: 4017-4023.

Wawro B, Greenfield NJ, Wear MA, Cooper JA, Higgs HN, Hitchcock-DeGregori SE. 2007. Tropomyosin regulates elongation by formin at the fast-growing end of the actin filament. *Biochem* 46: 8146-8155.

Wilson PJ, Forer A, Leggiadro C. 1994. Evidence that kinetochore microtubules in crane-fly spermatocytes disassemble during anaphase primarily at the poleward end. *J Cell Sci* 107: 3015-3027.

Woodrum DT, Rich SA, Pollard TD. 1975. Evidence for biased bidirectional polymerization of actin filaments using heavy meromyosin prepared by an improved method. *J Cell Biol* 67: 231-237.

Yin B and Forer A. 1996. Coordinated movements between autosomal half-bivalents in crane-fly spermatocytes: evidence that 'stop' signals are sent between partner half-bivalents. *J Cell Sci* 109: 155-163.

Xie L, Miyazaki JI, Hirabayashi T. 1991. Identification and distribution of tropomyosin isoforms in chicken digestive canal. *J Biochem* 109: 827-878.

Xie L and Forer A. 2008. Jasplakinolide, an actin stabilizing agent, alters anaphase chromosome movement in crane-fly spermatocytes. *Cell Motil Cytoskel* 65: 876-889.

Zhang D and Nicklas RB. 1996. "Anaphase" and cytokinesis in the absence of chromosomes. *Nature* 382: 466-468.

Zhang D, Rogers GC, Buster DW, Sharp DJ. 2007. Three microtubule severing enzymes contribute to the "Pacman-flux" machinery that moves chromosomes. *J Cell Biol* 231-242.

Appendix

Permissions: Figure 4

This Agreement between York University -- Jessica Di Salvo ("You") and Elsevier ("Elsevier") consists of your license details and the terms and conditions provided by Elsevier and Copyright Clearance Center.

License Number	4186760698471
License date	Sep 12, 2017
Licensed Content Publisher	Elsevier
Licensed Content Publication	Current Opinion in Structural Biology
Licensed Content Title	Architecture and function in the muscle sarcomere
Licensed Content Author	John M Squire
Licensed Content Date	Apr 1, 1997
Licensed Content Volume	7
Licensed Content Issue	2
Licensed Content Pages	11
Start Page	247
End Page	257
Type of Use	reuse in a thesis/dissertation
Intended publisher of new work	other
Portion	figures/tables/illustrations
Number of figures/tables/illustrations	1
Format	both print and electronic
Are you the author of this Elsevier article?	No
Will you be translating?	No
Original figure numbers	Figure 1
Title of your thesis/dissertation	Possible Roles for Tropomyosin During Anaphase Chromosome Movement
Expected completion date	Sep 2017
Estimated size (number of pages)	150
Requestor Location	York University 4700 Keele St. Toronto, ON M3J 1P3 Canada Attn: Forer
Total	0.00 USD

Permissions: Figure 6

This Agreement between York University -- Jessica Di Salvo ("You") and John Wiley and Sons ("John Wiley and Sons") consists of your license details and the terms and conditions provided by John Wiley and Sons and Copyright Clearance Center.

License Number	4186740542929
License date	Sep 12, 2017
Licensed Content Publisher	John Wiley and Sons
Licensed Content Publication	BioEssays
Licensed Content Title	The molecular basis for tropomyosin isoform diversity
Licensed Content Author	James P. Lees-Miller,David M. Helfman
Licensed Content Date	Feb 5, 2005
Licensed Content Pages	9
Type of use	Dissertation/Thesis
Requestor type	University/Academic
Format	Print and electronic
Portion	Figure/table
Number of figures/tables	1
Original Wiley figure/table number(s)	Figure 1
Will you be translating?	No
Title of your thesis / dissertation	Possible Roles for Tropomyosin During Anaphase Chromosome Movement
Expected completion date	Sep 2017
Expected size (number of pages)	150
Requestor Location	York University 4700 Keele St. Toronto, ON M3J 1P3 Canada Attn: Forer
Publisher Tax ID	EU826007151
Billing Type	Invoice
Billing Address	York University 4700 Keele St. Toronto, ON M3J 1P3 Canada Attn: Forer
Total	0.00 CAD

Permissions: Figure 7

This Agreement between York University -- Jessica Di Salvo ("You") and Springer ("Springer") consists of your license details and the terms and conditions provided by Springer and Copyright Clearance Center.

License Number	4186741189450
License date	Sep 12, 2017
Licensed Content Publisher	Springer
Licensed Content Publication	Journal of Muscle Research and Cell Motility
Licensed Content Title	Vertebrate tropomyosin: distribution, properties and function
Licensed Content Author	S.V. Perry
Licensed Content Date	Jan 1, 2001
Licensed Content Volume	22
Licensed Content Issue	1
Type of Use	Thesis/Dissertation
Portion	Figures/tables/illustrations
Number of figures/tables/illustrations	1
Author of this Springer article	No
Order reference number	
Original figure numbers	Figure 1
Title of your thesis / dissertation	Possible Roles for Tropomyosin During Anaphase Chromosome Movement
Expected completion date	Sep 2017
Estimated size(pages)	150
Requestor Location	York University 4700 Keele St. Toronto, ON M3J 1P3 Canada Attn: Forer
Billing Type	Invoice
Billing Address	York University 4700 Keele St. Toronto, ON M3J 1P3 Canada Attn: Forer
Total	0.00 USD

Permissions: Figure 10

This Agreement between York University -- Jessica Di Salvo ("You") and American Association for Cancer Research ("American Association for Cancer Research") consists of your license details and the terms and conditions provided by American Association for Cancer Research and Copyright Clearance Center.

License Number	4186750361897
License date	Sep 12, 2017
Licensed Content Publisher	American Association for Cancer Research
Licensed Content Publication	Cancer Research
Licensed Content Title	A Novel Class of Anticancer Compounds Targets the Actin Cytoskeleton in Tumor Cells
Licensed Content Author	Justine R. Stehn,Nikolas K. Haass,Teresa Bonello,Melissa Desouza,Gregg Kottyan,Herbert Treutlein,Jun Zeng,Paula R.B.B. Nascimento,Vanessa B. Sequeira,Tanya L. Butler,Munif Allanson,Thomas Fath,Timothy A. Hill,Adam McCluskey,Galina Schevzov,Stephen J. Palmer,Edna C. Hardeman,David Winlaw,Vivienne E. Reeve,Ian Dixon,Wolfgang Weninger,Timothy P. Cripe,Peter W. Gunning
Licensed Content Date	Aug 15, 2013
Licensed Content Volume	73
Licensed Content Issue	16
Type of Use	Thesis/Dissertation
Requestor type	academic/educational
Format	print and electronic
Portion	figures/tables/illustrations
Number of figures/tables/illustrations	1
Will you be translating?	no
Circulation	50
Territory of distribution	Worldwide
Title of your thesis / dissertation	Possible Roles for Tropomyosin During Anaphase Chromosome Movement
Expected completion date	Sep 2017
Estimated size (number of pages)	150
Requestor Location	York University 4700 Keele St. Toronto, ON M3J 1P3 Canada Attn: Forer
Billing Type	Invoice

Billing Address	York University 4700 Keele St. Toronto, ON M3J 1P3 Canada Attn: Forer
Total	0.00 USD

Permissions: Figure 11

Molecular Biology of the Cell (Online)

Order detail ID:70670782
Order License Id:4186821030564
ISSN:1939-4586
Publication Type:e-Journal
Volume:
Issue:
Start page:
Publisher: American Society for Cell Biology
Permission Status: **Granted**

Permission type: Republish or display content
Type of use: Thesis/Dissertation
Hide details

Requestor type	Academic institution
Format	Print, Electronic
Portion	image/photo
Number of images/photos requested	1
Title or numeric reference of the portion(s)	Figure 5
Title of the article or chapter the portion is from	A novel tropomyosin isoform functions at the mitotic spindle and Golgi in Drosophila
Editor of portion(s)	n/a
Author of portion(s)	Lauren M. Goins and R. Dyche Mullins
Volume of serial or monograph	26
Page range of portion	2491-2504
Publication date of portion	July 1 2015
Rights for	Main product
Duration of use	Life of current edition
Creation of copies for the disabled	no
With minor editing privileges	no
For distribution to	Worldwide
In the following language(s)	Original language of publication
With incidental promotional use	no
Lifetime unit quantity of new product	Up to 499
Made available in the following markets	education
The requesting person/organization	Jessica Di Salvo
Order reference number	
Author/Editor	Jessica Di Salvo
The standard identifier of New Work	Title
Title of New Work	Possible Roles for Tropomyosin During Anaphase Chromosome Movement
Publisher of New Work	York University
Expected publication date	Sep 2017
Estimated size (pages)	150